Mechanisms of B-cell arrest in acute lymphoblastic leukaemia (ALL) of childhood

- The interplay between the essential early B-cell factor EBF1 and
the multifunctional zinc finger protein OAZ -

Dissertation

zur Erlangung des Doktorgrades der Naturwissenschaften (Dr. rer. nat.)
am Department Biologie der Fakultät für Mathematik, Informatik und
Naturwissenschaften an der Universität Hamburg

Vorgelegt von

Dipl. Biologe Georg Eschenburg
geboren in Hamburg

Hamburg, Juni 2009

Genehmigt vom Department Biologie
der Fakultät für Mathematik, Informatik und Naturwissenschaften
an der Universität Hamburg
auf Antrag von Professor Dr. M. HORSTMANN
Weiterer Gutachter der Dissertation:
Herr Professor Dr. K. WIESE
Tag der Disputation: 17. April 2009

Hamburg, den   03. April 2009

Professor Dr. Jörg Ganzhorn
Leiter des Departments Biologie

Department Biologie

der Fakultät für Mathematik, Informatik und

Naturwissenschaften

Universität Hamburg

Martin Luther King-Platz 2

D-20146 Hamburg

Hamburg, 4. Februar 2009

Sehr geehrte Damen und Herrn,

hiermit bestätige ich, dass die von Herr Georg Eschenburg mit dem Titel ""Mechanisms of B-cell arrest in acute lymphoblastic leukaemia (ALL) of childhood - the interplay between the essential early B-cell factor EBF1 and the multifunctional zinc finger protein OAZ" vorgelegte Doktorarbeit in korrektem Englisch geschrieben ist.

Mit freundlichen Grüssen,

Carol Stocking

Dr. Carol Stocking

Leiterin der FG Molekulare Pathologie
Heinrich-Pette-Institut
(Amerikanerin),

Table of contents

A   List of figures

B   List of tables

1 Introduction

Transcriptome-wide expression analyses (Horstmann et al., unpublished) in paediatric acute lymphoblastic leukaemia (ALL) patient samples with TEL/AML1 rearrangement or hyperdiploid karyotype revealed an increased activation of the bone morphogenetic protein 2 (BMP2)-dependent pathway and its related transcription factor Olf/EBF1-associated zinc finger protein (OAZ/EBFAZ/Znf423) in the leukaemic cells. BMP2 directed target proteins and their transcriptional targets as the next layer of subcellular regulation could be of great importance in precursor B-cell ALL (pre-B ALL). An activated BMP2-pathway and/or an upregulation of OAZ could reflect either a bystanding phenomenon as a state of differentiation of leukaemic cells or a driving aberration of ALL, the modulation of which might affect the malignant phenotype.

1.1 Acute Lymphoblastic Leukaemia (ALL)

Leukaemia is the cancer of the blood or the bone marrow (from Greek leukos; white and aima; blood), characterised by an abnormal accumulation of immature progenitors of the white blood cell compartment[1]. By the displacement of normal haematopoiesis symptoms like anaemia, increased tendency to bleed and susceptibility for infections emerge. Without treatment the outcom usually is dismal. Characteristic for leukaemia is an unlimited capacity for self-renewal[2,3], a loss of normal proliferative control, a block in cell differentiation and resistance to death signals (apoptosis) in transformed cells[4]. It is assumed that leukaemogenesis is initiated by transforming genetic first hit events like aberrant expression of proto-oncogenes, chromosomal translocations that create fusion genes, or aneuploidy[4,5] necessary but usually not causal for leukaemia development following conventional two- or multistep models of cancer clone evolution[6,7,8].

The most prominent malignancy of childhood is the pre-B ALL, a specific form of leukaemia where progenitors of the B-lymphocytes go awry[5,9,10]. Today novel therapeutic strategies are necessary even though great therapy improvements were achieved in the last decades. Around 20% of the patients still succumb to the disease despite intensified therapy and leukaemia survivors are threatened by severe long-term complications such as secondary malignancies[1,11,12]. The TEL/AML1 fusion molecule resulting from a t(12;21)(p13;q22) illegitimate chromosomal translocation[13] is associated with a pre-B ALL phenotype with a favourable prognosis in children[14]. With up to 30% of the ALL cases it is the most frequent genetic abnormality in cancer of childhood (Figure 1)[5]. The t(12;21) translocation is thought to be a first-hit mutation occurring already in the uterus[15] which cellular origin is still a matter

of debate. The t(12;21) rearrangement likely originates in a committed B-cell progenitor[16,17] albeit several recent studies have suggested that the primary transformation event in ALLs frequently occurs in the HSC compartment[18,19,20]. The TEL/AML1 rearrangement results in a long-lived preleukaemic clone with increased self-renewal and survival properties, necessary but not sufficient for ALL transformation[21,22,23]. Only in one in a hundred (to thousand) cases TEL/AML1 rearranged cells accumulate critical additional mutations during their relatively long span of life leading to leukaemic transformation[15,24].
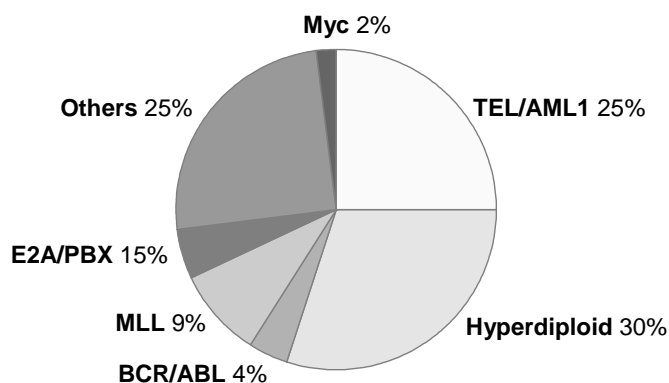
Figure 1: Chromosomal aberrations in childhood B-cell acute lymphoblastic leukaemia. The relative frequencies of specific alterations found in ALL are shown.

In TEL/AML1 leukaemia the two transcription factors TEL and Runx1, which have essential roles in haematopoiesis[13,25], are fused to a chimeric aberrant transcription factor that perturbs multiple pathways during haematopoiesis[21,26]. Studies in men and mice showed that TEL/AML1-expressing cells have a clonal advantage and give rise to increased numbers of myeloid cells[17,27,28]. Pro-B cells accumulate in the bone marrow at the expense of more differentiated pre-B cells, immature and mature B-cells leading to a pre-leukaemic state of the lymphoid lineage[21,22,28]. A lineal relationship between the cells propagating leukaemia and the initial preleukaemic cell where the TEL/AML1 fusion first occurred and/or had functional impact has been established by analysing a monochoric twin pair, one preleukaemic and one with frank leukaemia[29].

Molecular events like the TEL/AML1 rearrangement leading to a specific phenotype are suitable for the classification of ALL; the search for secondary or additional mutations responsible for leukaemia transformation nevertheless has become essential for the understanding and a targeted therapy of the disease. TEL/AML1 is often accompanied with a secondary TEL deletion of the non-rearranged allele, probably arising after birth[30,31]. Causal relations between accumulated mutations and TEL/AML1 leukaemia are still missing. A global analysis of more than 200 paediatric ALL patients using high-resolution SNP arrays, DNA sequencing, paired copy number and loss of heterozygosity (LOH) analyses showed

alterations in genes implicated in B-lymphocyte development in 40% of the cases[32]. More than 30% of these mutations affected the essential B-lineage commitment factor PAX-5[33]. Deletions also were detected in E2A, EBF1, LEF1, IKAROS and AIOLOS. Approximately 3% of the cases harboured monoallelic deletions of EBF1 likely responsible for the differentiation block characteristic for ALL. Another study showed microdeletions in PAX5, EBF1, IKAROS and RAG1/2[34]. Generally it is conceivable that the disruption of B-cell lineage genes and signalling contributes to the pathogenesis of leukaemia[32]. The identifcation of EBF1 mutations in a fraction of ALL might serve as a paradigmatic proof of concept, placing EBF1 into B-cell leukaemogenesis. This recent observation raises the question if there are other so far unidentified mechanisms leading to EBF1 deficiency and ultimately to frank acute lymphoblastic leukaemia?

1.2 Normal B-cell development

The haematopoiesis is the generation of all cellular blood components (Figure 2)[35].
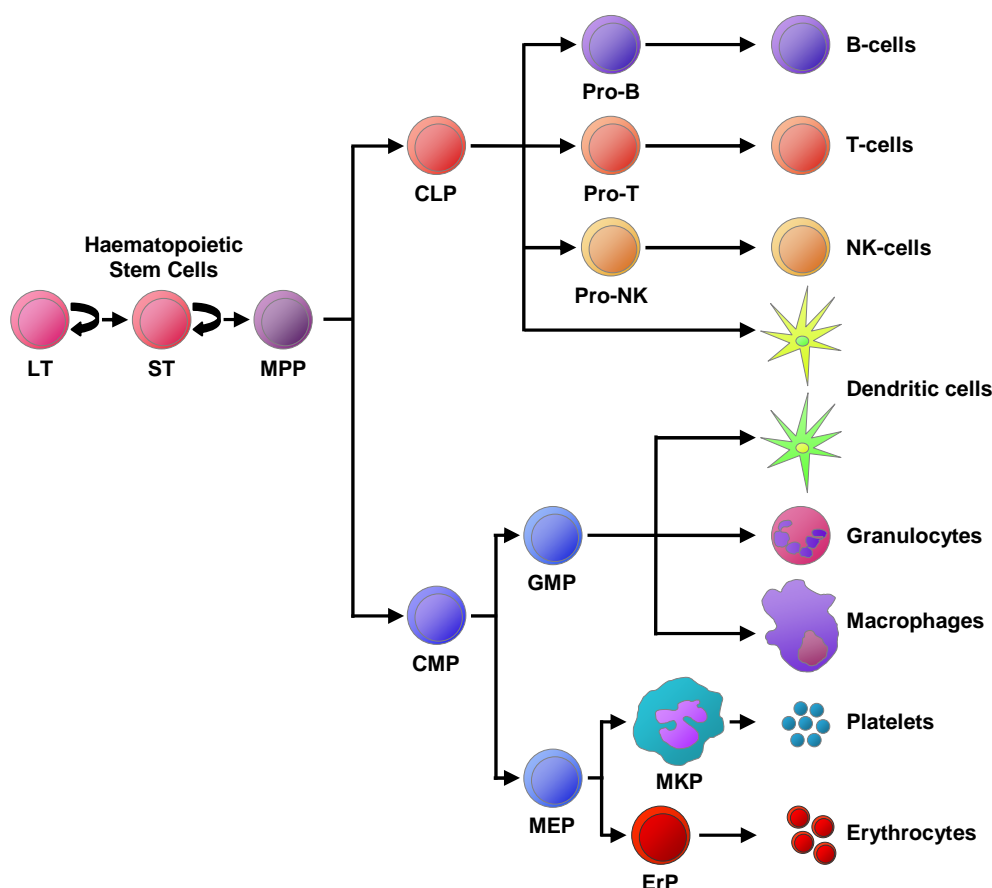
Figure 2: Schematic overview of haematopoiesis. Long-term (LT) and short-term (ST) haematopoietic stem cells differentiate to multipotent progenitors (MPPs) that give rise to common lymphoid progenitors (CLPs) and common myeloid progenitors (CMPs). CLPs develop into B-, T-, NK- and dendritic cells, CMPs into dendritic cells, granulocytes, macrophages, platelets and erythrocytes. GMP, granulocyte macrophage precursors; ErP, erythrocyte precursor; MEP, megakaryocyte erythrocyte precursor; MkP, megakaryocyte precursor, NK, natural killer.

Only 0.5-5% of human haematopoietic cells express CD34[36], this population contains the haematopoietic stem cells[37,38] that are able to generate vitally important lineages such as B-, T-, NK- dendritic and myeloid cells[38,39]. It is to notice that CD34 is not necessary for human haematopoiesis[40], it is needed for adhesion to the nourishing stromal microenvironment in the bone marrow[41].

B-lymphocytes (bursal or bone marrow derived) are a population of cells expressing clonally diverse surface specific antigenic epitopes[42]. B-cell development begins in primary lymphoid tissue like human fetal liver and fetal/adult bone marrow with a subsequent functional maturation in secondary lymphoid tissue (e.g. human lymph nodes and spleen)[42] a process that proceeds throughout life-time[43]. B-lymphocytes are multifunctional and are necessary for the production of antibodies and cytokines (IFN-γ, IL-6 and IL-10), lymphoid tissue organogenesis, tumour immunity, transplant rejection, wound healing, dendritic cell regulation, Th1/Th2 cytokine balance, co-stimulation of T-cells and antibody presentation (Figure 3)[42]. Plasma cells are the end point of B-cell development being terminally differentiated[42].
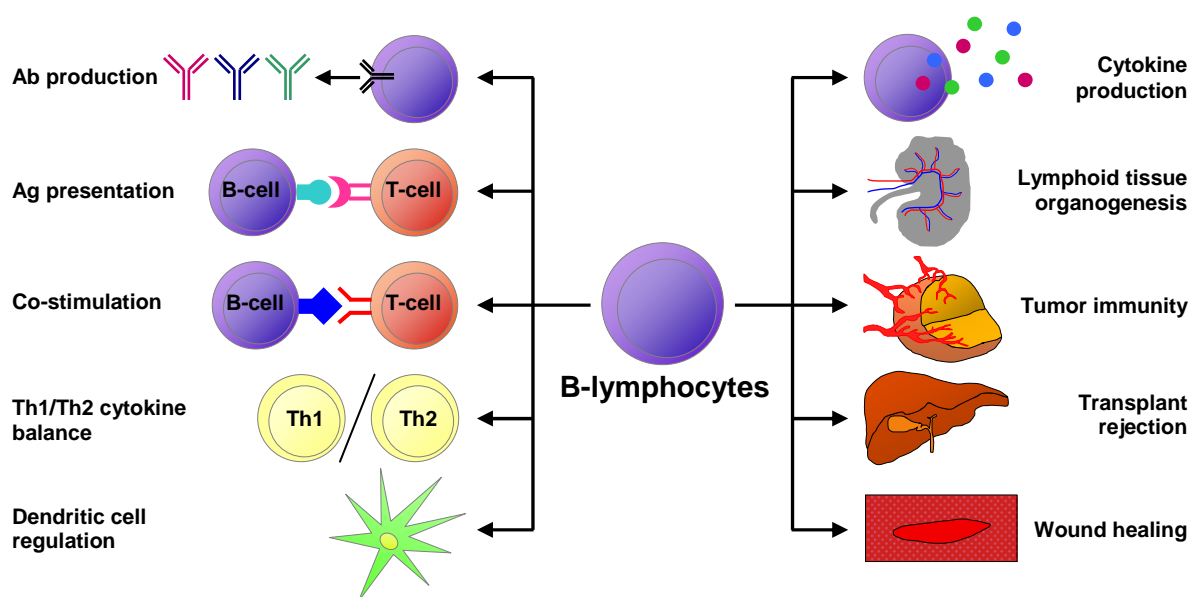
Figure 3: Functions of B-lymphocytes. Selection of processes regulated or mediated by B-cells.. Graphic adapted from LeBien and Tedder; Blood, 2008.

B-cell development starts with B-lineage-committed cells (Figure 4)[44,45] that pass through a CD34^{+}CD10^{+}CD19^{-} common lymphoid progenitor (CLP) early-B (E-B) stage[39,44,46], characterised by expression of transcriptional regulator proteins, which initiate the B-cell specific program[47,48]. The following differentiation goes along with an increase in CD19 and a decrease in CD10 expression. B-biased progenitors mature via CD34^{+}CD10^{+}CD19^{+} pro-B cells[45,49,50], that express CD19 but no cytoplasmic or cell surface μ heavy chains (HCs)[51], to

CD34$^-$CD10$^+$CD19$^+$ pre-B cells characterised by a loss of CD34 and TdT and an acquisition of cytoplasmic µHC in almost all cells[52,53]. Pre-B cells start to variably express cell surface µHCs associated with surrogate light chains (ΨLCs)[53], consisting of the two proteins IGLL1 (λ5) and VpreB[54], and the CD79a/CD79b signal transduction heterodimer[55] forming the pre-B-cell receptor (pre-BCR)[56,57]. Pre-B cells differentiate via CD34$^-$CD10$^+$CD19$^+$sIgM$^+$ immature B-cells (IM-B), expressing CD19 and cell surface µHCs associated with conventional κ or λLCs forming the B-cell receptor (BCR) [56,58], into CD34$^-$CD10$^-$CD19$^+$ mature B-cells[58,59].
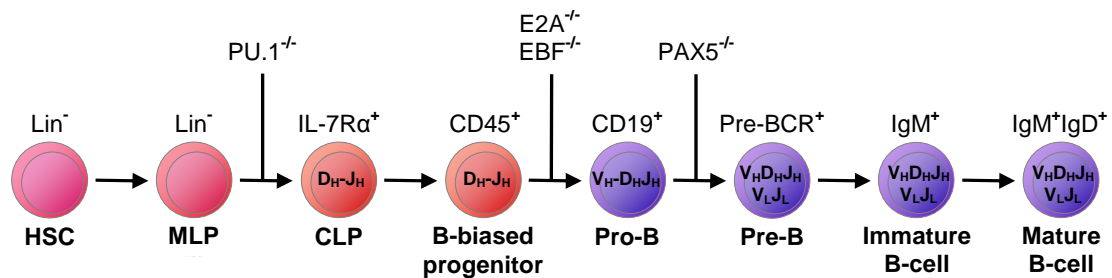
Figure 4: B-cell development. Murine B-cell lymphopoiesis with cell types indicated below, the status of V(D)J recombination indicated within and characteristic cell surface markers indicated above each cell. Point of block in B-lymphopoiesis for PU.1$^{-/-}$, E2A$^{-/-}$, EBF1$^{-/-}$ and PAX5$^{-/-}$ mice are shown above the cells. Lin$^-$ = lineage-specific markers. Graphic adapted from Hagman and Lukin; Trends in immunology, 2005.

The development of HSCs via lymphoid progenitors into early B-cells requires the concerted actions of a multitude of transcription factors (Figure 5)[59,60,61]. PU.1 and Ikaros act in parallel pathways to control transition of HSCs into lymphoid precursors[62,63,64]. EBF1 and E2A are important in promoting B-lineage specification and differentiation[65,66,67] and PAX5 is a multifunctional transcription factor maintaining the B-lymphoid commitment together with EBF1[68,69]. In the absence of PAX5, B-cells can dedifferentiate into functional T-, NK- and dendritic cells, macrophages, granulocytes and osteoclasts[68,69].

EBF1 and closely related proteins (EBF2, EBF3, EBF4, Collier Knot and Unc-3)[70] constitute a transcription factor family that possesses a highly conserved and distinct DNA-binding domain[71]. The human EBF1 gene is located on chromosome 5q34 and is highly homologous to the murine EBF1[72]. The EBF1 protein usually acts as a homodimer[73,74] which binds to promoter regions containing the consensus 5'-CCCNNGGG-3' sequence[71]. It is capable of directing chromatin modifications that are permissive for transcriptional activation[75,76]. Expression of the EBF gene has been detected in adipocytes, limb buds and the developing forebrain[73,77,78]. In the haematopoietic system it is exclusively expressed in the B-lymphoid lineage and is absent in terminally differentiated plasma cells, T- or myeloid cells[72,73,79]. Multipotent progenitor cells (MPPs) express E2A that controls EBF1, which in turn regulates PAX5[80,81,82]. MPPs lack expression of PAX5 and EBF1[51,83] until the commitment to the B-cell

lineage[45]. The onset of low EBF1 expression in common lymphoid progenitors (CLPs) occurs in response to PU.1 activation and IL-7 signalling (Figure 5)[60,71] leading to a repression of alternative differentiation pathways and activation of B-cell specific genes[84,85,86,87]. This directs haematopoietic progenitor cells to the B-lymphoid lineage.
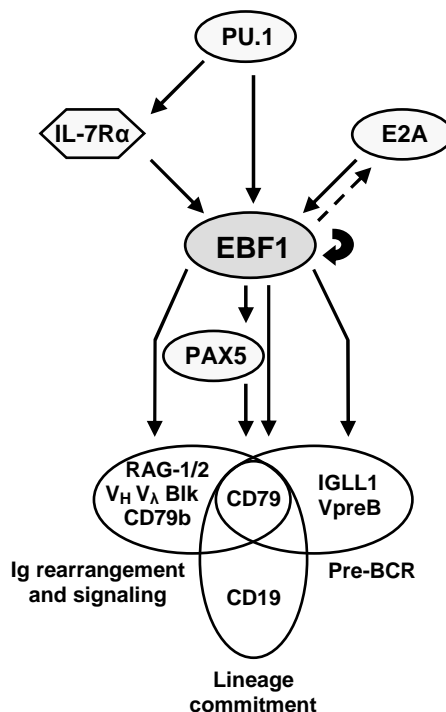
Figure 5: The essential role of EBF1. Regulation of murine early B-cell development by the transcription factor EBF1. Transcription of EBF1 is regulated by several other factors and a possible autoregulatory loop. EBF1 regulates genes, including PAX5, RAG1, λ5 (IGLL1), VpreB, B29 (CD79b), Blk, mb-1 (CD79a) and CD19. Lin⁻ = lineage-specific markers. Graphic adapted from Hagman and Lukin, Trends in immunology, 2005.

EBF1 acts downstream of E2A and can restore B-lymphopoiesis in E2A$^{-/-}$ progenitors[88]. Further commitment and differentiation to the B-cell lineage is promoted by EBF1-mediated enforced PAX5 expression, which in turn increases expression of EBF1[61,71,89]. Neither E2A nor PAX5 are able to efficiently rescue B-cell specific gene expression in EBF-deficient lymphoid progenitors[71]. Because EBF1 acts upstream of PAX5, its deficiency results in a developmental arrest at a later stage than that caused by EBF1[90]. Differentiation of progenitors to B-cells in mice is accompanied by the expression of the lineage markers B220, CD43 and IL-7Rα and the initiation of the V(D)J recombination resulting in gene rearrangement[71]. EBF1 is upregulated during this process with an increase from HSCs to early-B-cells and a maximum expression in pro-B and pre-B cells[72,91], concomitant with the onset of PAX5 expression[45,89]. The transcriptional regulation of essential B-cell genes and V(D)J rearrangement is mediated by an interaction with E2A, PAX5, E-proteins, STAT5 and RUNX1[92,93] and a potential EBF1 autoregulatory loop[81]. In the absence of EBF1, progenitor cells express the lineage markers B220, CD43, IL-7Rα and germline μ, but fail to express

genes necessary for pre-BCR and BCR signalling including CD79a, CD79b, IGll1, VpreB, RAG1/2, CD19 and PAX-5 [67,94]. Pre-B and B-cell receptor-dependent signals are essential for Ig chain allelic exclusion and proliferation of B-cells after the encounter with an antigen[95]. B-cell differentiation in EBF^{-/-} mice is blocked between the pro-B cell and early-B stage leading to a complete absence of functional Ig expressing mature B-cells[67]. Various non-lymphoid tissues that express EBF1 are apparently normal, including olfactory neurons in which EBF1 was originally identified as Olf1[74,96]. A reduction or a block of EBF1 expression can contribute to the development of disease in B-lineage cells[71]. A consequence could be the induction of leukaemia as suggested by a recent study detecting eight cases of B-cell progenitor ALL with mono- or biallelic deletions of the EBF1 gene in tumour cells in which EBF1 might act as a non-classical tumour suppressor[32].

1.3 TGF-β and BMP signalling

1.3.1 General signalling

Control and regulation of cellular functions are mediated by a panel of direct cell-cell signals, among which the transforming growth factor β (TGF-β) family of cytokines is of general importance[97]. A deregulation of this complex system network has fatal consequences. TGF-β signalling controls the proliferation, recognition and differentiation of cells as well as apoptosis and specification of developmental fate, depending on the differentiation state of the target cell, the tissue environment and the concentrations of crucial molecules[98,99]. The human genome encodes up to 42 TGF-β superfamily ligands[100], comprising the TGF-β/Activin/Nodal and BMP (bone morphogenetic protein)/GDF (growth and differentiation factor)/MIS (Müllerian inhibiting substance) subfamilies, and as well as seven type I and five type II receptors[101,102]. The BMPs make up the largest group within the TGF-β family and include BMP2, BMP4, BMP7 and GDF5 among others[103]. BMP2-signalling members are highly expressed in TEL/AML1 rearranged and hyperdiploid paediatric ALL patient samples (Horstmann et al., unpublished). The BMP proteins are characterised by six conserved cysteine residues[100] and exist as homodimers in their active form[104]. They can modulate gene expression by activation of a signalling cascade involving 8 distinct Smad proteins, constituting three functional classes designated as R-Smads (Smad1/2/3/5/8), Co-Smads (Smad4), and I-Smads (Smad6/7) (Figure 6)[102,105]. The receptor-activated Smad proteins (R-Smads) are phosphorylated subsequent to BMP ligand binding to serine/threonine kinase receptors type I and II[104]. In vertebrates, the type I receptors of BMP and GDF recognise Smad1/5/8[103,104]. Phosphorylated Smad proteins[106], bound to the cytoplasmic domain of the type I receptor, subsequently dissociate from the receptor multimer and form a complex with Smad4[104]. The inhibitory-Smads (I-Smads) negatively regulate BMP signalling by competing

with R-Smads for receptor or Smad4 interaction and by targeting the receptors for degradation[104]. The Smad complex then translocates into the nucleus leading to a regulation of target gene expression[102,103,107] by binding to a consensus Smad binding element (SBE) sequence[108,109].
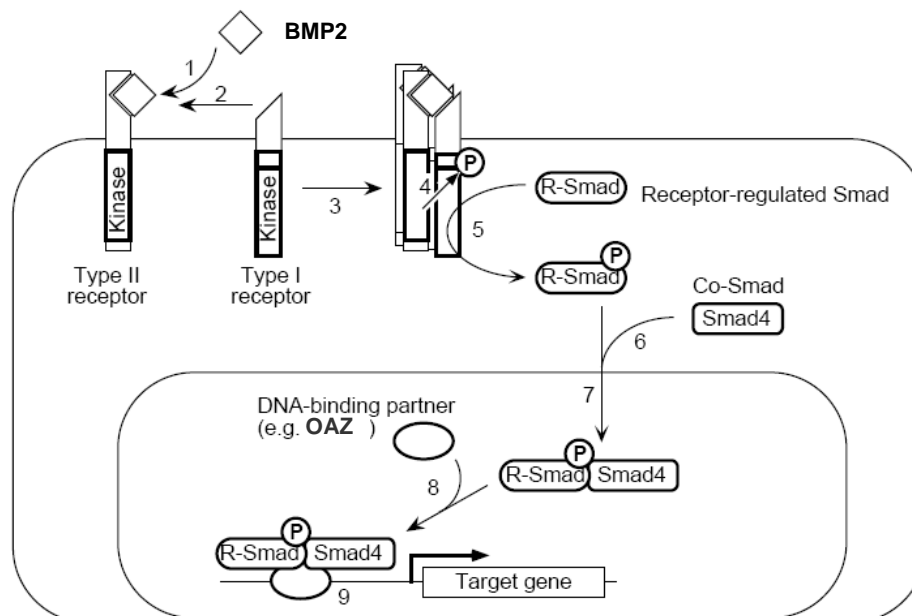
Figure 6: The Transforming growth factor *β* (TGF-*β*)/Smad pathway. Binding of a TGF-*β* family ligand like BMP2 to its type II receptor (1) together with a type I receptor (2) leads to receptor complex formation (3) and phosphorylation of the type I receptor (4). The activated type I receptor subsequently phosphorylates an R-Smad (5), leading to an association with Smad4 (6) and a translocation to the nucleus (7). In the nucleus, the Smad complex can bind to DNA-binding partners like OAZ (8). This higher complex binds to specific regulative DNA sequences in target genes (9) thereby activating transcription. Graphic from Massague; Annual review in biochemistry, 1998.

The Smad complex binds transcription factors such as OAZ[110,111] which can function independently of Smads in other cellular processes[97,103]. The regulation of BMP signalling is mediated by an interaction or "cross-talk" with other major signalling pathways like TGF-*β*/Activin, Notch, p38 MAPK (mitogen-activated protein kinase) and Toll[112,113] making it extremely versatile in the regulation of diverse cellular processes.

1.3.2 Specific functions of BMPs

From an evolutionary point of view the various isoforms of TGF-*β* and activin are distant from the BMPs[103]. TGF-*β* isoforms can either suppress or enhance proliferation, apoptosis, differentiation and terminally differentiated cell function[114]. TGF-*β* signalling in general exerts a negative effect on (haematopoietic) stem cell proliferation[114,115] and a deregulation of this pathway contributes to tumourigenesis[104]. Deregulated TGF-*β* signalling is known to be involved in a variety of human cancers, including those of the colon, pancreas, breast, prostate, head and neck and T-cell lymphoma[116,117,118]. The Smads are involved in HSC

renewal and mutations are rare in leukaemia, although have been associated with leukaemic transformation[114,119].

BMP expression is found in adult human bone marrow regulating the proliferation of highly purified primitive human haematopoietic progenitor and stem cells from adult and neonatal sources[120,121] and control the stem cell fate after transplantation into NOD/*scid* mice[122]. BMP2 is an inducer of a haematopoietic microenvironment including lymphoid, erythroid and myeloid progenitors in the rat[123]. BMPs are involved in negative regulation of mature B-cell growth, implicating their relevance in regulation of the immune response[124]. They were originally identified as playing an essential role in bone and cartilage remodelling and growth[125] especially during embryogenesis[103]. BMPs control such fundamental processes as somite and skeletal development, limp patterning, gastrulation, neurogenesis, chondrogeneis, intedigital apoptosis, organ and axial development of the whole body in men, frog and fly[126,127].

1.4 The multifunctional transcription factor OAZ

The Olf/EBF1-associated zinc finger gene (OAZ/EBFAZ/ Znf423) is located on human chromosome 16q12 and is expressed in brain, eye, olfactory epithelium, spleen and heart[128,129]. The encoded protein contains 30 C_2H_2 zinc-finger domains (Figure 7)[110] of the TFIIIA type and is one of the largest members of the Krüppel-like zinc-finger protein family[130]. OAZ fulfils multiple roles in signal transduction during development through an assumable mutually exclusive use of different clusters of zinc-fingers (Figure 7)[110].
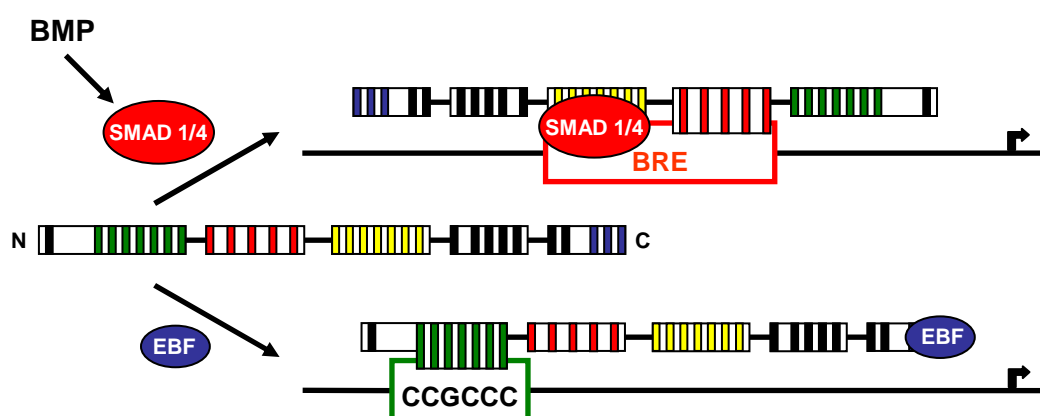
Figure 7: A model for the multifunctional role of OAZ by mutually exclusive use of different clusters of zinc-fingers. OAZ interacts with Smad1/Smad4 through zinc-fingers 14–19 and EBF1 with zinc-fingers 28–30. The binding to one of the partners may lead to a preference or just ability to bind to specific DNA sequences through different clusters of zinc-fingers. OAZ binds in company with BMP-activated Smad1/Smad4 to BMP responsive elements (BREs) through zinc-fingers 9–13 and binds the CCGCCC sequence through zinc-fingers 2-8 together with EBF1. Graphics and description modified from Hata et al.; Cell, 2000.

Each cluster of fingers has a different protein- or DNA-binding function whereby fingers 2-8 bind to SP1-like GC-rich DNA-sites, fingers 9-13 mediate binding to specific BMP responsive elements (BREs), fingers 14-19 bind to Smads and fingers 27-30 to EBF1[110,128,131].

OAZ is implicated in BMP signalling by binding to Smad1 and Smad4 in response to BMP2, forming a complex that transcriptionally activates genes with BREs like xenopus XVENT-2[110]. Cooperation of OAZ with BMP signalling is highly pathway specific excluding binding to TGF-β. Only specific consensus sequences are recognised by OAZ showing its target gene specificity[110]. EBF1 is the counterpart of the Smads; its overexpression inhibits the ability of OAZ to mediate XVENT-2 promoter activation by BMP2. Vice versa, the ability of OAZ to act as a transcriptional partner of EBF1 can be inhibited by BMP2 in a Smad-dependent manner[110]. OAZ and EBF1 are possibly able to transactivate so far unidentified target genes suggesting that the OAZ/EBF1 complex possesses DNA-binding activity via binding of OAZ to the CCGCCC DNA-sequence and transactivation activity mediated by EBF1[110,128,131].

The formation of a heteromeric complex of OAZ and EBF1 prevents the assembly of active EBF1 homodimers which can recognise native EBF1 binding-sites[128,131]. In consequence this abolishes EBF1-mediated transcriptional activation of the type III adenylyl cyclase (AC3) and olfactory marker protein (OMP) promoters showing OAZ' essential role in regulating the differentiation of olfactory neurons[128,131]. OAZ expression is also able to decrease the expression of the B-cell specific genes CD79b and IGLL1 in transfected HEK-293 cells[132], albeit OAZ is not expressed in normal haematopoietic cells[133]. It is likely that abnormal OAZ upregulation in haematopoietic cells could have severe consequences for normal B-cell development and could contribute to leukaemic transformation. This prediction is supported by the actuality that OAZ is highly expressed in TEL/AML1 rearranged and hyperdiploid paediatric ALL patient samples detected by previous transcriptome analyses (Horstmann et al., unpublished).

2 Working hypothesis

Precursor B-cell acute lymphoblastic leukaemia (pre-B ALL) is the most prominent form of leukaemia in childhood. Eminent therapeutic improvements were achieved in the last decades nevertheless it is necessary to further increase our knowledge of the disease. Almost 20% of the patients are not successfully treatable and patients exempt from leukaemia often get severe long-term complications. Leukaemogenesis in two- or multistep models of cancer clone evolution is initiated by first hit events like the common TEL/AML1 rearrangement that are necessary but not causal for leukaemic transformation. Therefore a deeper understanding of the molecular events and the detection of secondary or tertiary molecular abberations in the development of leukaemia is considered a prerequisite to design rational and targeted treatment strategies. Previous transcriptome-wide expression analyses (Horstmann et al., unpublished) in paediatric ALL showed an increased activation of the bone morphogenetic protein 2 (BMP2)-dependent pathway, which belongs to the TGF-β superfamily signalling network and of the pathway-related transcription factor Olf/EBF1-associated zinc finger protein (OAZ/EBFAZ/Znf423) in the leukaemic cells. We hypothesise that an activated BMP2-pathway and simultaneous OAZ expression does not reflect a state of differentiation of leukaemic cells but rather a specific aberration of ALL, which drives and maintains the malignant phenotype potentially by arresting the leukaemic cells in an immature state of differentiation.

The goal of this project is help to understand the multistep process to lymphoblastic leukaemia by dissecting and modulating molecular mechanisms of B-cell differentiation and its disturbances in ALL focusing on the interplay between the essential B-cell factor EBF1 and the BMP2 target protein OAZ. The aim is to assess the biological relevance of OAZ activation along the BMP2-signalling pathway in pre-B ALL of childhood. For this purpose it is necessary to clone relevant members of the BMP2-dependent pathway and EBF1 to gain specific expression plasmids as suitable tools for gene expression analyses of different ALL subgroups. Additionally shRNA plasmids have to be tested to gain specific vectors to downregulate EBF1 and OAZ in normal and leukaemic cells. If the activation of aberrant BMP2-signalling in ALL can be verified these would give a link between the characteristic B-cell maturation arrest in ALL and the known ability of OAZ to sequester EBF1 necessary for normal B-cell development. Functional *in-vitro* and *in-vivo* studies with the cloned expression plasmids would be the further experimental approach to proof that abnormal BMP2-signalling in haematopoietic cells could be a so far unknown second hit able to support or initiate leukaemic   transformation.

3 Material and Methods

3.1 Chemicals

Chemicals for standard laboratory procedures were used from Applied Biosystems/Ambion (Austin, USA), Bio-Rad (Hercules, USA), Calbiochem (San Diego, USA), Eurogentec (Cologne, Germany), Fluka (St. Louis, USA), GE Healthcare (Freiburg, Germany), Honywell Riedel-de Haën (Seelze, Germany), Invitrogen (Carlsbad, USA), J.T. Baker (Deventer, Netherlands), Merck (Darmstadt, Germany), Qiagen (Hilden, Germany), Roche (Mannheim, Germany), Roth (Karlsruhe, Germany) and Sigma Aldrich (St. Louis, USA).

3.2 Enzymes

Reagents were used from New England Biolabs (Ipswich, USA), Fermentas (St. Leon-Rot, Germany), Invitrogen (Carlsbad, USA) and Roche (Mannheim, Germany).

3.3 Kits

GFX *Micro* Plasmid Prep Kit	Amersham Biosciences (Freiberg, Germany)
LightCycler FastStart DNA Master	
SYBR Green I Kit	Roche (Mannheim, Germany)
Profection Mammalian Transfection	
System Calcium Phosphate	Promega (Mannheim, Germany)
Qiagen Plasmid Maxi Kit	Qiagen (Hilden, Germany)
Ultrafree-DA DNA Extraction	
from agarose gels	Millipore (Bedford, USA)
QIAquick Gel Extraction Kit	Qiagen (Hilden, Germany)
QIAquick PCR Purification Kit	Qiagen (Hilden, Germany)
BigDye Sequencing Kit	Applied Bios. (Darmstadt, Germany)
EasySep Human CD19 positive	
Selection Kit	StemCell Tech. (Vancouver, Canada
EasySep Human CD34 positive	
Selection Kit	StemCell Tech. (Vancouver, Canada)
Fix&Perm® Cell Permeabilization Kit	ADG (Vienna, Austria)
***DC* Protein Assay**	Bio-Rad (Hercules, USA)

3.4 Biological material

3.4.1 Bacteria

The *E.coli* strain TOP10F' (Invitrogen; Carlsbad, USA) was used for transformation and amplification of plasmid-DNA. The preparation, storage, and growth of chemical competent cells for transformation of plasmids were performed according to well established protocols[134].

3.4.2 Mice strains

Human CD34^{+} cells and samples from patients with ALL were injected intravenously into NOD/*scid* mice for further engraftment and differentiation[135,136].

3.4.3 Cell lines and primary cells

Suspension cells

697	Human B cell precursor leukaemia cell line with human near diploid karyotype; 46(45-48)<2n>XY, t(1;19)(q23;p13), del(6)(q21). DSMZ #ACC 42
CCRF-CEM	Human T cell leukaemia cell line with human near-tetraploid karyotype with extensive subclonal variation; 90(88-101)<4n>XX, -X, -X, +20, +20, t(8;9)(p11;p24)x2, der(9)del(9) (p21-22)del(9)(q11q13-21)x2; sideline with +5, +21, add(13) (q3?3), del(16)(q12). DSMZ #ACC 240
MHH-CALL-2	Human B cell precursor leukaemia cell line with human hyperdiploid karyotype with 13% polyploidy; 52(50-52)<2n>XX, +8, +10, +18, +18, +21, +21; hyperdiploidy with tetrasomy 21 associated with pre B-ALL in children - resembles published karyotype. DSMZ #ACC 341
MHH-CALL-3	Human B cell precursor leukaemia cell line with human pseudodiploid karyotype; 46(45-46)<2n>XX, del(6)(q15), der(9) t(9;9)(p21;q11), der(19) t(1;19) (q23;p13); carries t(1;19) primary and 6q- secondary rearrangements associated with pre B-ALL. DSMZ #ACC 339
Nalm-6	Human B cell precursor leukaemia cell line with human near diploid karyotype; 46(43-47)<2n>XY, t(5;12) (q33.2;p13.2). DSMZ #ACC 128
REH	Human B cell precursor leukaemia cell line with human pseudodiploid karyotype; 46(44-47)<2n>X, -X, +16, del(3) (p22), t(4;12;21;16) (q32;p13; q22;q24.3)-inv(12)(p13q22), t(5;12)(q31-q32;p12), der(16)t(16;21) (q24.3; q22); sideline with inv(5)der(5)(p15q31),+18; carries t(12;21) and del(12) producing TEL-AML1 fusion and deletion of residual TEL. DSMZ #ACC 22

SEM	Human B cell precursor leukaemia cell line with human hypodiploid karyotype with 1.5% polyploidy; 45(40-46)<2n>XX, -13, t(4;11)(q21;q23), del (7)(p14); carries t(4;11) with breakpoints at AF4 and MLL. DSMZ #ACC 546
SUP-B15	Human B cell precursor leukaemia cell line with human pseudodiploid karyotype; 46<2n>XY, der(1)t(1;1)(p11;q31), add(3)(q2?7), der(4) t(1;4) (p11;q35), t(9;22)(q34;q11), add(10) (q25), ?del(14)(q23q31), der(16)t(9;16) (q11;p13). DSMZ #ACC 389

Adherent cells

HEK-293	Human embryonal kidney cell line with human near-triploid karyotype with 6% polyploidy. DSMZ #ACC 305
HEP-G2	Human hepatocellular carcinoma cell line with human hyperdiploid karyotype; 52(47-54)<2n>XY. DSMZ #ACC 180
HCT-116	Human colon carcinoma cell line with human near-diploid karyotype with 3% polyploidy; 45(44-46)<2n>X/XY. DSMZ #ACC 581
hTERT-BMSC	Human telomerase reverse transcriptase (TERT)-immortalised bone marrow mesenchymal cell line with normal human karyotype. Used as a stromal layer to support growth and culture of leukaemic lymphoblasts and normal CD34^{+} haematopoietic cells *in-vitro*[137]
NCI-H1299	Non-small cell lung cancer cell line. ATCC #CRL-5803
Mewo	Human malignant melanoma cell line. ATCC # HTB-65
Phoenix-gp	Derivate of human embryonal kidney cell line 293T with stable expression of *gag* and *pol* gene products. ATCC #3514

Primary cells

Stromal Cells	Adherent mesenchymal cells harvest from human bone marrow
CD19^{+} cells	CD19^{+} cells were isolated from human umbilical cord blood or bone marrow
CD34^{+} cells	CD34^{+} cells were isolated from human umbilical cord blood or bone marrow

3.4.4 Acute Lymphoblastic Leukaemia (ALL) samples

Samples with TEL-AML1 rearrangement

ALL #	Sex	Age	Type	Blasts (BM)	ALL #	Sex	Age	Type	Blasts (BM)
16	male	5 years	Pre-B ALL	94%	83	male	1 year	Pre-B ALL	66%
19	male	4 years	C-ALL	94%	88	female	11 years	C-ALL	100%
26	male	4 years	C-ALL	98%	90	female	4 years	C-ALL	98%
28	female	4 years	C-ALL	90%	109	female	7 years	C-ALL	97%
38	male	8 years	C-ALL	98%	115	female	3 years	C-ALL	99%
40	male	2 years	C-ALL	97%	124	male	6 years	C-ALL	85%
43	male	6 years	C-ALL	99%	131	male	3 years	C-ALL	97%
45	female	2 years	C-ALL	90%	140	female	5 years	C-ALL	99%
47	male	3 years	C-ALL	86%	145	male	4 years	C-ALL	92%
52	female	3 years	C-ALL	95%	147	male	3 years	C-ALL	96%
53	male	2 years	Pre-B ALL	97%	148	female	4 years	C-ALL	95%
57	female	3 years	Pre-B ALL	99%	151	female	1 year	C-ALL	96%
60	male	8 years	Pre-B ALL	92%	154	male	4 years	Pre-B ALL	96%
61	male	5 years	C-ALL	94%	164	male	6 years	C-ALL	98%
72	female	10 years	C-ALL	98%	169	female	4 years	C-ALL	97%
74	male	2 years	C-ALL	99%	192	male	3 years	C-ALL	95%
75	female	3 years	C-ALL	97%	193	male	11 years	C-ALL	86%
79	male	10 years	C-ALL	97%	194	male	1 year	Pre-B ALL	95%
80	male	9 years	C-ALL	98%					

Table 1: Samples from patients with paediatric B-cell precursor ALL with TEL/AML1 rearrangement. Shown above are ALL case number, sex and age of the patients, subtype of ALL and percentage of leukaemic blasts in the bone marrow.

Samples with hyperdiploidy (≥50 chromosomes) and no TEL-AML1 rearrangement

ALL #	Sex	Age	Type	Blasts (BM)	DNA index
6646	male	8 years	C-ALL	93%	1.24 (24% of blasts)
6684	male	3 years	C-ALL	98%	1.2 (85% of blasts)
6718	female	1 year	C-ALL	98%	1.37 (88% of blasts)
6721	male	7 years	C-ALL	84%	1.17 (77% of blasts)
6750	male	8 years	C-ALL	90%	1.25 (88% of blasts)
6772	male	7 years	Pre-B ALL	83%	1.17 (85% of blasts)
6775	female	6 years	?	?	1.18 (80% of blasts)
6801	male	14 years	C-ALL	84%	1.42 (46% of blasts)
6804	male	5 years	C-ALL	95%	1.15 (85% of blasts)
6869	male	3 years	C-ALL	97%	1.18 (90% of blasts)
6898	male	14 years	C-ALL	93%	1.17 (86% of blasts)
6910	female	3 years	?	?	1.22 (90% of blasts)
6921	female	4 years	Pre-B ALL	91%	1.39 (87% of blasts)
6926	female	2 years	C-ALL	97%	1.35 (95% of blasts)
6939	male	4 years	C-ALL	92%	1.18 (86% of blasts)
6963	female	5 years	C-ALL	95%	1.29 (85% of blasts)
7033	male	10 years	C-ALL	91%	1.14 (95% of blasts)
7051	female	1 year	C-ALL	91%	1.2 (85% of blasts)
7128	male	2 years	Pre-B ALL	98%	1.16 (45% of blasts)
7131	female	4 years	C-ALL	87%	1.16 (87% of blasts)
7134	male	6 years	Pre-B ALL	88%	1.12 (86% of blasts)
7138	male	2 years	C-ALL	96%	1.13 (89% of blasts)
7145	male	3 years	Pre-B ALL	91%	1.23 (85% of blasts)
7185	female	3 years	C-ALL	98%	1.25 (80% of blasts)
7196	male	6 years	C-ALL	97%	1.22 (90% of blasts)

Table 2: Samples from patients with paediatric B-cell precursor ALL with hyperdiploid karytopyte and no TEL/AML1 rearrangement. Shown above are ALL case number, sex and age of the patients, subtype of ALL, percentage of leukaemic blasts in the bone marrow and DNA index of blast subpopulations.

Samples with no TEL-AML1 rearrangement or hyperdiploidy (≥50 chromosomes)

ALL #	Sex	Age	Type	Blasts (BM)	ALL #	Sex	Age	Type	Blasts (BM)
6652	female	7 years	Pre-B ALL	?	6933	female	14 years	Pre-B ALL	73%
6658	female	2 years	C-ALL	96%	6943	female	4 years	C-ALL	82%
6662	male	4 years	Pre-B ALL	57%	6956	male	13 years	Pre-B ALL	96%
6698	female	13 years	Pre-B ALL	72%	6984	male	11 years	C-ALL	95%
6705	male	2 years	C-ALL	98%	6986	female	3 years	Pre-B ALL	99%
6725	female	3 years	C-ALL	98%	6991	female	2 years	C-ALL	94%
6778	male	1 week	Pro-B ALL	60%	6993	female	7 years	C-ALL	97%
6787	male	15 years	Pre-B ALL	?	6997	male	2 years	C-ALL	93%
6820	male	11 years	Pre-B ALL	?	7018	male	13 years	Pre-B ALL	85%
6838	female	4 years	C-ALL	93%	7047	female	2 years	C-ALL	93%
6839	female	2 years	C-ALL	?	7065	male	5 years	C-ALL	?
6845	male	9 years	C-ALL	?	7105	male	2 years	Pro-B ALL	?
6903	female	4 years	C-ALL	?	7118	male	1 year	C-ALL	97%
6919	male	13 years	Pre-B ALL	56%	7123	female	1 year	Pro-B ALL	92%
6922	male	1 year	C-ALL	?	7137	female	8 years	Pro-B ALL	98%
6923	male	1 year	Pre-B ALL	89%	7139	female	4 years	C-ALL	95%
6924	male	11 years	C-ALL	91%	7141	male	6 years	Pre-B ALL	96%

Table 3: Samples from patients with paediatric B-cell precursor ALL with neither TEL/AML1 rearrangement nor hyperdiploid karyotype. Shown above are ALL case number, sex and age of the patients, subtype of ALL and percentage of leukaemic blasts in the bone marrow.

3.5 Media

3.5.1 Media for bacterial culture

Growth and expansion of bacteria was performed with Luria-Bertani (LB)-media or -agar. Dissolved media were autoclaved for 20 min at 121℃; agar was cooled at 55℃ before addition of carbenicillin (100 ng/ml) or kanamycin (50 ng/ml) (Roth; Karlsruhe, Germany) for selection and was subsequently plated. Antibiotics were added to the liquid media directly before use.

3.5.2 Cell culture media and reagents

FBS	Fetal bovine serum (Gibco/Invitrogen; Carlsbad, USA)
PBS	Phosphate buffered saline. 200 µg/ml KCl, 136 µg/ml KH_2PO_4, 58 µg/ml NaCl and 268µg/ml Na_2HPO_4*$7xH_2O$ (Gibco/ Invitrogen; Carlsbad, USA)
Penicillin/Streptomycin	10000 u/ml penicillin and 10000 µg/ml streptomycin (Gibco/ Invitrogen; Carlsbad, USA)
Puromycin dihydrochloride	P7255, 25µg (Sigma Aldrich; St. Louis, USA)
L-Glutamine	29.2 mg/ml (Gibco/Invitrogen; Carlsbad, USA)
Trypsin, 0.05%/EDTA	0.5 mg/ml trypsin and 0.2 mg/ml EDTA*4xNa in HBSS (Gibco/ Invitrogen; Carlsbad, USA)

HEPES	1M HEPES (Gibco/Invitrogen; Carlsbad, USA)
Sodium Pyruvate MEM	100 mM (Gibco/Invitrogen; Carlsbad, USA)
D-MEM	Dulbecco's modified Eagle's medium, 4500 µg/ml D-Glucose (Gibco/Invitrogen; Carlsbad, USA)
D-MEM culture medium	DMEM, 10% (v/v) FBS, 2 mM L-Glutamine, 1 mM sodium pyruvate and 10 mM HEPES
RPMI-1640 medium	Roswell Park Memorial Institute medium (Gibco/Invitrogen; Carlsbad, USA)
RPMI-1640 culture medium	RPMI, 10% FBS (v/v), 2 mM L-Glutamine and 1% penicillin-streptomycin
RPMI-1640 selection medium	RPMI, 10% FBS (v/v), 2 mM L-Glutamine, 1% penicillin-streptomycin and 1 µg/ml puromycin dihydrochloride
McCoy's 5A medium	Gibco/Invitrogen (Carlsbad, USA)
McCoy's 5A culture medium	80% McCoy's 5A + 20% FBS (v/v), 2 mM L-Glutamine and 1% penicillin-streptomycin
Biocoll seperating solution	1,077 g/ml, 10 mM HEPES (Biochrom; Berlin, Germany)
Freezing medium	90% FBS and 10% DMSO
SFEM	Serum free expansion medium (CellSystems; St. Katharinen, Germany)
HBSS	Gibco/Invitrogen (Carlsbad, USA)
Polybrene	8 µg/ml
Chloroquine	1000x
Retronectin	Human fibronectin fragment, T100B 25 mg (TaKaRa; Saint-Germain-en-Laye, France)
hFLT3-L	Human FLT3 Ligand (CellSystems; St. Katharinen, Germany)
hSCF	Human stem cell factor (CellSystems; St. Katharinen, Germany)
hTPO	Human thrombopoietin (CellSystems; St. Katharinen, Germany)
hIL-6	Human interleukin 6 (CellSystems; St. Katharinen, Germany)
hIL-7	Human interleukin 7 (CellSystems; St. Katharinen, Germany)
CD34$^+$ expansion medium	SFEM, 2% L-Glutamine, 2% penicillin/streptomycin, 100 ng/ml hFLT3-L, 100 ng/ml hSCF, 20 ng/ml hTPO and 20 ng/ml hIL-6
B-cell differentiation medium	SFEM, 2% L-Glutamine, 2% penicillin/streptomycin, 10 ng/ml hFLT3-L,100 ng/ml hSCF and 20 ng/ml hIL-7

3.6 Buffer and solutions

10x TBS	1.5 M NaCl and 0.5 M Tris (pH 7.3-7.4)
1x TBST	1x TBS, 0.05% Tween-20
TE buffer	10 mM Tris/HCl (pH 8.0), 0.1 mM EDTA (pH 8.0)
Modified TAE buffer	50x buffer diluted to 1x with ddH$_2$O (Millipore; Bedford, USA)

3.7 Oligonucleotides

Primer	Application	Binding to	Sequence 5'-3'
BMP2.1/full fw	Amplification of hBMP2 CDS	NM_001200	acc atg gtg gcc ggg acc cgc tgt c
BMP2.1/full HA rev	Amplification of hBMP2 CDS and addition of a c-terminal HA-TAG	NM_001200	cta agc gta gtc tgg gac gtc gta tgg gta gcg aca ccc aca acc ctc cac aac c
BMP2/807 fw	Sequencing of hBMP2 CDS	NM_001200	ctt cta gcg ttg ctg ctt cc
BMP2/1025 fw	Sequencing of hBMP2 CDS	NM_001200	aga cct gta tcg cag gca ct
BMP2/1222 fw	Sequencing of hBMP2 CDS	NM_001200	cct cag cag agc ttc agg tt
BMP2/1355 fw	Sequencing of hBMP2 CDS	NM_001200	act ttt gga cac cag gtt gg
BMP2/1631 fw	Sequencing of hBMP2 CDS	NM_001200	tca agc caa aca caa aca gc
BMP2/1945 fw	Sequencing of hBMP2 CDS	NM_001200	aca tgg ttt tgg agg gtt gt
BMP2/2242 fw	Sequencing of hBMP2 CDS	NM_001200	caa ccc cag cac atg aag ta
EBF.2/CDS fw	Amplification of hEBF1 CDS	NM_024007	ggg gga gga gat ttt cca caa gaa aag g
EBF.2/CDS rev	Amplification of hEBF1 CDS	NM_024007	cct gca ctt gca gat ccc tct tcc a
EBF/383 fw	Sequencing of hEBF1 CDS	NM_024007	aca gca atg gga taa gga cgg a
EBF/793 fw	Sequencing of hEBF1 CDS	NM_024007	acg ccc tct tat ctg gaa cat g
EBF/1200 fw	Sequencing of hEBF1 CDS	NM_024007	act gta tgg gat gcc aca caa c
EBF/1580 fw	Sequencing of hEBF1 CDS	NM_024007	atg cca tag tgc cat cca gcc
OAZ.2/CDS Flag fw	Amplification of hOAZ CDS and addition of a n-terminal Flag-TAG	NM_015069	acc atg *gac tac aag gac gac gat gac aag* cat aag aag agg gtt gaa gag ggg gag gcc tc
OAZ.1/CDS rev	Amplification of hOAZ CDS	NM_015069	tca ctg tgc gtg ctg gct cat c
OAZ/317 fw	Sequencing of hOAZ CDS	NM_015069	ctc cct cca gca agg atg tt
OAZ/664 fw	Sequencing of hOAZ CDS	NM_015069	ttc aag tgc act gtg tgc aag c
OAZ/1009 fw	Sequencing of hOAZ CDS	NM_015069	ggt gtc tac tgc cac ctg g
OAZ/1351 fw	Sequencing of hOAZ CDS	NM_015069	ccc acc ctc tac aac ctc aa
OAZ/1719 fw	Sequencing of hOAZ CDS	NM_015069	ctt tgg ctc cat cct gaa act c
OAZ/2092 fw	Sequencing of hOAZ CDS	NM_015069	gac aag caa ttt tcc tcg gtg g
OAZ/2426 fw	Sequencing of hOAZ CDS	NM_015069	gta agt tct gca gca ggg cc
OAZ/2807 fw	Sequencing of hOAZ CDS	NM_015069	cac gga ctt tct tct cgg ag
OAZ/3172 fw	Sequencing of hOAZ CDS	NM_015069	cag ggg ctg cag agc tc
OAZ/3544 fw	Sequencing of hOAZ CDS	NM_015069	gag atc caa atc cac gtt gcc
Smad1/181 fw	Sequencing of hSmad1 CDS	NM_005900	ccg agt aac tgt gtc acc att c
Smad1/481 fw	Sequencing of hSmad1 CDS	NM_005900	caa aat gag cct cac atg cca c
Smad1/781 fw	Sequencing of hSmad1 CDS	NM_005900	cag gcg gtt gct tat gag gaa
Smad1/1083 fw	Sequencing of hSmad1 CDS	NM_005900	cta cca tca tgg att tca tcc tac
Smad4/241 fw	Sequencing of hSmad4 CDS	NM_005359	agg ctt cag gtg gct ggt c
Smad4/541 fw	Sequencing of hSmad4 CDS	NM_005359	acc atc agc atc cca cca agt a
Smad4/841 fw	Sequencing of hSmad4 CDS	NM_005359	cct cac cac caa aac ggc cat
Smad4/1141 fw	Sequencing of hSmad4 CDS	NM_005359	ttg cac ata ggc aaa ggt gtg c
Smad4/1441 fw	Sequencing of hSmad4 CDS	NM_005359	gct atc agt ctg tca gct gct
Smad5/181 fw	Sequencing of hSmad5 CDS	NM_005903	ccg agt aac tgt gtc acc att c
Smad5/481 fw	Sequencing of hSmad5 CDS	NM_005903	caa aat gag cct cac atg cca c
Smad5/781 fw	Sequencing of hSmad5 CDS	NM_005903	cag gcg gtt gct tat gag gaa
Smad5/1077 fw	Sequencing of hSmad5 CDS	NM_005903	ctg caa cta cca tca tgg att tca t
T7	Sequencing of cloned inserts in pcDNA3.1(+) MCS		taa tac gac tca cta tag gg
BGH	Sequencing of cloned inserts in		tag aag gca cag tcg agg

	pcDNA3.1(+) MCS		
R1331 fw	Sequencing of cloned inserts in R1331-pRmys-iV MCS		cct tca aag tag acg gca tc
R1331 rev	Sequencing of cloned inserts in R1331-pRmys-iV MCS		ggc ctt att cca agc ggc tt
pLKO.1 fw	Sequencing of shRNA sequence in pLKO.1-puro		ttc ttg ggt agt ttg cag ttt t
M13 Forward (-20)	Sequencing of cloned inserts in pCR2.1-TOPO, pCR4-TOPO and pCR-XL-TOPO		gta aaa cga cgg cca g
M13 Reverse	Sequencing of cloned inserts in pCR2.1-TOPO, pCR4-TOPO and pCR-XL-TOPO		cag gaa aca gct atg ac
B2M.1 q-RT fw	real time PCR of hB2M CDS	NM_004048	ttc tgg cct gga ggc tat c
B2M.1 q-RT rev	real time PCR of hB2M CDS	NM_004048	tca gga aat ttg act ttc cat tc
BMP2.1 q-RT fw	real time PCR of hBMP2 CDS	NM_001200	tca agc caa aca caa aca gc
BMP2.1 q-RT rev	real time PCR of hBMP2 CDS	NM_001200	agc cac aat cca gtc att cc
BMP4.1 q-RT fw	real time PCR of hBMP4 CDS	NM_001202	tcc aca gca ctg gtc ttg ag
BMP4.1 q-RT rev	real time PCR of hBMP4 CDS	NM_001202	ctg gga tgt tct cca gat gtt
BMPRIa.1 q-RT fw	real time PCR of hBMPRIa CDS	NM_004329	gga cga aag cct gaa caa aa
BMPRIa.1 q-RT rev	real time PCR of hBMPRIa CDS	NM_004329	gca att ggt att ctt cca cga
BMPRII.1 q-RT fw	real time PCR of hBMPRII CDS	NM_001204	gcc cag ggg agg aag ata
BMPRII.1 q-RT rev	real time PCR of hBMPRII CDS	NM_001204	tgg tgc cat ata tct gat agt gc
EBF.1 q-RT fw	real time PCR of hTIEG2 CDS	NM_024007	agc tgc caa ctc ccc cta t
EBF.1 q-RT rev	real time PCR of hTIEG2 CDS	NM_024007	ggg agg ctt gtg gag gag
OAZ1.2 q-RT fw	real time PCR of hOAZ CDS	NM_015069	gtg gac cac cgt gac ctc
OAZ1.2 q-RT rev	real time PCR of hOAZ CDS	NM_015069	gat gca ctg gta tgt ctt ttt cc
SMAD1.1 q-RT fw	real time PCR of hSmad1 CDS	NM_005900	tgt gta cta tac gta tga gct ttg tga
SMAD1.1 q-RT rev	real time PCR of hSmad1 CDS	NM_005900	taa cat cct ggc ggt ggt a
SMAD4.2 q-RT fw	real time PCR of hSmad4 CDS	NM_005359	cct gtt cac aat gag ctt gc
SMAD4.2 q-RT rev	real time PCR of hSmad4 CDS	NM_005359	gca atg gaa cac caa tac tca g
SMAD5.1 q-RT fw	real time PCR of hSmad5 CDS	NM_005903	gga cca gga agt cca ttt ca
SMAD5.1 q-RT rev	real time PCR of hSmad5 CDS	NM_005903	agg tgg cat ata ggc agg ag
TIEG2.1 q-RT fw	real time PCR of hTIEG2 CDS	NM_003597	ctt cca ttc ttt atc gac tct gtg
TIEG2.1 q-RT rev	real time PCR of hTIEG2 CDS	NM_003597	gat ggc tcc acg aga tca g
TGIF.1 q-RT fw	real time PCR of hTGIF CDS	NM_170695	tcc aga atg aaa ggc aag aaa
TGIF.1 q-RT rev	real time PCR of hTGIF CDS	NM_170695	aga aag gtc aaa ggg aat gtc
DNTT q-RT fw	real time PCR of hDNTT CDS	NM_004088.3	tac gag cg tcg tgc ctt t
DNTT q-RT rev	real time PCR of hDNTT CDS	NM_004088.3	ata gcg ccg gag gtc tct
RAG1 q-RT fw	real time PCR of hRAG1 CDS	NM_000448.1	aat atc aac caa att gca gac atc
RAG1 q-RT rev	real time PCR of hRAG1 CDS	NM_000448.1	gcc atg ctg gct gag gta
CD79a q-RT fw	real time PCR of hCD79a CDS	NM_001783.3	caa gaa ccg aat cat cac agc
CD79a q-RT rev	real time PCR of hCD79a CDS	NM_001783.3	cgt tct gcc atc gtt tcc
CD79b q-RT fw	real time PCR of hCD79b CDS	NM_000626.2	ttg ctg ctg ctg ctc tca
CD79b q-RT rev	real time PCR of hCD79b CDS	NM_000626.2	cgc gaa caa gca cta cct tt
PAX5 q-RT fw	real time PCR of hPAX5 CDS	NM_016734.1	acg ctg aca ggg atg gtg
PAX5 q-RT rev	real time PCR of hPAX5 CDS	NM_016734.1	cct cca gga gtc gtt gta cg
IL7R q-RT fw	real time PCR of hIL7R CDS	NM_002185.2	gct ttt gag gac cca gat gt
IL7R q-RT rev	real time PCR of hIL7R CDS	NM_002185.2	agg cac ttt acc tcc acg ag
Spi1 q-RT fw	real time PCR of hSpi1 CDS	NM_001080547.1	cag ggg atc tga ccg act c
Spi1 q-RT fw	real time PCR of hSpi1 CDS	NM_001080547.1	agg tct tct gat ggc tga gg
E2A q-RT fw	real time PCR of hE2A CDS	NM_003200.1	ccc aga cca aac tgc tca tc
E2A q-RT rev	real time PCR of hE2A CDS	NM_003200.1	ctg ctt tgg gat tca ggt tc
VpreB q-RT fw	real time PCR of hVpreB CDS	NM_007128.2	cat gct gtt tgt cta ctg cac a
VpreB q-RT rev	real time PCR of hVpreB CDS	NM_007128.2	gcg gat tgt ggt tcc aag
IGLL1 q-RT fw	real time PCR of hIGLL1 CDS	NM_020070.2	tgg tgt gtc tca tga atg act tt
IGLL1 q-RT rev	real time PCR of hIGLL1 CDS	NM_020070.2	ggt gat ggg ggt acc atc t

Table 4: The used oligonucleotides are shown with their name, kind of application, specific binding locus (NM numbers from NCBI database), and sequence (5'-3')

3.8 Plasmids and retroviral vectors

3.8.1 Plasmids for subcloning of PCR-products

pCR2.1-TOPO +   TA-cloning plasmids for Taq-amplified PCR fragments. Designed for
pCR4-TOPO   further subcloning in an expression plasmid; with amp and kan
resistance (Invitrogen; Carlsbad, USA).

pCR-XL-TOPO   TA-cloning plasmid for Taq-amplified PCR fragments of 3-10 kb length.
Designed for further subcloning in an expression plasmid; with kan and
zeo resistance (Invitrogen; Carlsbad, USA).

3.8.2 Cloned plasmids for further subcloning

pCR2.1-TOPO-   pCR2.1-TOPO with cDNA CDS of hEBF1 (NCBI, NM_024007).
HsEBF1(wt)

pCR4-TOPO-   pCR4-TOPO with cDNA CDS of hBMP2 (NCBI, NM_001200) and HA-
HsBMP2(wt)HA   TAG (c-terminal).

pCR-XL-TOPO-   pCR-XL-TOPO with cDNA CDS of hOAZ (NCBI, NM_015069) and Flag-
FlagHsOAZ(wt)   TAG (n-terminal).

3.8.3 Expression plasmids

pcDNA3.1(+)   Designed for high-level stable and transient expression in mammalian
hosts; with amp and neo resistance (Invitrogen; Carlsbad, USA).

-HsBMP2(wt)HA   pcDNA3.1(+) with cDNA CDS of hBMP2 (NCBI, NM_001200) and HA-
TAG (c-terminal).

-HsEBF1(wt)   pcDNA3.1(+) with cDNA CDS of hEBF1 (NCBI, NM_024007).

-FlagHsOAZ(wt)   pcDNA3.1(+) with cDNA CDS of hOAZ (NCBI, NM_015069) and Flag-
TAG (n-terminal).

-FlagHsSmad1   pcDNA3.1(+) with cDNA CDS of hSmad1 (NCBI, NM_005900) and Flag-
(wt)   TAG (n-terminal).

-FlagHsSmad4   pcDNA3.1(+) with cDNA CDS of hSmad4 (NCBI, NM_005359) and Flag-
(wt)   TAG (n-terminal).

-FlagMmSmad5   pcDNA3.1(+) with cDNA CDS of mSmad5 (NCBI, NM_008541) and
(wt)   Flag-TAG (n-terminal).

pEGFP-C2   eGFP expression vector with CMV promoter and kan resistance.
Subcloning in MCS results in eGFP fusion proteins (Clontech; St-
Germain-en-Laye, France).

3.8.4 Retroviral vectors

3.8.4.1 Lentiviral plasmids

Packaging plasmids for virus production

pMDLg-pRRE (#583)   Packaging plasmid for production of lentiviral particles with amp resistance. pHIV-1 GAG/POL[138].

pRSV-Rev (#584)   Packaging plasmid for production of lentiviral particles with amp resistance. pRev[138].

phCMV-RD114/ TR (#652)   Packaging plasmid for production of lentiviral particles with amp resistance. RD114 virus envelope glycoprotein (RD114 GP) was further modified to express the RD114/TR chimeric glycoprotein carrying the MLV-A GP cytoplasmic tail (TR)[139,140].

Lentiviral constructs

pLKO.1-puro   Empty lentiviral shRNA expression vector[141] for transient or stable transfection of mammalian cells and production of lentiviral particles. Stable integration is selected using the puromycin selectable marker while self-inactivating replication incompetent viral particles can be produced in packaging cells (Phoenix-gp) e.g.) by co-transfection with compatible packaging plasmids[142].

-shRNA-SCR- puro/YFP   Scrambled shRNA vectors serving as controls for unspecific effects of shRNA transfection or transduction on gene expression (The RNAi Consortium, TRC). Selection via puromycin resistance or YFP expression respectively.

-HsEBF1(30/31)- puro/YFP   Vectors to downregulate hEBF1 (NCBI, NM_024007) with shRNA targeting CDS of EBF1 mRNA (The RNAi Consortium, TRC). Selection via puromycin resistance or YFP expression respectively.

-HsOAZ(76/77)- puro/YFP   Vectors to downregulate hOAZ (NCBI, NM_015069) with shRNA targeting CDS of OAZ mRNA (The RNAi Consortium, TRC). Selection via puromycin resistance or YFP expression respectively.

3.8.4.2 *γ*-retroviral plasmids

Packaging plasmids for virus production

pSV40-gag/pol (R690)   Packaging plasmid for production of *γ*-retroviral particles with amp resistance. MoMLV *gag*- and *pol*-genes under control of the SV40

promoter (kindly provided by Stocking C.).

phCMV-RD114 (R916)   Packaging plasmid for production of *γ*-retroviral particles with amp resistance. RD114 virus envelope glycoprotein (kindly provided by Stocking C.).

γ-retroviral constructs

R1331-pRMys   Expression vector for production of *γ*-retroviral particles with amp resistance. Self-inactivating replication incompetent viral particles can be produced in packaging cells (Phoenix-gp e.g.) by co-transfection with compatible packaging plasmids. Positive cells with integrated vector can be selected via Venus (improved YFP)[143] expression (kindly provided by Stocking C.)[144].

-HsEBF1(wt)   R1331-pRMys-iV with cDNA CDS of hEBF1 (NCBI, NM_024007).

-FlagHsOAZ(wt)   R1331-pRMys-iV with cDNA CDS of hOAZ (NCBI, NM_015069) and Flag-TAG (n-terminal).

3.9 Antibodies

3.9.1 Primary Antibodies

anti-BMP2   Mouse monoclonal (IgG2b) antibody binding to human BMP2. Alpha Diagnoistic (San Antonio, USA) #BMP21-M (used 1:1000).

anti-Smad1   Mouse monoclonal (IgG1) antibody binding to human Smad1. Santa Cruz Biotechnology (Santa Cruz, USA) #sc-7965, clone A-4 (used 1:1000).

anti-pSmad1   Rabbit polyclonal (IgG) antibody binding to human phospho-Smad1 (Ser463/465). Millipore (Bedford, USA) #06-702 (used 1:500).

anti-EBF1   Mouse monoclonal (IgG1) antibody binding to human EBF1. Abnova (Taipei City, Taiwan) # H00001879-M01, clone 1C12 (used 1:1000).

anti-EBF1   Goat polyclonal (IgG) antibody binding to human EBF1. Santa Cruz Biotechnology (Santa Cruz, USA) #sc-15888, clone C-20 (used 1:1000).

anti-OAZ   Goat polyclonal (IgG) antibody binding to human OAZ, Santa Cruz Biotechnology (Santa Cruz, USA) #sc-10488, clone E-20 (used 1:1000).

anti-OAZ   Rabbit polyclonal (IgG) antibody binding to human OAZ, Santa Cruz Biotechnology (Santa Cruz, USA) #sc-48785, clone H-105 (used 1:1000).

anti-Actin   Mouse monoclonal (IgG2a) antibody binding to human Actin. Sigma

Aldrich (St. Louis, USA) #A5316 (used 1:5000).

anti-Flag   Mouse monoclonal (IgG2a) antibody binding to the FLAG®-epitope. Sigma Aldrich (St. Louis, USA) #F1804, clone M2 (used 1:3000).

3.9.2 Secondary Antibodies

Donkey anti-mouse (PE)   Donkey polyclonal antibody binding to mouse IgG (H+L), conjugated with R-phycoerythrin (PE). Beckman Coulter (Krefeld, Germany) #732970 (20 µl of a 1:20 dilution per reaction).

Rabbit anti-goat (FITC)   Rabbit polyclonal antibody binding to goat IgG (H+L), conjugated with fluorescein isothiocyanate (FITC). Beckman Coulter (Krefeld, Germany) #732914 (20 µl of a 1:20 dilution per reaction).

Goat anti-mouse (HRP)   Goat polyclonal antibody binding to mouse IgG conjugated with horseradish peroxidase (HRP). Dako Cytomation (Hamburg, Germany) #P0447 (1:5000).

Goat anti-rabbit (HRP)   Goat polyclonal antibody binding to rabbit IgG conjugated with horseradish peroxidase (HRP). Dako Cytomation (Hamburg, Germany) #P0448 (1:5000).

Rabbit anti-goat (HRP)   Rabbit polyclonal antibody binding to goat IgG conjugated with horseradish peroxidase (HRP). Dako Cytomation (Hamburg, Germany) #P0449 (1:5000).

3.9.3 FACS Antibodies

anti-CD10 (PE)   Mouse monoclonal (IgG1, κ) antibody binding to human CD10 conjugated with R-phycoerythrin (PE). Biolegend (San Diego, USA) #309904, clone ME-78.

anti-CD10 (PE-Cy7)   Mouse monoclonal (IgG1, κ) antibody binding to human CD10 conjugated with R-phycoerythrin-Cy7 (PE-Cy7). BD Biosciences (Heidelberg, Germany) #341112, clone HI10a.

anti-CD19 (APC)   Mouse monoclonal (IgG1, κ) antibody binding to human CD19 conjugated with allophycocyanin (APC). Beckman Coulter (Krefeld, Germany) #IM2470, clone J4.119.

anti-CD19 (PerCP-Cy5.5)   Mouse monoclonal (IgG1, κ) antibody binding to human CD19 conjugated with peridinin chlorophyll protein-Cy5.5 (PerCP-Cy5.5). BD Biosciences (Heidelberg, Germany) #332780, clone SJ25C1.

anti-CD34   Mouse monoclonal (IgG1) antibody binding to human CD34 conjugated

(FITC)	with fluorescein iso-thiocyanate (FITC). Beckman Coulter (Krefeld, Germany) #IM1870, clone 581.
anti-CD38 (APC)	Mouse monoclonal (IgG1, *κ*) antibody binding to human CD38 conjugated with allophycocyanin (APC). BD Biosciences (Heidelberg, Germany) #345807, clone HB7.
anti-CD38 (PC5)	Mouse monoclonal (IgG1) antibody binding to human CD38 conjugated with R-phycoerythrin-Cy5.1 (PC5). Beckman Coulter (Krefeld, Germany) #A07780, clone LS198-4-3.
anti-CD45 (APC-H7)	Mouse monoclonal (IgG1, *κ*) antibody binding to human CD45 conjugated with allophycocyanin-H7 (APC-H7). BD Biosciences Pharmingen (Heidelberg, Germany) #560178, clone 2D1.
anti-IgM (APC)	Mouse monoclonal (IgG1, *κ*) antibody binding to human IgM conjugated with allophycocyanin (APC). BD Biosciences Pharmingen (Heidelberg, Germany) #551062, clone G20-127.

3.10 Instrumentation

Equipment important for the analysis of samples and generation of data is mentioned.only Other laboratory equipment meets today's usual lab-standards and is not cited separately.

Flow cytometer	BD FACS Canto Flow Cytometer with FACS Diva Software (Becton Dickinson; Heidelberg, Germany)
Flow cytometer	BD FACS Aria Flow Cytometer with function for sorting of cells; FACS Diva Software (Becton Dickinson; Heidelberg, Germany)
Real Time PCR machine	LightCycler® 480 System with LightCycler® software version 1.2.0.0625 (Roche; Mannheim, Germany)

3.11 Nucleic Acid–Based Methods

3.11.1 DNA isolation and analysis

TE served as a standard buffer in which dissolved DNA is protected against degradation through DNases and can be stably stored at 4℃ for short-term or at -20℃ for long-term.

Preparation of plasmid DNA

In general it can be discriminated between mini- and maxi-preparations when plasmid-DNA is isolated from bacteria. Finally just the amount of used bacteria is relevant; the mechanisms of action are practically identical. For Plasmid preparations of 1-2 ml of culture the Plasmid

Mini preparation method and for 100 ml (high copy plasmids) to 500 ml (low copy plasmids) of culture the Plasmid Maxi preparation method were used.

Plasmid Mini preparation (GFX *Micro* Plasmid Prep Kit)

Solution I	100mM Tris-HCl (pH 7.5), 10mM EDTA and 400 µg/ml RNase I
Solution II	1M NaOH, 5.3% (w/v) SDS, before use diluted with 65ml ddH$_2$O
Solution III	Buffered solution containing acetate and chaotrope
Wash buffer	Tris-EDTA buffer, before use 100ml EtOH abs. is added
GFX columns	MicroSpin^{TM} columns pre-packed with a glass fibre matrix
Collection tubes	2 ml capless microcentrifuge tubes
Heraeus Biofuge pico	Thermo Fisher Scientific (Waltham, USA)

1-1.5 ml of bacterial culture was harvested, plasmid DNA isolated according to the manufacturers manual and finally eluted from the columns by addition of usually 100 µl TE-buffer or ddH$_2$O

Plasmid maxi preparation (Qiagen Plasmid Maxi Kit)

Buffer P1 [resuspension buffer]	50 mM Tris-HCl (pH 8) 10 mM EDTA, 100 µg/ml RNase
Buffer P2 [lysis buffer]	200 mM NaOH, 1% SDS (w/v)
Buffer P3 [neutralization buffer]	3 M KAc, pH 5.5
Buffer QBT [equilibration buffer]	750 mM NaCl, 50 mM MOPS (pH 7), 15% isopropanol (v/v), 0.15% Triton X-100 (v/v)
Buffer QC [wash buffer]	1 M NaCl, 50 mM MOPS (pH 7), 15% isopropanol (v/v)
Buffer QF [elution buffer]	1.25 M NaCl, 50 mM Tris-HCl (pH 8.5), 15% isopropanol (v/v)

Qiagen-tip 500

50 ml centrifugation tubes

Fluted Filter (S+S, 185mm)

Isopropanol

70% ethanol

Heraeus Multifuge 3S-R	Thermo Fisher Scientific (Waltham, USA)

100-500 ml of bacterial culture was harvested, plasmid DNA isolated according to the manufacturers manual and the DNA-pellet was finally dissolved by addition of usually 300 µl TE-buffer or ddH$_2$O.

3.11.2 RNA Isolation

TRIzol® Reagent   Invitrogen (Carlsbad, USA)
Chloroform
Isopropanol
75% ethanol (in DEPC-treated water)
RNase-free water
1.5 m reaction tubes
Eppendorf 5810R centrifuge   Eppendorf (Wesseling-Berzdorf, Germany)

To isolate RNA, fresh or cryopreserved material (cell lines, leukaemic samples, primary cells or cells from mice organs) was used. $5\text{-}10\text{x}10^6$ cells in a 1.5 ml reaction tube were mixed and resuspended in 1 ml Trizol, a monophasic solution of phenol and guanidine isothiocyanate. For cell numbers $\leq 5\text{x}10^5$, only 200μ Trizol was used and the volumes of the other reagents were adjusted. The homogenised samples were lysed for 5-10 min at RT. After lysis 200μl chloroform was added, the samples mixed well, incubated for 2-3 min at RT and centrifuged with 11500 rpm (15 min, 4°C). The addition of chlor oform and the subsequent centrifugation step led to a separation of the solution in an aqueous (RNA phase) and an organic phase. The aqueous (upper) phase was transferred to a new 1.5 ml reaction tube and the pellet (interphase with proteins and DNA, lower phase with DNA only) was discarded. The aqueous phase was mixed with 1 volume isopropanol to precipitate the RNA and was incubated at -20°C for at least 15 min and was subsequently cent rifuged with 13000 rpm (15 min, 4°C). The supernatant was discarded; the RNA pellet mixed with 1 ml of 75% ethanol and was centrifuged with 13000 rpm (5 min, 4°C). The supern atant was discarded again and the RNA pellet was air-dried for 5-10 min. The pellet was usually resuspended in 25-50 μl RNase-free water; RNA was stored at -80°C.

3.11.3 cDNA synthesis

Oligo p(dT)15 primers   40μg, dissolved in 80μl ddH$_2$O (Roche; Mannheim, Germany)
dNTP-Mix (10mM each)
ddH$_2$O
5x First-Strand Buffer   Invitrogen (Carlsbad, USA)
0,1M DTT   Invitrogen (Carlsbad, USA)
SuperScript II Reverse Transcriptase   Invitrogen (Carlsbad, USA)

To transcribe RNA into cDNA, isolated RNA-transcripts (0.5-1 µg) were used in a reverse transcription reaction. The First Strand cDNA synthesis was performed with SuperScript II RT and Oligo p(dT)15 primers following the First-Strand cDNA Synthesis Using SuperScript™ II RT manual from Invitrogen (Carlsbad, USA).

3.11.4 PCR and Sequencing

3.11.4.1 PCR

Polymerase chain reactions (PCRs) were performed according to standard protocols[145].

3.11.4.2 Sequencing

Plasmid DNA or PCR products were sequenced according to the didesoxy-chain-termination method following Sanger[146] with the commercial BigDye® Terminator v1.1 Cycle System (Amersham Biosystems; Foster City, USA).

Reaction for sequencing:

Plasmid DNA (150-300 ng) or PCR product (10-50 ng)	4 µl
Buffer HT	3 µl
Big Dye® (v1.1)	1 µl
Primer for sequencing (15 pmol)	1.5 µl
ddH$_2$O	10.5 µl
Reaction mix	20 µl

The sequencing-reactions were incubated in a 96-well plate thermocycler according to following sequencing program.

Sequencing program:

Temperature	time	cycles
60°C	break	1x
95°C	5 min	1x
95°C	30 s	
x°C, x= Primer annealing temp.	30 s	50x
60°C	4 min	
10°C	break	1x

After the thermocycling 4 µl of the sequencing reactions were diluted with 16 µl ddH$_2$O and were analysed in the sequencing facility of the Klinik und Poliklinik für Pädiatrische Hämatologie und Onkologie (Universitätsklinikum Eppendorf; Hamburg, Germany).

3.11.5 Cloning of DNA

Plasmid DNA was sequenced with specific primers (3.7), received sequences were analysed with the Lasergene Suite (DNASTAR, Inc.; Madison, USA) and compared with the wild-type sequences for mutations.

3.11.5.1 Cloning of *Taq*-amplified PCR products

TOPO® TA Cloning Kit
(with pCR2.1-TOPO or pCR4-TOPO)   Invitrogen (Carlsbad, USA)
TOPO® XL PCR Cloning Kit
(with pCR-XL-TOPO)   Invitrogen (Carlsbad, USA)

The cloning of PCR products, amplified with the Expand High Fidelity PCR System (Roche; Mannheim, Germany), was performed with commercial TA Cloning Kits from Invitrogen (Carlsbad, USA) according to the manufacturer's manuals. PCR products generated with *Taq* polymerase have single deoxyadenosine (A) overhangs at the 3' end making it possible to ligate them easily and efficiently with the single deoxythymidine (T) overhangs at the 5' end of the linearised TOPO vectors.

Cloning of hBMP2 CDS

The hBMP2 CDS was amplified with specific primers (3.7) using cDNA of the cell line REH generating a c-terminal HA-TAG. The purified PCR product was ligated in the pCR4-TOPO vector and the isolated plasmid DNA was digested with *EcoRI*, to check for insert size. Insert containing plasmids were sequenced with BMP2 sequencing primers (3.7).

Cloning of hEBF1 CDS

The hEBF1 CDS was amplified with specific primers (3.7) using cDNA of the cell line 697. The purified PCR product was ligated in the pCR2.1-TOPO vector and the isolated plasmid DNA was digested with *HindIII* and *NotI* or *EcoRI* alone, to check for insert size. Insert containing plasmids were sequenced with EBF1 sequencing primers (3.7).

Cloning of hOAZ CDS

The hOAZ CDS was amplified with specific primers (3.7) using cDNA of the cell line REH thereby generating an n-terminal FLAG-TAG. The purified PCR product was ligated in the pCR-XL-TOPO vector and the isolated plasmid DNA was digested with *EcoRI*, to check for insert size. Insert containing plasmids were sequenced with OAZ sequencing primers (3.7).

3.11.5.2 Subcloning into pcDNA3.1(+) expression plasmid

Subcloning of hBMP2 into pcDNA3.1(+)

The plasmid pCR4-TOPO-HsBMP2(wt)HA was digested with *EcoRI* resulting in two fragments with 1239 bp and 3938 bp length. The 1239 bp fragment was subsequently cloned in the plasmid pcDNA3.1(+) (Invitrogen; Carlsbad, USA) linearised with *EcoRI*.

Subcloning of hEBF1 into pcDNA3.1(+)

The plasmid pCR2.1-TOPO-HsEBF1(wt) was digested with *BamHI* and *XhoI* resulting in two fragments with 2088 bp and 3849 bp length. The 2088 bp fragment was subsequently cloned in the plasmid pcDNA3.1(+) (Invitrogen; Carlsbad, USA) linearised with *BamHI* and *XhoI*.

Subcloning of hOAZ into pcDNA3.1(+)

The plasmid pCR-XL-TOPO-FlagHsOAZ(wt) was digested with *EcoRI* and *DraI* resulting in three fragments with 1205 bp, 2296 bp and 3901 bp length. The 3901 bp fragment was subsequently cloned in the plasmid pcDNA3.1(+) (Invitrogen; Carlsbad, USA) linearised with *EcoRI*.

Subcloning of hSmad1 into pcDNA3.1(+)

The plasmid pBabe-puro4-FlagHsSmad1(wt) was digested with *BamHI* and *XhoI* resulting in two fragments with 1455 bp and 5160 bp length. The 1455 bp fragment was subsequently cloned in the plasmid pcDNA3.1(+) (Invitrogen; Carlsbad, USA) linearised with *BamHI* and *XhoI*.

Subcloning of hSmad4 into pcDNA3.1(+)

The plasmid pBabe-puro4-FlagHsSmad4(wt) was digested with *BamHI* and *XhoI* resulting in two fragments with 1701 bp and 5160 bp length. The 1701 bp fragment was subsequently cloned in the plasmid pcDNA3.1(+) (Invitrogen; Carlsbad, USA) linearised with *BamHI* and *XhoI*.

Subcloning of mSmad5 into pcDNA3.1(+)

The plasmid pBabe-puro4-FlagMmSmad5(wt) was digested with *BamHI* and *XhoI* resulting in two fragments with 1517 bp and 5160 bp length. The 1517 bp fragment was subsequently cloned in the plasmid pcDNA3.1(+) (Invitrogen; Carlsbad, USA) linearised with *BamHI* and *XhoI*.

3.11.5.3　Subcloning into R1331-pRMys-iV *γ*-retroviral vector

Subcloning of hEBF1 into R1331-pRMys-iV

The plasmid pCR2.1-TOPO-HsEBF1(wt) was digested with *BamHI* and *XhoI* resulting in two fragments with 2088 bp and 3849 bp length. The 2088 bp fragment was subsequently cloned in the plasmid R1331- pRMys-iV linearised with BamHI and XhoI

Subcloning of hOAZ into R1331-pRMys-iV

The plasmid pCR-XL-TOPO-FlagHsOAZ(wt) was digested with EcoRI and DraI resulting in three fragments with 1205 bp, 2296 bp and 3901 bp length. The 3901 bp fragment was subsequently cloned in the plasmid R1331- pRMys-iV linearised with EcoRI

3.11.5.4　Insertion of YFP into pLKO.1-puro vectors

The Puromycin cassettes of pLKO.1-shRNA-SCR-puro, pLKO.1-shRNAHsEBF1(30)-puro, pLKO.1-shRNAHsEBF1(31)-puro, pLKO.1-shRNAHsOAZ(76)-puro and pLKO.1-shRNA HsOAZ-(77)-puro were exchanged with a YFP-casette via the BamHI/NsiI cutting sites. The YFP expression can be used to select transfected cells in *in-vitro* co-cultures and *in-vivo* experiments.

3.11.6　Real Time PCR

Real time PCR is a technique based on the normal PCR to simultaneously amplify and quantify the amount of a specific DNA or cDNA target. Amplified DNA can be quantified in "*real time*" because the DNA is accumulated after each cycle of amplification and can be detected with SYBR Green that intercalates unspecific into double-stranded DNA[147]. SYBR Green emits a strong fluorescence signal that increases in the same way as the amount of DNA increases during amplification. The increase in fluorescence intensity is measured after each cycle of real time PCR. The calculation of the crossing point (CP) at a specific cycle number at which fluorescence becomes detectable above background signal allows to quantify the amount of original DNA in the sample. The more specific transcripts are in the sample the lower is the CP value. To normalise the results and make a relative quantification of amount of original DNA transcript, two different methods using beta-2-microglobulin (NM_004048), an accurate housekeeping gene for leukocytes[148], as an internal control were used. An internal control is a transcript whose signal is used to adjust the amount and quality of initial DNA in different samples, is easily to detect and whose expression is not regulated during cell cycle, in different cell types or as a result of treatment of cells during experiments.

Relative standard curve method

The relative standard curve method was used to calculate the relative expression of target genes in cell lines, primary cells or ALL samples. For both the gene of interest and the internal control gene linear standard curves produced by real time PCR of serial dilutions (e.g. undiluted, 1:10, 1:100, 1:1000 etc) were run. The template for the standard curve was usually a cDNA sample from a cell line or plasmid DNA. It is important to note that the expression level of the sample should fall within the limits of the standard curve. The CP values of the gene of interest and the internal control were used to calculate the relative mean concentrations with the help of the known concentrations of the standard curve dilutions and the LightCycler® software. To relatively quantify the gene of interest following formula was used:

$$\text{Relative amount of transcript} = \frac{\text{Mean concentration gene of interest}}{\text{Mean concentration beta-2-microglobulin}}$$

Δ-Δ-CP-method

The Δ-Δ-CP-method was used to calculate the relative expression of EBF1 target genes in retroviral infected CD34^{+} cells. Relative expressions were measured as n-fold differences with help of the Δ-Δ-CP value. Important for the use of this method were similar efficiencies of the participating PCR reactions. The CP value of the internal control gene was subtracted from the CP value of the gene of interest giving the Δ-CP value. Then the Δ-CP values of two samples (e.g. infected and not infected) were subtracted from each other giving the Δ-Δ-CP value which is inserted in the formula n-fold expression (e.g. infected to not infected):

$$\text{Relative amount of transcript} = 2^{-(\Delta\text{-}\Delta\text{-CP})}$$

3.11.6.1   Real Time PCR procedure

LightCycler FastStart DNA Master   Roche (Mannheim, Germany)
SYBR Green I Kit

For the relative quantification of transcripts, cDNA or plasmid DNA were used in a real time PCR reaction with the LightCycler FastStart DNA Master SYBR Green I Kit and the LightCycler 480 machine.

Reaction for real time PCR:

cDNA or Plasmid DNA	2 µl
SYBR-Green mixture	2 µl
forward primer	1 µl
reverse primer	1 µl
ddH$_2$O	4 µl
Reaction mix	10 µl

The real time PCR reactions were incubated and measured in a LightCycler® 480 System according to following sequencing program.

Program for real time PCR:

Program	Temperature	time	cycles
Pre-incubation	95℃	10 min	1x
Amplification	95℃	10 s	45x
	x℃, x= Primer annealing temp.	10 s	
	72℃	10 s	
Melting curve	95℃	1 s	1x
	65℃	15 s	
	95℃ →65℃	slope 0.1℃/s	
Cooling	40℃	30 s	1x

3.12 Cell culture

3.12.1 Culture of adherent cells

All cells were cultivated at 37℃, 5% CO$_2$-atmosphere and a relative humidity of 95%. Coated cell culture flasks or plates were used for culture in subconfluent conditions. Depending on the density, cells were split usually every 3-4 days and reseeded in a dilution of 1:3 to 1:10. For the passaging cells were washed at least once with PBS, were detached from the surface with trypsin and were resuspended in fresh medium.

3.12.2 Culture of suspension cells

Cells in suspension were cultured under the same conditions described above for adherent cells. Depending on density and proliferation cells were split usually every 3-4 days and were reseeded in a dilution of 1:10 to 1:20.

3.12.3 Thawing and freezing of cells

Frozen cells, stored in a freezer at -80℃ (short-t erm) or at approximately -200℃ in liquid nitrogen, were thawed in a 37℃ warm water bath. Af terwards cells were diluted in pre-warmed culture medium to prevent the cytotoxic effects of the DMSO-containing freezing

medium. The cells were centrifuged with 1200 rpm (5-10 min, 4°C), the supernatant was discarded and they were diluted in an appropriate volume of culture medium for further culture. For long term storage usually 5×10^6 cells were resuspended in 1 ml of freezing medium, were transferred to cryotubes (Nunc; Langenselbold, Germany) and were frozen at -80°C. After some days the cells were transferred t o liquid nitrogen.

3.12.4 Thawing of ALL samples

Frozen ALL samples in cryotubes (1×10^7 cells) were hold on dry ice and were mixed with 1 ml of pre-warmed RPMI/FCS (1:1 (v/v)). They were thawed directly in a 37°C warm water bath. The thawed cells were transferred to 15 ml centrifugation tubes, diluted with 10 ml of pre-warmed RPMI and centrifuged with 1500 rpm (10 min, RT and without brake). The supernatant was discarded and the cells were mixed with culture medium or PBS.

3.12.5 Analysis of cells with the Flow cytometer

The flow cytometer enables the detection of fluorescence, emitted by fluorescence dyes, which is generated either by reporter genes like GPF/YFP or fluorochrome-coupled antibodies. To analyse cell surface molecules standard procedures for antibody staining were used[149]. To detect intracellular or cytoplasmic molecules the Fix&Perm® Cell Permeabilization Kit (ADG; Vienna, Austria) was used according to the manufacturer's manual. If two ore more different dyes were used simultaneously, compensation controls were used to eliminate the overlap of the emission spectra of different fluorochromes with the help of the automated compensation of the flow cytometer. Usually measurements were performed with volumes between 200 and 500 µl.

3.12.6 Sorting of cells

Cells were sorted according to their differential expression of reporter genes or binding of fluorochrome-coupled antibodies. The sorting was performed with a BD FACS Aria flow cytometer with sorting function and the kind help of Arne Düsedau (Heinrich-Pette-Institut; Hamburg, Germany).

3.12.6.1   Sorting strategy for hematopoietic and B-cell subgroups

For the analysis of ALL patient samples adequate normal cells were separated from healthy human BM as control. BM mononuclear cells were gained by density gradient separation (3.12.7) and were further separated by CD19$^+$ or CD34$^+$ immunomagnetic selection (3.12.8). The sorting of hematopoietic stem cells/progenitors, Pro-B, Pre-B and mature B-cells was

performed with three different fluorochrome-coupled antibodies and following sorting strategy:

Antibody used	HSCs/ progenitors	Pro-B	Pre-B	mature B
Anti-CD34-FITC	+	+	-	-
Anti-CD10-PE	-	+	+	-
Anti-CD19-APC	-	+	+	+

Table 5: Sorting strategy for haematopoietic and B-lineage subfractions. Shown are the antibodies used for the sorting of the four subfractions: HSCs/progenitors, Pro-B, pre-B and mature B cells. + = specific CD antigen is expressed in this subfraction, - = specific CD antigen is nor expressed in this subfraction, HSCs = Haematopoietic stem cells, Ab. = antibody

3.12.7 Density gradient separation of mononuclear cells

Biocoll separating solution   Biochrom (Berlin, Germany)

PBS

RPMI-1640 culture medium

50 ml reaction tubes

To isolate mononuclear cells from heparinised whole blood, cord blood or bone marrow, cells were mixed 1:2 (v/v) with RPMI-1640 culture medium and separated by density gradient with the help of the Biocoll Separating Solution according to the manufacturer's instructions.

3.12.8 Immunomagnetic CD19$^+$ and CD34$^+$ cell selection

EasySep Human CD19 positive Selection Kit   StemCell Tech. (Vancouver, Canada)

EasySep Human CD34 positive Selection Kit   StemCell Tech. (Vancouver, Canada)

EasySep Magnet   StemCell Tech. (Vancouver, Canada)

5 ml PS Round-Bottom Tubes

PBS, 2% FBS, 1 mM EDTA, Ca^{++} and Mg^{++} free

EasySep is an immunomagnetic cell selection procedure using monoclonal antibodies directed against specific cell surface molecules like CD19 or CD34. Antibody-labelled cells are crosslinked to magnetic nanoparticles allowing the removal of non-bound cells with the help of the high gradient magnetic field of the EasySep magnet leading to a high purity of positive cells after several rounds of washing. Due to the small size of the nanoparticles, cells can be easily detected with other antibodies by flow cytometry. CD19$^+$ or CD34$^+$ cells were separated from umbilical cord blood or bone marrow according to the manufacturer's manual.

3.12.9 Transfection of plasmid DNA into eukaryotic cells

For transient or stable transfection of plasmid DNA into eukaryotic cells Lipofectamine 2000 (Invitrogen; Carlsbad, USA) was used according to the manufacturer's manual.

3.12.10 Production of infectious virus particles

The production of infectious virus particles was performed via co-transfection of phoenix-gp cells with suitable packaging plasmids and calcium phosphate. A lentiviral or γ-retroviral expression plasmid was co-transfected with plasmids encoding for the viral structural proteins, enzymes and core proteins *gag*, *pol* and *env*. The Profection Mammalian Transfection Kit Calcium Phosphate (Promega; Mannheim Germany) was used for the transfection. 5×10^6 Phoenix-gp cells were seeded in 10 cm cell culture dishes 16 h before transfection. Directly before transfection, medium was changed and new medium with 25 µM chloroquine was given on the cells. Plasmid DNA was diluted in ddH$_2$O and 62.5 µl CaCl$_2$ solution to give a total volume of 500 µl.

Production of lentiviral particles	10 µg of lentiviral vector, 10 µg pMDLg-pRRE, 5 µg pRSV-Rev and 10 µg of phCMV-RD114/TR were used per dish
Production of *γ*-retroviral particles	5 µg of *γ*-retroviral vector, 10µg pSV40-gag/pol and 3 µg of phCMV-RD114 were used per dish

DNA/CaCl$_2$ solution was given dropwise to 500 µl 2x HBS while simultaneously air was blown in the solution with a stuffed Pasteur pipette. After vigorous vortexing the solution was incubated for 15 min. The developed calciumphosphate-DNA precipitate was given dropwise to the cells and was mixed with caution. 6-8 h later, the medium was approved and exchanged with 6 ml of fresh medium lacking chloroquine. Up to 5 times every 8-16 h (12 h are optimal) virus containing supernatant was removed and exchanged with 6 ml of fresh medium. The viral supernatants were filtrated with a 0.22 µm sterile filter (Millipore; Bedford, USA) and were frozen at -80℃ until use.

3.12.11 Calculation of virus titres

To compare the quality of different virus supernatants virus titres were determined to calculate the amount of infectious viral particles. 293-HEK cells were split 1:3 one day before infection. The next morning, 5×10^4 cells/well (of a 24-well plate) were seeded in 500 µl medium (with polybrene) and in the evening 20µl or 100 µl of virus supernatant were given directly to the cells followed by centrifugation with 2000 rpm (1 h, RT). The next morning the

medium was exchanged with fresh medium without virus. 48 h later the medium was discarded; cells were washed once with PBS and detached with trypsin. The reaction was stopped with medium/FCS, cells were centrifuged with 1200 rpm (10 min, 4°C) and the cell pellet was resuspended in 500 µl PBS. Cells were transferred to FACS tubes and YFP- or Venus-containing cells were detected using the flow cytometer. The amount of infectious units per ml (IU/ml) was calculated with following formula:

$$\text{Titer} = \text{IU/ml} = \frac{\text{Seeded cells per well x Percent YFP/Venus positive cells}}{\text{ml of used virus supernatant per infection}}$$

3.12.12 Infection of suspension cells with virus particles

RPMI-1640 selection medium
Polybrene (8 µg/ml)
6-well cell culture plates
15 ml reaction tube
Heraeus Multifuge 3S-R centrifuge   Thermo Fisher Scientific (Waltham, USA)

The cell line REH was infected with lentiviral particles containing constructs harbouring a puromycin antibiotic resistance gene allowing selection by application of puromycin (1 µg/ml) to the medium. $5x10^5$ cells were resuspended in 3 ml of a suitable viral supernatant (leftover stored at 4°C) and 3 µl polybrene and were transferred to one well of a 6-well plate. The plate was centrifuged with 2000 rpm (1 h, RT) and incubated over night. The next day cells were resuspended in the viral supernatant and pelleted by centrifugation in a 15 ml reaction tube. Cells were again resuspended in 3 ml of a fresh viral supernatant with 3 µl polybrene and handled like before. The other day cells were resuspended, centrifuged and cell pellets were mixed in a suitable volume of RPMI-1640 selection medium. Successful infections became obvious usually after 5 days of culture.

3.12.13 Viral infection of human CD34$^+$ cells

CD34$^+$ expansion medium
Retronectin
Blocking solution   PBS, 2% BSA
Washing solution   HBSS, 2.5% HEPES
6-well bacteria plates (non-coated)
Heraeus Multifuge 3S-R centrifuge   Thermo Fisher Scientific (Waltham, USA)

Human CD34$^+$ cells were seeded at an optimal density of 5-8x10^5/ml in 2.5-3.5 ml of CD34$^+$ expansion medium per well of a 6-well plate. 12-24 h before the first infection plates were hold in suitable boxes with additional vessels containing ddH$_2$O to increase the humidity for optimal growth. 2 ml Retronectin were used per infection to coat the wells; the plates were hold at 4℃ until the next day. The Retronectin was removed and stored at -20℃ for reuse (4-5 times possible). The wells were blocked with 2 ml blocking solution for 30 min and were washed with 3 ml of washing solution. Wells were coated 3-6 times with 1-2 ml of virus supernatant each. After application of supernatant, plates were centrifuged with 2000 rpm (20 min, 4℃) and the old supernatant was exchanged with new supernatant. After the last coating step ~1.5x10^6 CD34$^+$ cells in expansion medium were given in the wells; plates were cultivated over night. The next day a new Retronectin-coated plate was handled and coated with virus supernatant as described before. After the last coating step, already infected CD34$^+$ cells were transferred to the wells of the new plate, fed with 200 µl fresh medium per well and were cultivated overnight or for additional two days. The infected cells were analysed and YFP/Venus expressing cells sorted for further experiments or analysis.

3.12.14 *In-vitro* culture and differentiation of CD34$^+$ cells

24-well cell culture plates
hTERT-BMSC
B-cell differentiation medium

hTERT-BMSC cells[137] were used to support the growth of lymphocytes due to cell-cell contact and secretion of growth factors in a co-culture system. hTERT-BMSC stop proliferating if they become confluent but maintain an active metabolism. hTERT-BMSC cells were split 1:2 in 24-well plates in RPMI culture medium one week before use to give a dense stromal layer for co-culture with CD34$^+$ cells[150,151]. The medium was removed and cells were washed once with PBS. 5x10^3-2x10^4 CD34$^+$ cells were resuspended in B-cell differentiation medium and were given directly on the stromal layer. Differentiation medium contained the cytokines SCF, FLT-3 and IL-7 known to support the generation of B-lymphocytes[152,153,154]. Plates were cultured in suitable boxes with additional vessels containing ddH$_2$O to increase the humidity for optimal growth of CD34$^+$ cells. Cells were grown for 1-2 weeks depending on the density of the cells and were removed from the stromal layer for further analysis.

3.13 Protein Biochemistry

3.13.1 Cell lysis with SDS buffer

1 x Loading/lysis protein buffer (Laemmli buffer):   62.5 mM Tris (pH 6.8), 2.3% SDS, 10% glycerol, and 0.02% Pyronin-Y; addition of 50µl/ml β-mercapto-ethanol directly before use

Eppendorf 5810R centrifuge   Eppendorf (Wesseling-Berzdorf, Germany)

To lyse cells directly they were resuspended in an appropriate volume of Laemmli buffer, boiled for 10 min at 95°C and centrifuged at 14000 rpm (10 min, 4°C). The supernatant was directly used for SDS-PAGE or frozen at -80°C for f urther use.

3.13.2 Cell lysis with KLB' buffer

KLB lysis buffer   25 mM Tris, 150 mM NaCl, 5 mM EDTA, 10% glycerol, 1% Triton X-100, 10 mM Na-pyrophosphat, 1 mM Na-ortho-vanadate and 10 mM glycerolphosphate

KLB' lysis buffer   Addition of following reagents to KLB lysis buffer directly before cell lysis: 1 µl/ml 1 M PMSF, 10 µl/ml aprotinin, 20 µl/ml 0,5 M NaF and 2 µl/ml 40 mM Na-pervanadate (always freshly prepared: to 100µl of 50mM orthovanadate add 16µl H_2O_2, incubate for 30 min at RT)

2 x Loading buffer (Laemmli buffer)   125 mM Tris (pH 6.8), 4.6% SDS, 20% glycerol, 0.04% Pyronin Y; ad 50µl/ml β-mercaptoethanol directly before use

Eppendorf 5810R centrifuge   Eppendorf (Wesseling-Berzdorf, Germany)

To lyse cells with KLB' buffer, 5-10x10^6 adherent or suspension cells were washed twice with PBS, resuspended in 500-1000 µl of ice cold and freshly prepared KLB' buffer and transferred to 2 ml tubes. Cells were incubated for 30 min on ice for efficient lysis and resuspended occasionally. The lysate was centrifuged at 14000 rpm (10 min, 4°C) and the supernatant was transferred to a fresh 1.5 ml tube afterwards. The lysate was aliquoted and frozen at -80°C for storage. To determine the prote in concentrations, the *DC* Protein Assay (Bio-Rad; Hercules, USA) following Bradford[155] was used according to the manufacturer's manual. Before use, lysates were mixed with 2x loading buffer 1:1 (v/v), boiled for 10 min at 95°C and were centrifuged at 14000 rpm (10 min, 4°C). Supernatants were used in SDS-PAGE.

3.13.3 Isolation of core proteins[156] (modified[157])

Buffer A	10 mM HEPES*KOH (pH 7.9), 1.5 mM MgCl$_2$, 10 mM KCl, 0.5 mM DTT, 2 mM PMSF, 20 mM NaPP, 10 mM NaF and 1 mM Na$_3$VO$_4$
Buffer C	20 mM HEPES*KOH (pH 7.9), 25% glycerol, 420 mM NaCl, 1,5 mM MgCl$_2$, 0.2 mM EDTA, 0.5 mM DTT, 2 mM PMSF, 20 mM NaPP, 10 mM NaF and 1 mM Na$_3$VO$_4$
2 x Loading buffer (Laemmli buffer)	125 mM Tris (pH 6.8), 4.6% SDS, 20% glycerol, 0.04% Pyronin Y; ad 50µl/ml *β*-mercaptoethanol directly before use
Eppendorf 5810R centrifuge	Eppendorf (Wesseling-Berzdorf, Germany)

Buffer A and C were prepared in volumes of 50 ml, were aliquoted and stored at -80℃ until use. To isolate nuclear proteins, 5×10^5 to 1×10^7 cells were washed twice in PBS and cell pellets were resuspended in 400 µl ice cold buffer A. Cells were lysed on ice under hypotonic conditions for 10 min following vigorous vortexing for 10 s. Lysates were centrifuged with 4000 rpm (3 min, 4℃), supernatants were discarded and pellets resuspended cautious in 60 µl of buffer C. Extraction of nuclei was carried out by incubation under high salt conditions on ice for 30 min following vigorous vortexing for 15 s. Lysates were centrifuged with full speed (3 min, 4℃), supernatants were transferred and ali quoted into new reaction tubes and stored at -80℃. Before use, lysates were mixed with 2x lo ading buffer 1:1 (v/v), boiled for 10 min at 95℃ and centrifuged at 14000 rpm (10 min, 4℃). Su pernatants were used in SDS-PAGE.

3.13.4 SDS-PAGE

SDS-PAGE stacking gel (5%)	0.83 ml acrylamide mix (30%), 0.63 ml Tris (1 M, pH 6.8), 0.05 ml SDS (10%), 0.05 ml APS (10%), 0.004 ml TEMED, fill to 5 with ddH$_2$O for approx. 2 small gels
SDS-PAGE resolving gel (12%)	6ml acrylamide mix (30%), 3.8 ml Tris (1.5 M, pH 8.8), 0.15 ml SDS (10%), 0.15 ml APS (10%), 0.006 ml TEMED, fill to 15 ml with ddH$_2$O for approx. 2 small gels
10x SDS-PAGE running buffer	60.5 g Tris, 288 g glycine and 200 ml SDS 10% fill to 2 l with ddH$_2$O

The SDS-PAGE was used to separate denatured proteins according to their molecular weight. The preparation and running of gels was performed following standard procedures[158].

3.13.5 Immunoblot and detection of proteins

PVDF membranes (Immobilion-P)	Millipore (Bedford, USA)
Nitrocellulose membranes	GE Healthcare (Freiburg, Germany)
(Amersham Hybond ECL)	
Transfer buffer (semi-dry)	18.2 g Tris, 86.5 g glycine, fill to 4 l with ddH$_2$O
	and adjust pH to 8.3-8.4. Fill to 6 l with ddH$_2$O
CAPS transfer buffer (wet-blot)	20 ml CAPS (0.5 M, pH 11.0), 200 ml methanol
	fill to 1 l with ddH$_2$O
1 x TBST (for washing)	
TBST- 5% skim milk	50 ml TBST, 2.5 g skim milk powder
(for blocking and antibody dilution)	
Amersham ECL solution RPN2106	GE Healthcare (Freiburg, Germany)
Amersham Hyperfilm MP (18 × 24 cm)	GE Healthcare (Freiburg, Germany)
Immunoblot stripping buffer	62.5 ml Tris (1 M, pH 6.8), 200 ml 10% SDS, 7
	ml β-mercaptoethanol fill to 1 l with ddH$_2$O

Proteins separated by SDS-PAGE were transferred to PVDF or nitrocellulose membranes enabling the detection by antibody-binding and an HRP-mediated chemiluminiscence reaction. The transfer of proteins in semi-dry or wet-blot chambers, the blocking and washing of membranes and the primary- and secondary antibody-binding were performed according to standard procedures[159]. To detect specific proteins membranes were incubated with ECL solutions for 2 min and exposed in the dark on an autoradiographic film.

In some cases immunoblot membranes were stripped to detach the bound antibodies for an additional detection with a different antibody. After the first detection membranes were washed twice with ddH$_2$O and were transferred to a closable vessel with an appropriate amount of stripping buffer. The membranes were incubated in a 50°C warm shaking water bath for 30-60 min, depending on the stringency of the stripping, were washed twice with TBST and blocked again. The stripped membranes were then handled as described above.

3.13.6 (Co)-Immunoprecipitation/(Co)-IP

Protein G Plus Agarose (sc-2002)	Santa Cruz Biotechnology (Santa Cruz, USA)
0.5 ml reaction tubes	
Eppendorf 5810R centrifuge	Eppendorf (Wesseling-Berzdorf, Germany)

The immunoprecipitation (IP) technique was used to enrich proteins out of whole cell lysates. Co-IP analysis was used to detect protein-protein interactions. First, 2.5 µg of an antibody

specific for the protein of interest was added to 20 µl of Protein G Plus Agarose and mixed for 2h at 4°C on a horizontal shaker. 150 µl of who le cell or nuclear lysate was transferred to the pre-coated antibody and was mixed and incubated over night at 4°C on an overhead shaker, leading to a precipitation of the protein through the antibody-Protein G Agarose complex. If there are any proteins/molecules bound to the first protein they will also be precipitated. The tubes were centrifuged the next day with full speed (1 min, 4°C) and the supernatants were discarded or transferred to new reaction tubes (IP supernatant). The pellet consisting of agarose beads was washed twice with 200 µl KLB lysis buffer (3.13.2) and the supernatants were discarded. After the second washing step a maximal amount of supernatant was aspirated without disturbing the agarose beads. Beads were mixed with 50-60 µl of 1x Laemmli buffer (3.13.1), boiled for 10 min at 95°C and were centrifuged at 14000 rpm (10 min, 4°C). Supernatants were directly used for SDS-PAGE or frozen at -80°C for further use. The detection of the co-precipitated protein was performed with a specific antibody.

4 Results

Previous transcriptome-wide expression analyses (Horstmann et al., unpublished) in TEL-AML1 rearranged ALL and hyperdiploid ALL showed an increased activation of the bone morphogenetic protein 2 (BMP2)-dependent pathway, which belongs to the TGF-β superfamily signalling network. The goal of the present study was to assess the biological relevance of BMP2 signalling and its potential transcriptional targets in paediatric ALL. We hypothesised that an activated BMP2-pathway does not reflect a state of differentiation of leukaemic cells but rather a specific aberration of ALL, which drives and maintains the malignant phenotype potentially by arresting the leukaemic cells in an immature state of differentiation. We sought mechanistic insight into the molecular events of B-cell differentiation and its disturbances in ALL focusing on the interplay between the essential B-cell factor EBF1 and the BMP2 target protein OAZ.

For this purpose relevant members of the BMP2-dependent pathway were cloned and further subcloned to gain specific expression plasmids as suitable tools for gene expression analyses and to use them for further functional studies. Additionally EBF1 was cloned, the expression of which is essential for the normal B-cell development (1.2). Mutations in the gene have been identified in a minor fraction of pre-B-ALL[32,34] and deregulation of EBF1 is possibly directly linked to the characteristic B-cell maturation arrest observed in leukaemia[4]. EBF1-mediated target gene transactivation can be inhibited by expression of the multifunctional zinc-finger protein OAZ, which is able to sequester the EBF1 protein and hereby to prevent its binding at specific consensus DNA sequences of target genes (1.4). The aberrantly high expression levels of OAZ in leukaemic lymphoblasts detected by the previous transcriptome analyses might be related to the molecular pathogenesis of ALL, insomuch as critical EBF1 target genes could be indirectly blocked by an EBF1/OAZ protein complex (1.2).

4.1 Cloning of human BMP2, OAZ and EBF1

Using non-quantitative RT-PCR it was initially confirmed that key components of the BMP2 signalling pathway were expressed in different ALL cell lines (data not shown). The human BMP2 and OAZ CDSes were amplified by PCR from REH cells; the EBF1 CDS was amplified from 697 cells. The PCR products were subsequently inserted in a TA-cloning vector. The integrity of the CDSes was verified by DNA sequencing and suitable clones were further subcloned in an expression vector (see 3.11.5.2).

4.1.1 Cloning of human BMP2

The human BMP2 CDS was Taq-amplified and ligated in the pCR4-TOPO vector as described before (3.11.5.1). The isolated plasmid DNA was digested with *EcoRI* (Figure 8) and insert containing plasmids were subsequently sequenced. The insert of plasmid clone #1 showed a 100% sequence homology with the wild type sequence of hBMP2 and was designated as pCR4-TOPO-HsBMP2(wt)HA.
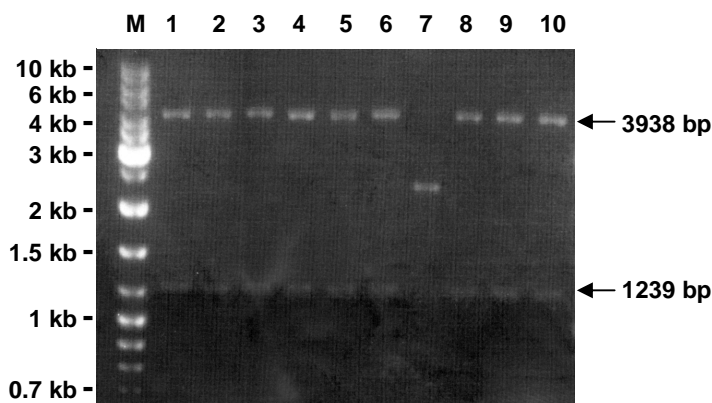

Figure 8: Cloning of hBMP2 into pCR4-Topo vector. *EcoRI* digest of 10 clones of amplified hBMP2 CDS ligated in pCR4-Topo vector separated on a 1.2% TAE-Agarose gel. The size of the hBMP2 CDS insert is 1239 bp, pCR4-TOPO backbone 3938 bp. M (GeneRuler DNA Ladder Mix size marker), 1-10 (number of different plasmid clones).

4.1.2 Cloning of human EBF1

The human EBF1 CDS was Taq-amplified and ligated in the pCR2.1-TOPO vector as described before (3.11.5.1). The isolated plasmid DNA was digested with *HindIII* and *NotI* (Figure 9) or *EcoRI* alone and insert containing plasmids were sequenced. The insert of clone #2 showed 100% sequence homology with the wild type sequence of hEBF1 at the nucleotide (nt) level and was designated as pCR2.1-TOPO-HsEBF1(wt).
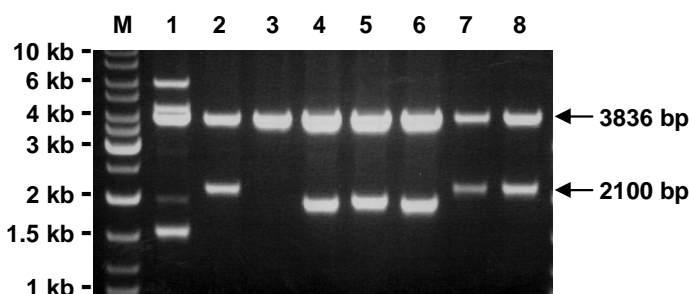

Figure 9: Cloning of hEBF1 into pCR2.1-Topo vector. *HindIII* and *NotI* digest of 8 clones of amplified hEBF1 CDS ligated in pCR2.1-Topo vector separated on a 1 % TAE-Agarose gel. The size of the hEBF1 CDS insert is 2100 bp, pCR2.1-TOPO backbone 3836 bp. M (GeneRuler DNA Ladder Mix size marker), 1-8 (number of different plasmid clones).

4.1.3 Cloning of human OAZ

The human OAZ CDS was Taq-amplified and ligated in the pCR-XL-TOPO vector as described before (3.11.5.1). The isolated plasmid DNA was digested with *EcoRI* (Figure 10) and insert containing plasmids were sequenced. The insert of clone #2 showed 100% sequence homology with the wild type sequence of hEBF1 at the nucleotide level and was designated as pCR4-TOPO-HsBMP2(wt)HA.
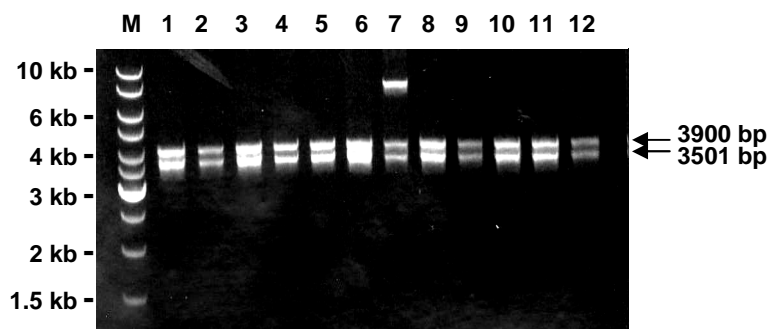

Figure 10: Cloning of hOAZ into pCR-XL-Topo vector. *EcoRI* digest of 12 clones of amplified hOAZ CDS ligated in pCR-XL-Topo vector separated on a 1 % TAE-Agarose gel. The size of the hOAZ CDS insert is 3900 bp, pCR-XL-TOPO backbone 3501 bp. M (GeneRuler DNA Ladder Mix size marker), 1-12 (number of different plasmid clones).

4.2 Subcloning into expression plasmids

4.2.1 Subcloning of human BMP2

The plasmid pCR4-TOPO-HsBMP2(wt)HA was used to subclone the human BMP2 CDS into pcDNA3.1(+) as described before (3.11.5.2). A clone with sequence integrity and correct orientation was designated as pcDNA3.1(+)-HsBMP2(wt)HA. The expression of hBMP2 was confirmed by transfection of HEK-293 cells (3.12.9) with this plasmid and the BMP2 protein (3.13.1) was detected by Western Blot (3.13.4 and 3.13.6) (results not shown).

4.2.2 Subcloning of human EBF1

The plasmid pCR2.1-TOPO-HsEBF1(wt) was used to subclone the human EBF1 CDS into pcDNA3.1(+) as described before (3.11.5.2).
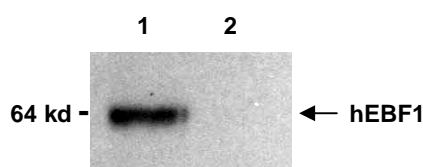

Figure 11: Detection of hEBF1 in whole protein lysate of HEK-293 cells transfected with pcDNA3.1(+)-HsEBF1(wt) (1) or empty vector (2). 12% SDS-PAGE gel, nitrocellulose membrane and detection by Abnova anti-hEBF1 antibody (1:1000).

A clone with sequence integrity and correct orientation was designated as pcDNA3.1(+)-HsEBF1(wt). The expression of hEBF1 was confirmed by transfection of HEK-293 cells (3.12.9) with this plasmid and detection of EBF1 protein (3.13.1) by Western Blot (3.13.4 and 3.13.6) (Figure 11).

4.2.3 Subcloning of hOAZ into pcDNA3.1(+)

The plasmid pCR-XL-TOPO-FlagHsOAZ(wt) was used to subclone the human OAZ CDS into pcDNA3.1(+) as described before (3.11.5.2). A clone with sequence integrity and correct orientation was designated as pcDNA3.1(+)-FlagHsOAZ(wt). The expression of hOAZ-Flag fusion protein (further designated as hOAZ) was confirmed by transfection of HEK-293 cells (3.12.9) with this plasmid and detection of Flag-Tag and hOAZ protein (3.13.1) by Western Blot (3.13.4 and 3.13.6) (Figure 12).
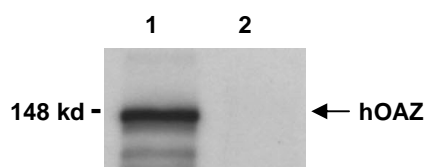

Figure 12: Detection of hOAZ in whole protein lysate of HEK-293 cells transfected with pcDNA3.1(+)-FlagHsOAZ(wt) (1) or empty vector (2). 12% SDS-PAGE gel, nitrocellulose membrane and detection by Sigma Aldrich anti-Flag antibody (1:3000).

4.2.4 Subcloning of human Smad1, 4 and murine Smad5

The plasmids pBabe-puro4-FlagHsSmad1(wt), -FlagHsSmad4(wt) and -FlagMmSmad5(wt) were used to subclone the human Smad1 and Smad4 CDSes and murine Smad5 CDS, which is almost 99% homologous with human Smad5 at the protein level, into pcDNA3.1(+) as described before (3.11.5.2). Clones with sequence integrity and correct orientation were designated as pcDNA3.1(+)-FlagHsSmad1(wt), -FlagHsSmad4(wt) and -FlagMmSmad5(wt). The expression of human Smad1-Flag and Smad4-Flag and murine Smad5-Flag fusion proteins (further designated as hSmad1, hSmad4 and mSmad5) was confirmed by transfection of HEK-293 cells (3.12.9) with these plasmids and detection of Flag fusion proteins (3.13.1) by Western Blot (3.13.4 and 3.13.6) (Figure 13).
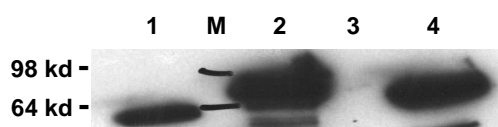

Figure 13: Detection of murine Smad5 and human Smad4 and Smad1 and in whole protein lysates of HEK-293 cells transfected with pcDNA3.1(+)-FlagMmSmad5(wt) (1), -FlagHsSmad4(wt) (3), -FlagHsSmad1(wt) (4) or empty vector (3). 15% SDS-PAGE gel, nitrocellulose membrane and detection by Sigma Aldrich anti-Flag antibody (1:1000).

4.3 shRNA vectors to knock-down EBF1 and OAZ

shRNA vectors were tested in addition to the cloned expression plasmids to establish the experimental tools for the specific downregulation of EBF1 and OAZ in normal and leukaemic cells. The encoded shRNAs of several different vectors were compared for their ability to effectively knock-down the EBF1 or OAZ transcript levels[141]. Phoenix-gp cells were co-transfected (3.12.10) with pLKO.1-puro EBF1 shRNA or pLKO.1-puro OAZ shRNA constructs and the control vector pLKO.1-shRNA-SCR-puro in combination with suitable packaging plasmids encoding lentiviral proteins with the help of the calcium-phosphate method. Lentiviral supernatants were harvested and used for the infection of the TEL/AML1 ALL cell line REH (3.12.12). Infected cells containing the puromycin resistance gene of the pLKO.1-puro vector were selected by the antibiotic puromycin. Infected cells were harvested after a minimum of 120 hours of growth under selection conditions.

The quantitation of the EBF1 transcript levels in REH cells infected with EBF1 shRNA vectors showed two vectors with efficient EBF1 knock-down respectively (Figure 14). EBF1 transcript levels were almost 40-60% reduced in comparison to the scrambled shRNA vector pLKO.1-shRNA-SCR-puro, which served as a control for shRNA effects. The two vectors pLKO.1-shRNAHsEBF1(30)-puro and pLKO.1-shRNAHsEBF1(31)-puro were chosen to be used for further EBF1 knock-down experiments

Figure 14: Testing of EBF1 shRNA vectors. EBF1 expression levels of REH cells infected with lentiviral shRNA vectors quantitated by real time PCR. EBF1 expression relative to B2M was normalized to 1 for scrambled (SCR) shRNA vector in comparison to a significant reduction to 0.63 for the EBF30 and 0.40 for the EBF31 shRNA vectors.

The quantitation of the OAZ transcript levels in REH cells infected with OAZ shRNA vectors showed two vectors with strong OAZ knock-down. OAZ transcript levels were more than 70-80% reduced in comparison to the scrambled shRNA vector pLKO.1-shRNA-SCR-puro

(Figure 15). The two vectors pLKO.1-OAZ(76)-puro and pLKO.1-shRNAHsOAZ(77)-puro were chosen to be used for further further OAZ knock-down experiments.
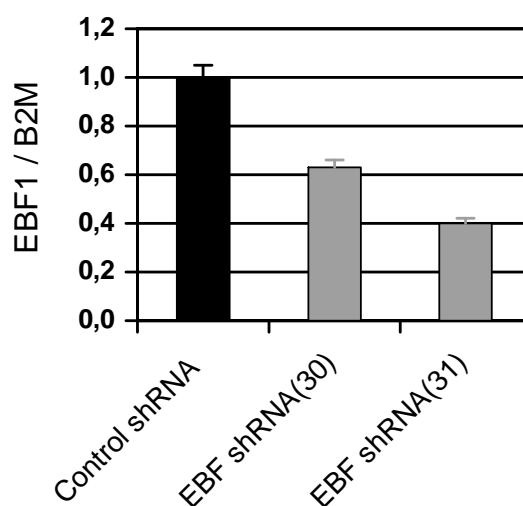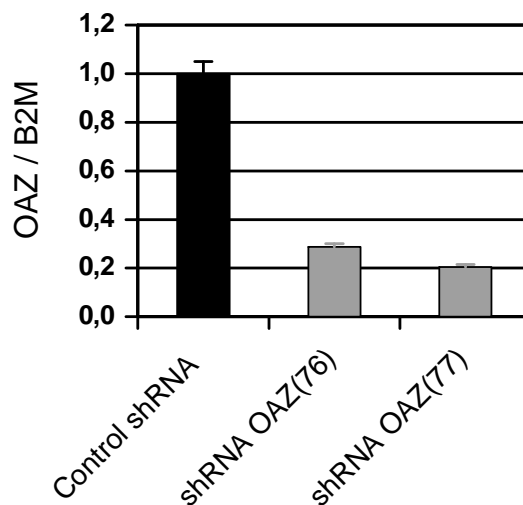

Figure 15: Testing of OAZ shRNA vectors. OAZ expression levels of REH cells infected with lentiviral shRNA vectors quantitated by real time PCR. OAZ expression relative to B2M was normalized to 1 for scrambled (SCR) shRNA vector in comparison to a significant reduction to 0.29 for the OAZ76 and 0.20 for the OAZ77 shRNA vectors.

4.3.1 Insertion of a YFP reporter into pLKO.1-puro vectors

To use the tested shRNA vectors that were suitable for an effective downregulation of EBF1 and OAZ respectively, a consistent application of the antibiotic puromycin during cultivation is absolutely necessary. For *in-vitro* culture conditions in a stromal cell dependent co-culture system or in the *in-vivo* NOD/*scid* mouse model this is not feasible because of non-resistance of the stromal cells or the mice towards puromycin. Therefore we decided to exchange the puromycin cassettes in the shRNA vectors for an YFP reporter gene as described before (3.11.5.4) (data not shown). The YFP expression of the constructs can be used in the future to select transfected cells in *in-vitro* co-culture and *in-vivo* experiments.

4.4 Analysis of the BMP2 Pathway in ALL

4.4.1 Gene expression analysis of cell lines

Cell lines were used to quantify the expression levels of genes which were crucial for BMP2-signalling. They served as a model for different subgroups of paediatric ALL. Non-leukaemia cell lines obtained from different human tissues acted as controls. RNA was isolated (3.11.2) from 7 paediatric B-ALL cell lines, one T-ALL cell line, 4 other cancer cell lines and the standard human embryonic kidney cell line HEK-293 to quantify the expression levels of different genes. After testing of RNA for quality and quantity, RNA was reverse transcribed into cDNA (3.11.3) which was used for the real time PCR analysis (3.11.6).

4.4.1.1 BMP2 gene expression

The analysis of BMP2 (Figure 16) showed a high expression level in the hyperdiploid ALL cell line MHH-CALL2 and the TEL-AML1 rearranged ALL cell line REH. This was consistent with the initial transcriptome analyses data on leukaemic cells from hyperdiploid and TEL-AML1 positive ALL patients, exhibiting a strong expression of BMP2.
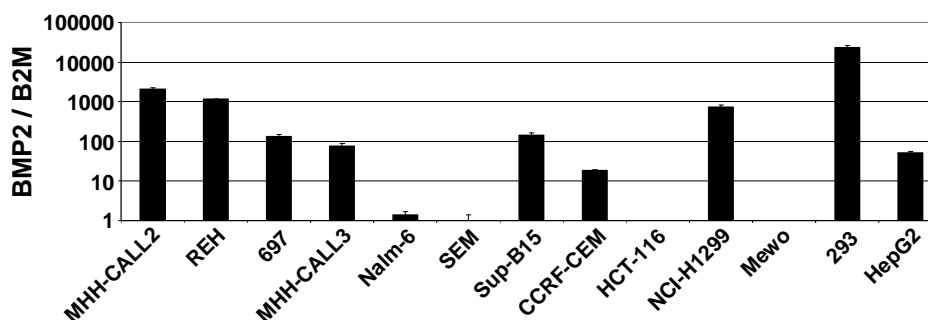

Figure 16: Quantification of BMP2 expression by real time PCR. BMP2 expression levels quantitated by real time PCR. Bars show mean (± sd) BMP2 expression relative to B2M in the cell lines MHH-CALL2 (hyperdiploid ALL), REH (t(12;21) / TEL-AML1 ALL), 697 (t(1;19) / E2A-PBX ALL), MHH-CALL3 (t(1;19) / E2A-PBX ALL), Nalm-6 (t(5;12) / TEL-PDGFRβ), SEM (t(4;11) / MLL-AF4), SUP-B15 (t(9;22) / BCR-ABL (P185)), CCRF-CEM (T-ALL), HCT-116 (colon carcinoma), NCI-H1299 (Non-small cell lung cancer), Mewo (malignant melanoma), HEK-293 (embryonal kidney) and HepG2 (hepatocellular carcinoma). sd = standard deviation.

The expression of BMP2 in the cell line MHH-CALL2 was up to 2000-fold higher and in the TEL/AML1 rearranged cell line REH up to 1000-fold higher than in the other ALL cell lines tested. The human embryonic kidney cell line HEK-293 nevertheless showed the by far highest expression of all cell lines.

4.4.1.2 BMP receptor expression

BMP receptor II (BMPRII) expression, which is the ubiquitous type II receptor for all BMPs, was detectable in all cell lines except the E2A-PBX ALL cell line MHH-CALL3 (data not shown). The highest expression of BMPRII was detetctable in the embryonic kidney cell HEK-293 whose expression was up to 20-fold higher than in the other cell lines.

The expression of the BMP receptor Ia (BMPRIa), one of the two type I receptors used by all BMPs, was detectable in all non-ALL cell lines (data not shown). The embryonic kidney cell HEK-293 showed the highest expression. Only in the TEL-PDGFRβ ALL cell line Nalm-6 and the MLL-AF4 ALL cell line SEM were basal levels of BMPRIa detectable. The other ALL cell lines showed BMPRIa levels that were not quantifiable by the used real time PCR technique.

The other type I receptor used from the BMPs is the BMP receptor Ib (BMPRIb). This receptor was not detectable in the used cell lines due to technical problems.

4.4.1.3 Smad1, Smad4 and Smad5 gene expression

Subsequently Smad1, an essential signalling mediator in the BMP2-pathway, was measured in the cell lines (1.2 and Figure 17). BMP2-binding leads to a phosphorylation and activation of the BMP receptor complex and a subsequent Smad1 phosphorylation. Phospho-Smad1 forms a complex with Smad4, shuttles into the nucleus resulting in a transmission of the BMP2 signal to transcriptional transactivation. Smad1 expression was detectable in all ALL cell lines with the highest expression in the E2A-PBX ALL cell line MHH-CALL3 and the TEL/AML1 rearranged ALL cell line REH. The expression of Smad1 in non-ALL cell lines was in general much stronger with a maximum in the colon carcinoma cell line HCT-116.
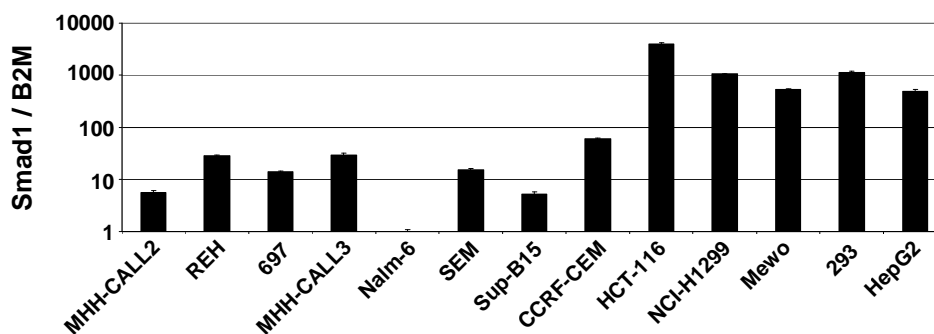

Figure 17: Quantification of Smad1 expression by real time PCR. Smad1 expression levels quantitated by real time PCR. Bars show mean (± sd) Smad1 expression relative to B2M in the cell lines MHH-CALL2 (hyperdiploid ALL), REH (t(12;21) / TEL-AML1 ALL), 697 (t(1;19) / E2A-PBX ALL), MHH-CALL3 (t(1;19) / E2A-PBX ALL), Nalm-6 (t(5;12) / TEL-PDGFRβ), SEM (t(4;11) / MLL-AF4), SUP-B15 (t(9;22) / BCR-ABL (P185)), CCRF-CEM (T-ALL), HCT-116 (colon carcinoma), NCI-H1299 (Non-small cell lung cancer), Mewo (malignant melanoma), HEK-293 (embryonal kidney) and HepG2 (hepatocellular carcinoma). sd = standard deviation.

The complexing partner of the receptor activated Smads (Smad1/5/8), Smad4, was detectable in all ALL and non-ALL cell lines tested consistent with its ubiquitous role in BMP and TGF-β signalling in general (Figure 18). The variability of Smad 4 expression among the tested cells lines was significantly smaller in comparison to Smad1. The Smad4 expression in the ALL cell lines just ranged over one log distance and was usually slightly higher in the non-ALL cell lines.
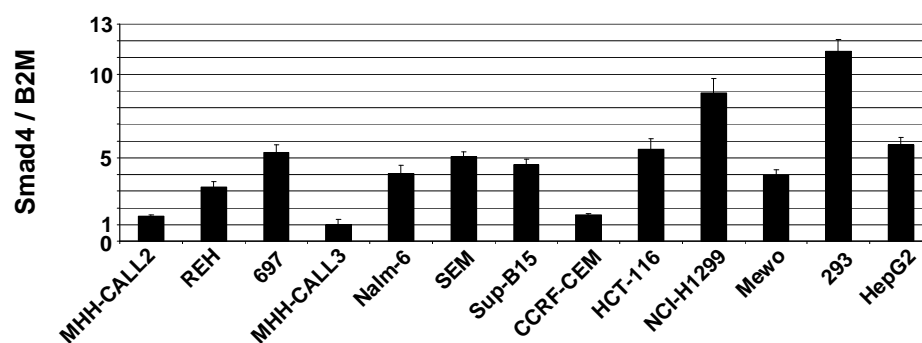
Figure 18: Quantification of Smad4 expression by real Time PCR. Smad4 expression levels quantitated by real time PCR. Bars show mean (± sd) Smad4 expression relative to B2M in the cell lines MHH-CALL2 (hyperdiploid ALL), REH (t(12;21) / TEL-AML1 ALL), 697 (t(1;19) / E2A-PBX ALL), MHH-CALL3 (t(1;19) / E2A-PBX ALL), Nalm-6 (t(5;12) / TEL-PDGFR*β*), SEM (t(4;11) / MLL-AF4), SUP-B15 (t(9;22) / BCR-ABL (P185)), CCRF-CEM (T-ALL), HCT-116 (colon carcinoma), NCI-H1299 (Non-small cell lung cancer), Mewo (malignant melanoma), HEK-293 (embryonal kidney) and HepG2 (hepatocellular carcinoma). sd = standard deviation.

Smad5, like Smad1 transmitting BMP2 signals into the nucleus, was detectable in all ALL and non-ALL cell lines tested (Figure 19). The picture was similar to Smad4 with about one log range difference in expression between the E2A/PBX ALL cell line 697 and the hyperdiploid ALL cell line MHH-CALL2. The highest expression of Smad5 was measurable in the embryonic kidney cell HEK-293.

Figure 19: Quantification of Smad5 expression by real time PCR. Smad5 expression levels quantitated by real time PCR. Bars show mean (± sd) Smad4 expression relative to B2M in the cell lines MHH-CALL2 (hyperdiploid ALL), REH (t(12;21) / TEL-AML1 ALL), 697 (t(1;19) / E2A-PBX ALL), MHH-CALL3 (t(1;19) / E2A-PBX ALL), Nalm-6 (t(5;12) / TEL-PDGFR*β*), SEM (t(4;11) / MLL-AF4), SUP-B15 (t(9;22) / BCR-ABL (P185)), CCRF-CEM (T-ALL), HCT-116 (colon carcinoma), NCI-H1299 (Non-small cell lung cancer), Mewo (malignant melanoma), HEK-293 (embryonal kidney) and HepG2 (hepatocellular carcinoma). sd = standard deviation.

4.4.1.4 OAZ gene expression

OAZ is a zinc-finger protein with implications in BMP2 signalling and in the posttranslational regulation of the essential B-cell differentiation gene EBF1 on protein level as described before (1.4). The measurement of OAZ showed an extraordinary high expression level in the TEL-AML1 rearranged ALL cell line REH which was up to 35-fold higher than the expression

levels in the other ALL cell lines tested (Figure 20). In the TEL/PDGFR*β* ALL cell line Nalm-6, the MLL/AF4 ALL cell line SEM and the two non-ALL cell lines NCI-H1299 and Mewo, OAZ was not detectable at all
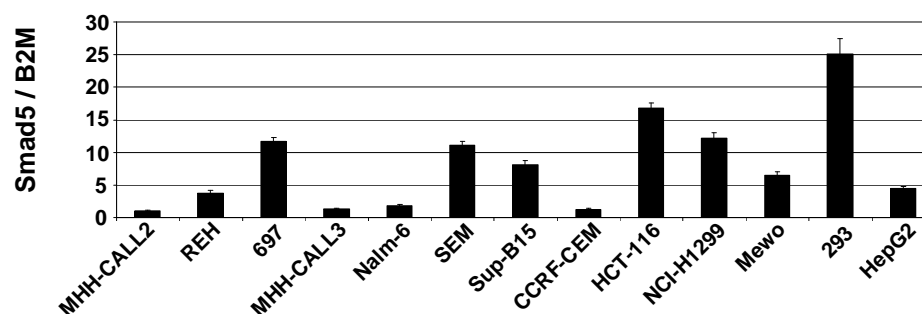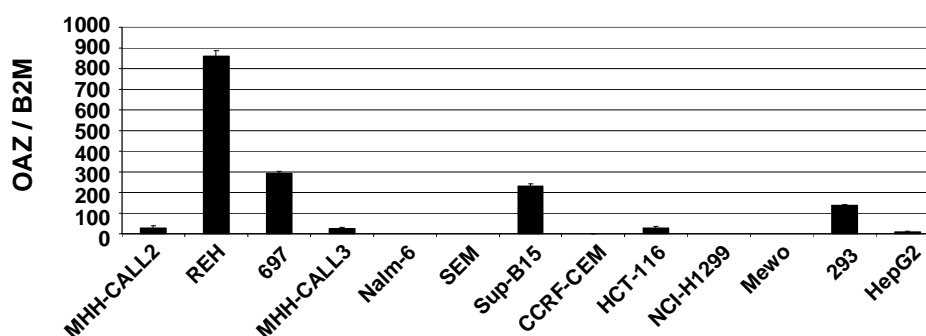

Figure 20: Quantification of OAZ expression by real time PCR. OAZ expression levels quantitated by real time PCR. Bars show mean (± sd) OAZ expression relative to B2M lines MHH-CALL2 (hyperdiploid ALL), REH (t(12;21) / TEL-AML1 ALL), 697 (t(1;19) / E2A-PBX ALL), MHH-CALL3 (t(1;19) / E2A-PBX ALL), Nalm-6 (t(5;12) / TEL-PDGFR*β*), SEM (t(4;11) / MLL-AF4), SUP-B15 (t(9;22) / BCR-ABL (P185)), CCRF-CEM (T-ALL), HCT-116 (colon carcinoma), NCI-H1299 (Non-small cell lung cancer), Mewo (malignant melanoma), HEK-293 (embryonal kidney) and HepG2 (hepatocellular carcinoma). sd = standard deviation.

4.4.1.5 EBF1 gene expression

EBF1 a transcription factor usually expressed during B-cell development from early to mature B-cells (1.2) was found to be differentially expressed in the ALL cell lines (Figure 21). The general expression of EBF1 in the ALL cell lines was not surprising due to their B-lymphoid origin. The highest expression levels were detected in the TEL/AML1 rearranged ALL cell line REH and the E2A/PBX ALL cell line 697 showing a more than two log range difference to the MLL-AF4 ALL cell line SEM. The human embryonic kidney cell line HEK-293 was the only non-ALL cell line with a detectable expression level of EBF1.
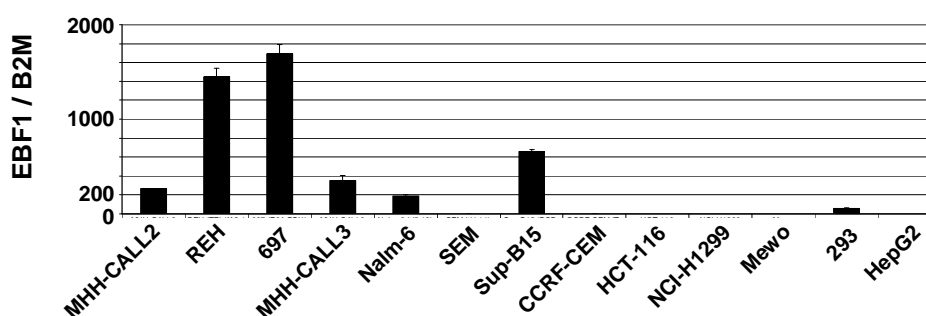
Figure 21: Quantification of EBF1 expression by real time PCR. EBF1 expression levels quantitated by real time PCR. Bars show mean ± sd. EBF1 expression relative to B2M in the cell lines MHH-CALL2 (hyperdiploid ALL), REH (t(12;21) / TEL-AML1 ALL), 697 (t(1;19) / E2A-PBX ALL), MHH-CALL3 (t(1;19) / E2A-PBX ALL), Nalm-6 (t(5;12) / TEL-PDGFR*β*), SEM (t(4;11) / MLL-AF4), SUP-B15 (t(9;22) / BCR-ABL (P185)), CCRF-CEM (T-ALL), HCT-116 (colon carcinoma), NCI-H1299 (Non-small cell lung cancer), Mewo (malignant melanoma), HEK-293 (embryonal kidney) and HepG2 (hepatocellular carcinoma). sd = standard deviation.

4.4.1.6 Overview of gene expression in ALL cell lines

The quantification of the gene expression of crucial members of the BMP2 signalling pathway showed usually at least basal expression levels in all pre-B ALL cell lines tested. The exception was the zinc-finger protein OAZ which was not detectable in two ALL cell lines, but showed an abundant expression in the TEL/AML1 rearranged ALL cell line REH. In order to directly compare the expression signatures of all ALL cell lines it was necessary to classify the measured values (Table 6).

Cell line	ALL-subtype	BMP2	BMPR II	BMPR Ia	Smad 1	Smad 4	Smad 5	OAZ	EBF1
MHH-CALL2	hyperdipl.	++++	+	-	+	++	+	+	+
REH	TEL/AML1	+++	+++	-	++	+++	++	++++	++++
697	E2A/PBX	+	++++	-	+	++++	++++	++	++++
MHH-CALL3	E2A/PBX	+	-	-	++	+	+	+	+
Nalm-6	TEL-PDGFRβ	(+)	+++	++	+	++++	+	-	+
SEM	MLL/AF4	(+)	+	++++	++	++++	++++	-	(+)
SUP-B15	BCR/ABL	+	++	-	+	++++	+++	++	++
CCRF-CEM	T-ALL	(+)	+	-	++++	++	+	(+)	(+)

Table 6: Gene expression of BMP2 signalling and EBF1 in ALL cell lines. Expression values were quantitated by real time PCR. The relative quantity of specific transcripts is indicated as (-) undetectable, ((+)) very low, (+) low, (++) moderate, (+++) high and (++++) abundant. Classification was calculated for each transcript depending on the cell line with the strongest expression defined as 100%; (-) stands for 0% expression, ((+)) for <1%, (+) for 1-25%, (++) for 26-50%, (+++) for 51-75% and (++++) for 76-100%.

4.4.2 Gene expression analysis of ALL patient samples

The analysis of different ALL cell lines supported the results gained from the initial transcriptome analyses of TEL/AML1 rearranged and hyperdiploid ALL patient samples. The expression of BMP2 necessary for binding at the BMP receptor complex and activation of the downstream BMP2 signalling cascade was high in the hyperdiploid ALL cell line MHH-CALL2 and the TEL-AML1 rearranged ALL cell line REH. A strong expression of the zinc-finger protein OAZ was noted in the TEL/AML1 rearranged ALL cell line REH, the expression of which was detected before in TEL/AML1 ALL patient samples. In the following, a greater cohort of patient samples was included in order to recapitulate 'in vivo' the BMP2 dependent signaling events and its downstream targets. Patient samples were obtained from the Klinik und Poliklinik für Pädiatrische Hämatologie und Onkologie of the UKE (Hamburg, Germany)

after written informed consent and approval of the ethics committee of the City of Hamburg. We focused onto the two defined TEL/AML1 rearranged and hyperdiploid subclasses of ALL as well as a control group, containing patients with precursor B-ALL that were neither TEL/AML1 positive nor did they exhibit a hyperdiploid karyotype (3.4.4). 37 cases with TEL-AML1 rearranged ALL, 25 cases of hyperdiploid ALL and 34 cases of the control subgroup were included. Bone marrow samples from initial diagnosis were used for quantification by real time PCR (3.11.6). To analyse if the expression and activation of the BMP2 pathway is specific for leukaemic cells, different normal cell fractions served as a control. For this purpose haematopoietic stem cells/progenitors, Pro-B, Pre-B and mature B-cells were sorted from human bone marrow aspirates drawn from healthy donors (3.12.6.1). Additionally, bone marrow stromal cells were isolated and analysed as an additional control, which constitute an essential component of the haematopoietic stem cell niche.

The measurement of the BMP2 expression showed a wide range in the expression values for the ALL samples with several samples showing strong BMP2 expression contrary to generally low expression in the normal controls (Figure 22).

Figure 22: Quantification of BMP2 expression by real time PCR in leukaemic and healthy BM cells. All expression values for the samples of one group are displayed as squares. The mean values (±sd) of a group are additionally shown as bars next to the expression values. BMP2 median expression relative to B2M was 254 (mean 479±434; n=36) in the TEL-AML1 rearranged ALL group in comparison to 515 (mean 739±659; n=23) in the hyperdiploid ALL group, 117 (mean 325±476; n=33) in the control ALL group with different (other ALL) cases, 7 (mean 8±8; n=3) in HSCs/progenitors (CD34$^+$CD10$^-$CD19$^-$), 132 (mean 161±172; n=4) in Pro-B cells (CD34$^+$CD10$^+$CD19$^+$), 17 (mean 17±13; n=4) in Pre-B cells (CD34$^-$CD10$^+$CD19$^+$), 66 (mean 66±86; n=2) in mature B-cells (CD34$^-$CD10$^-$CD19$^+$) and 55 (mean 64±51; n=3) in mesenchymal cells from human BM (stromal cells). Asterisks, analysis of means with Welch's t-test; ∗, p<0.01 (except Pro-B cells, p<0.03) compared with the TEL-AML1 ALL subgroup.

The BMP2 expression values for the TEL-AML1 rearranged samples were distributed over a wide range. The median BMP2 expression was slightly lower in the TEL-AML1 group than in the hyperdiploid ALL group but higher than in the control ALL subgroup. By contrast, the comparison of the TEL/AML1 ALL subgroup with the healthy control cells showed significant differences. The median BMP2 expression was higher than in the normal Pro-B cells (p<0.03), which had the highest expression of the control cells, and was considerably higher (p<0.01) than in the HSCs/progenitor subset. The results are in accordance with the expression data generated in the analyses of the cell lines showing that the hyperdiploid ALL cell line MHH-CALL2 had a higher expression of BMP2 than the TEL-AML1 ALL cell line REH and a significantly higher expression than the other ALL cell lines tested. It is conceivable that the strong expression of BMP2 in hyperdiploid and TEL-AML1 rearranged ALL reflects a pathway dependence, which could be exploited therapeutically.

The expression of Smad1, Smad4 and Smad5 was only measured in the ALL samples. The Smad1 median expression of the TEL-AML1 rearranged ALL subgroup was almost 3-fold higher than in the hyperdiploid ALL and the control ALL subgroup. The distributions of the expression values showed substantial deviations in the TEL-AML1 and control ALL subgroup. The differences in the expression values for Smad4 and Smad5 were only marginal between the three ALL subgroups; Smad4 median expression in the hyperdiploid ALL subgroup was slightly higher than in the TEL-AML1 and the control ALL subgroups; Smad5 median expression in the TEL-AML1 ALL and the hyperdiploid ALL subgroup were almost equal and slightly higher than in the control ALL subgroup.

The analysis of the OAZ expression showed significant differences between the three ALL subgroups and a significantly stronger expression in the ALL samples in comparison to the normal haematopoietic cells (Figure 23). OAZ was highly expressed in the TEL-AML1 ALL subgroup. The OAZ median expression in this subgroup was significantly higher than in the hyperdiploid ALL (p<0.01) and higher than in the control ALL subgroup. The OAZ expression values in the ALL subgroups were widely distributed and were almost not detectable in the haematopoietic samples. The comparison with the haematopoietic controls showed the highest expression in Pro-B cells, the median expression of which nevertheless was almost one log ratio lower than in the TEL/AML1 ALL samples, with minimum basal levels in HSCs/progenitors. The median expression of OAZ in the BM stromal cells was approximately on the level of the TEL-AML1 ALL subgroup, consistent with its known role in regulating BMP signalling essential for bone and cartilage formation[160,161].
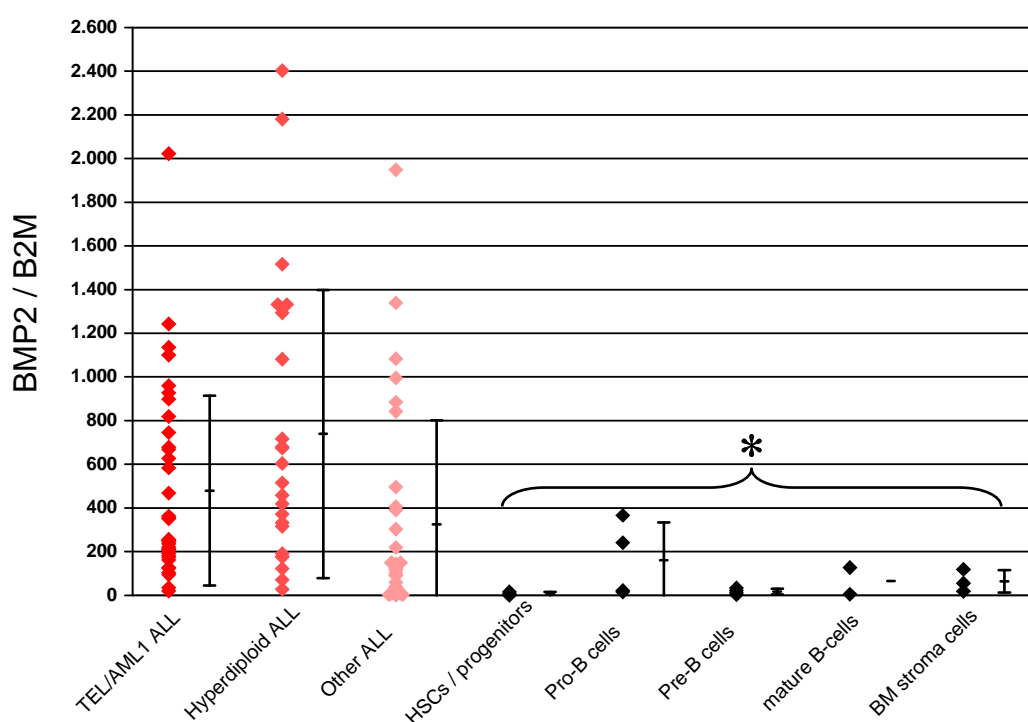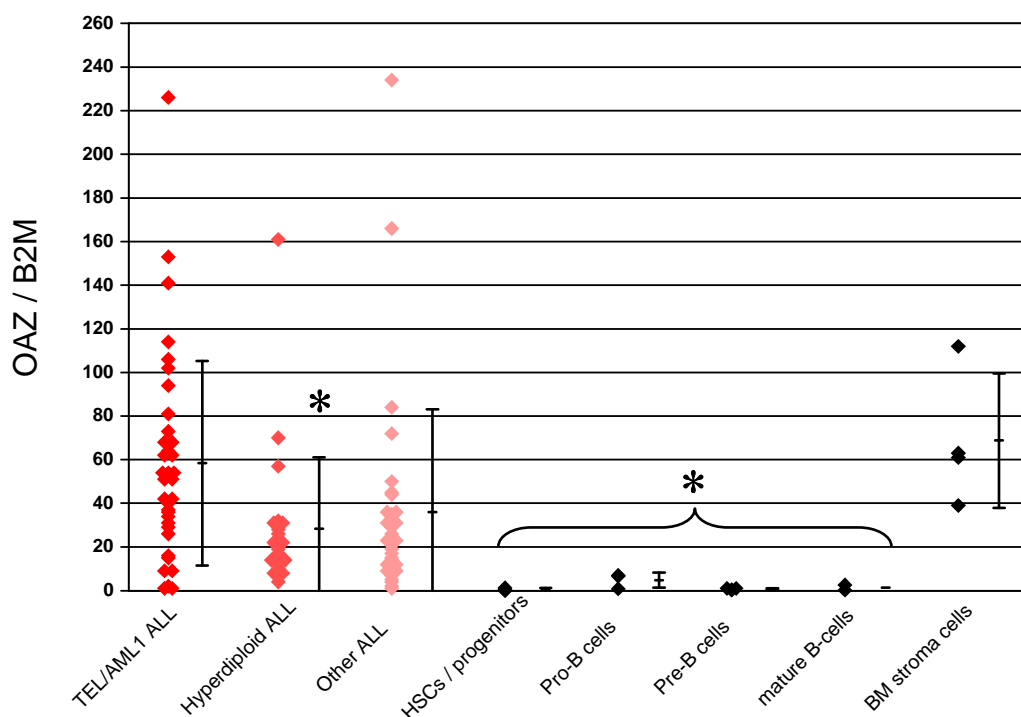
Figure 23: Quantification of OAZ expression by real time PCR in leukaemic and healthy BM cells. All expression values for the samples of one group are displayed as squares. The mean values (±sd) of a group are additionally shown as bars next to the expression values. OAZ median expression relative to B2M was 52 (mean 58±47; n=36) in the TEL-AML1 rearranged ALL group in comparison to 19 (mean 28±33; n=23) in the hyperdiploid ALL group, 23 (mean 36±47; n=33) in the control ALL group with different (other ALL) cases, 0.3 (mean 0.5±0.7; n=3) in HSCs/progenitors (CD34$^+$CD10$^-$CD19$^-$), 6.6 (mean 4.8±3.5; n=3) in Pro-B cells (CD34$^+$CD10$^+$CD19$^+$), 0.7 (mean 0.7±0.4; n=4) in Pre-B cells (CD34$^-$CD10$^+$CD19$^+$), 1.4 (mean 1.4±1.7; n=2) in mature B-cells (CD34$^-$CD10$^-$CD19$^+$) and 62 (mean 69±31; n=4) in mesenchymal cells from human BM (stroma cells). Asterisks, analysis of means with Welch's t-test:; ∗, p<0.01; compared with the TEL-AML1 ALL subgroup.

The expression pattern of EBF1 was comparable in all three ALL subgroups (Figure 24) and differences between the subgroups were not significant. In the normal control cells an increase of EBF1 from basal levels in HSCs/progenitors to a maximum level in Pro-B cells was detectable, which was lower but comparable to the ALL samples. The EBF1 expression gradually decreased from the pre-B cell stage to mature B-cells. This observation is in line with the normal onset of EBF1 activity during B-cell development (see 1.2). To test for a potential correlation between OAZ and EBF1 expression levels in the leukaemic patient samples, a Pearson correlation was calculated. Including all the samples from the three ALL subgroups the coefficient was 0.19, for the TEL-AML1 ALL subgroup 0.16, for the hyperdiploid ALL subgroup 0.6 and for the control ALL subgroup 0.3. Overall, there is no correlation between the expression of OAZ and EBF1 in the ALL samples tested.
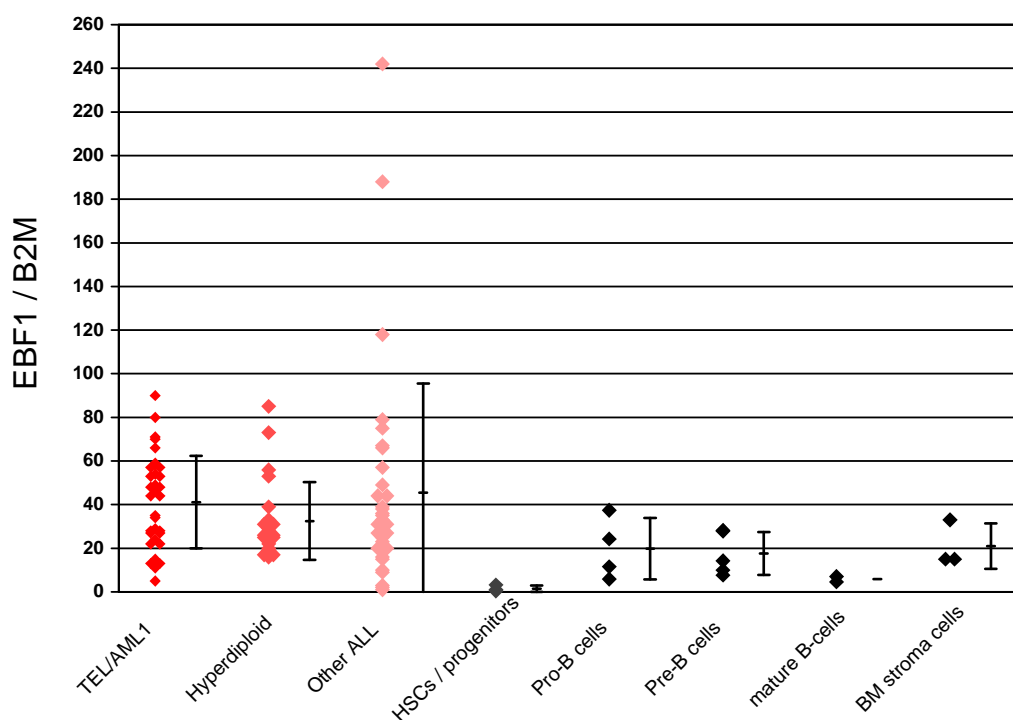
Figure 24: Quantification of EBF1 expression by real time PCR in leukaemic and healthy BM cells. All expression values for the samples of one group are displayed as squares. The mean values (±sd) of a group are additionally shown as bars next to the expression values. EBF1 median expression relative to B2M was 44 (mean 41±21; n=35) in the TEL-AML1 rearranged ALL group in comparison to 26 (mean 32±18; n=23) in the hyperdiploid ALL group, 31 (mean 46±50; n=34) in the control ALL group with different (other ALL) cases, 1 (mean 1.5±1.5; n=3) in HSCs/progenitors (CD34$^+$CD10$^-$CD19$^-$), 18 (mean 20±14; n=4) in Pro-B cells (CD34$^+$CD10$^+$CD19$^+$), 14 (mean 18±10; n=5) in Pre-B cells (CD34$^-$CD10$^+$CD19$^+$), 5.9 (mean 5.9±1.8; n=2) in mature B-cells (CD34$^-$CD10$^-$CD19$^+$) and 15 (mean 21 ±10; n=3) in mesenchymal cells from human BM (stromal cells).

4.4.3 OAZ

After measurement of high OAZ mRNA expression levels, especially in TEL-AML1 ALL patient samples, the goal was to detect OAZ on the protein level. Specific antibodies were tested successfully on Western Blot level with isolated whole cell protein lysates from HEK-293 cells transfected with the cloned OAZ expression plasmid. The detection of OAZ in cell lines and in frozen primary ALL samples failed using conventional techniques. Also enrichment by immunoprecipitation did not improve the detection of endogenous OAZ in the available protein samples. Therefore ALL cell lines were additionally analysed by flow cytometry. Only one cell line tested, the TEL-AML1 rearranged cell line REH, was highly positive for OAZ. More than 93% of the REH cells showed a strong and specific fluorescence signal (Figure 25). This result underlines the relevance and former observed high OAZ expression for TEL/AML1 rearranged ALL.
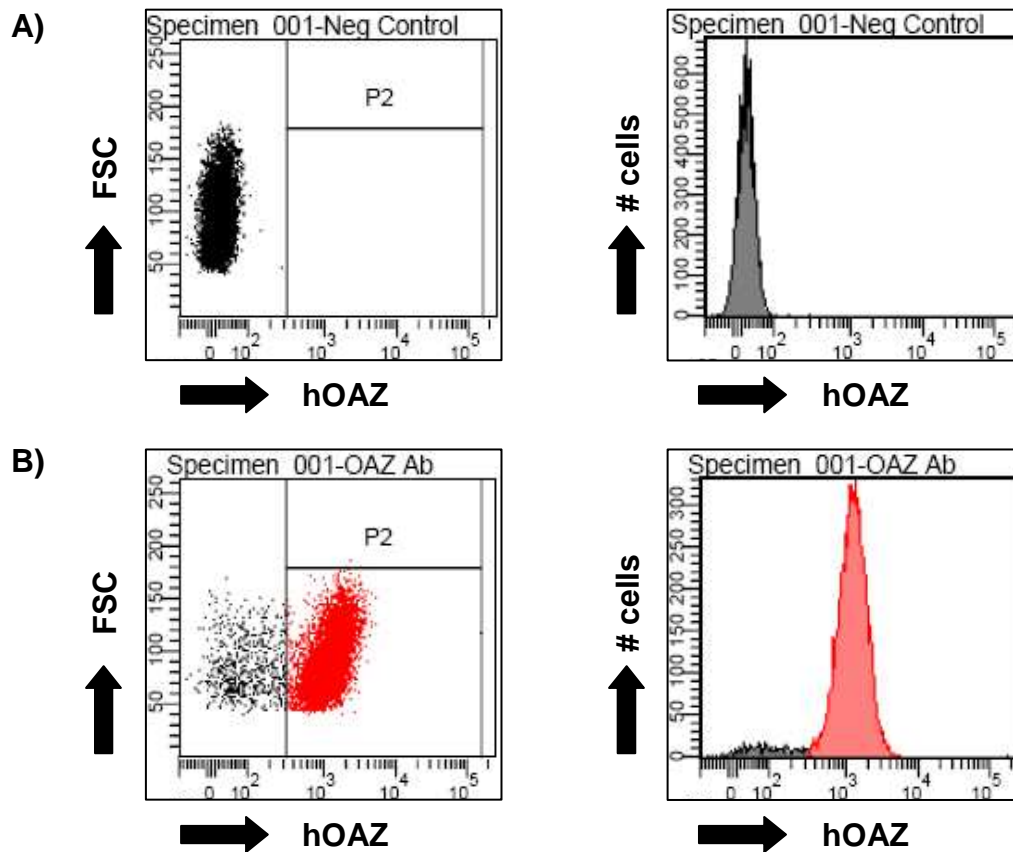
Figure 25: OAZ expression in TEL/AML1 ALL cell line REH. REH cells were isolated and human OAZ detected by FACS. The upper plots (A) show the negative control sample and the lower plots (B) the sample stained with OAZ primary and FITC secondary antibodies showing that more than 93% of the cells were OAZ positive. hOAZ = detection of human OAZ protein in the FITC channel of the FACS, FSC = forward scatter

4.5 OAZ/EBF1 protein-protein interactions

It was previously shown that the zinc-finger protein OAZ can modulate the transcriptional activity of EBF1 by specifically binding to it with its zinc-fingers 28-30[110,128,131]. OAZ protein bound EBF1 in a yeast two-hybrid system and a stable complex of both could be detected by co-immunoprecipitation (Co-IP) and *in-vitro* binding assays. EBF1-mediated transcriptional activation was suppressed in reporter assays by enforced expression of OAZ[128]. On the other hand it is known that OAZ is able to associate with an BMP2-mediated active Smad1/Smad4 complex with its zinc fingers 14-19, thereby forming a higher complex, which is able to activate specific target genes containing BMP responsive elements (BRE)[110]. The use of the different zinc fingers in the binding of EBF1 or the Smad1/Smad4 complex is thought to be mutually exclusive and suggests a dual role of OAZ in the regulation of different signalling pathways[110].

To test the possible interaction of OAZ and EBF1 in native leukaemia, a Co-IP system (3.13.6) was established. HEK-293 cells were either transfected (3.12.9) with OAZ or EBF expression plasmids (3.8.3) or co-transfected with both of them. Nuclear extracts of the transfected cells were isolated (3.13.3) and used in Co-IPs. Specific pull down of one of the interaction partners by IP was performed by anti-EBF1 or anti-OAZ/anti-Flag antibodies leading to a co-pulldown of the other. The co-precipitated OAZ/EBF complex partner was detected after separation and blotting (3.13.4/3.13.5) of the immunoprecipitate by the use of anti-OAZ/anti-Flag or anti-EBF antibodies. The Co-IPs were also performed to reconfirm the published data[128,131] and to further test the cloned OAZ and EBF1 expression plasmids in their ability to generate wild type OAZ and EBF1 proteins necessary for further functional *in-vitro* and *in-vivo* studies. The interaction of OAZ and EBF1 was examined by anti-EBF1 antibody Co-IP with OAZ protein in the presence of EBF1 protein (Figure 26). OAZ could be co-immunoprecipitated in the presence of EBF1 protein (lane 1), but not when EBF1 was replaced by the pcDNA3.1(+) empty vector (lane 3), supporting the observation of a specific interaction between OAZ and EBF1.
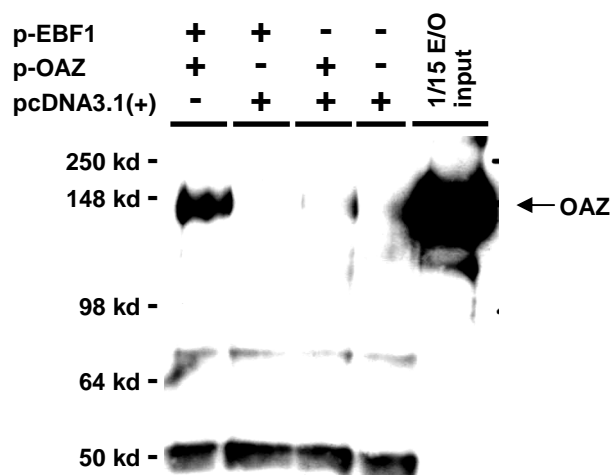
Figure 26: Co-immunoprecipitation of OAZ and EBF1 with anti-EBF1 antibody. Nuclear cell extracts from HEK-293 cells transfected with different expression constructs were mixed with anti-EBF1 antibody (#sc-15888) and Protein-G agarose beads. After being washed, proteins were extracted from the beads with 60 µl of 1x Leammli buffer and loaded on a 12% SDS-PAGE and detected after Western Blot with the use of Sigma Aldrich anti-Flag antibody. One-fifteenth of the input of the OAZ and EBF1 co-transfected lysate was used as a reference.

The reverse Co-IP with anti-OAZ antibody or anti-Flag antibody (pull down of the OAZ-FLAG fusion protein) was also successful (data not shown). EBF1 could only be co-immunoprecipitated in the presence of OAZ protein, but not when OAZ was replaced by the pcDNA3.1(+) empty vector. In conclusion, it was possible to demonstrate a protein-protein interaction of OAZ and EBF1 by Co-IP from nuclear extracts of HEK-293 cells transfected with OAZ and EBF1 expression plasmids. For the co-precipitation of OAZ respectively EBF1

only the specific anti-OAZ and anti-EBF1 antibodies were suitable. Since OAZ was not detectable in ALL cell lines by Western Blot or IP as well as in cryopreserved ALL patient samples, we were not able to show the OAZ/EBF1 interaction in leukaemic cells on the protein level.

4.6 Transplantation of ALL cells into NOD/*scid* mice

The strong OAZ expression measured in ALL cell lines and patient samples (4.4.1 and 4.4.2) is a possible cause for the maturation arrest in TEL-AML1 rearranged ALL and potentially also beyond that subgroup. Using immunodeficient NOD/*scid* mice, which serve as a model for human haematopoietic engraftment and differentiation[135,136,162], we studied the behaviour of ALL cells in an *in-vivo* situation. The mouse model is also suitable for the xenotransplantation of treated CD34^{+} cells to test their ability to induce a gross leukaemia. The goal was to engraft ALL patient cells and amplify them *in-vivo*. Upon apparent illness of the mice, ALL cells were isolated from bone marrow, spleen or peripheral blood and were further analysed for the expression of OAZ, EBF1 and BMP2. It was restudied if the expression levels initially measured in the patient samples stood constant in the *in-vivo* situation and was not an unspecific artifact. Additionally, engrafted cells were sorted if possible, depending on the expression of different cell surface antigens. Hereby, leukaemic subpopulations could be further characterised regarding BMP2-dependent signalling and target protein expression. In a first experiment (# 1) ALL samples from nine different ALL patients (Table 7), (TEL/AML1, n=3; hyperdiploid, n=3 and BCR/ABL, n=3), were used and transplanted into two mice per patient. Between 0.05-1.67x10^{7} vital cells were transplanted into sublethal irradiated (5.5 min with 350 cGy) NOD/*scid* mice by tail vein injection. The viability of the thawed cells varied from 20% to 84%.

ALL #	ALL Subtype	Viability	# of cells / mice
7168		83,3%	0.48 x 10e7
7172	BCR-ABL	64,7%	0.40 x 10e7
7208		57,5%	0.51 x 10e7
131		84,2%	0.98 x 10e7
136	TEL/AML1	20,0%	0.05 x 10e7
140		59,2%	0.40 x 10e7
7145		73,5%	1.67 x 10e7
7185	hyperdiploid	54,0%	0.47 x 10e7
7196		21,6%	0.29 x 10e7

Table 7: ALL patient samples used for the NOD/*scid* mice transplantation experiment #1. The ALL # (3.4.4), the specific ALL subtype, viability of the used cells after thawing and the # of calculated viable cells used per mice and patient is listed.

Engraftment of human ALL cells in the mice was analysed after 5 to 26 weeks post transplantation. When the mice became ill (or died) they were sacrificed and their organs were analysed. In five of 18 mice between 0.9-98% human cells could be detected either in

the BM or the spleen (Table 8 and Figure 27). The engraftment was detectable in two mice transplanted with cells from two TEL/AML1 rearranged ALL patients (#131 and #140) and in three mice transplanted with cells from two hyperdiploid ALL patients (#7145 and 7196).

ALL #	ALL Subtype	Mouse #	Time post transpl.	% human cells
131	TEL-AML1	2	136 days	69% CD10 in BM / 98% CD10 in spleen
140		2	76 days	11% CD45 in spleen
7145	hyperdiploid	1	79 days	2.3% CD45 in BM / 2.2% CD45 in spleen
		2	105 days	22% CD45 in BM
7196		2	169 days	0.9% CD45 in BM

Table 8: Initial transplantation of human ALL samples into NOD/*scid* mice (experiment #1). ALL samples with successful human engraftment in NOD/*scid* mice after transplantation of human ALL samples are shown with ALL # (3.4.4), the specific ALL subtype, the # of the transplanted mice, the time after transplantation when the mice were analysed and the percentage of human engraftment in different organs detected by the described specific human CD antibodies.

From the spleen of mice #2, transplanted with TEL/AML1 sample #131, human cells could be isolated. They were analysed by FACS and sorted based on CD34, CD10 and CD19 expression. Two subpopulations were attained that showed either a CD34⁻CD10⁺CD19⁺ or CD34⁺CD10⁺CD19⁺ antigen expression. The two subpopulations were used for the analysis of specific gene expression (Figure 27 and Figure 31).

Figure 27: Engraftment of ALL sample #131 after transplantation into NOD/*scid* mice #2. Spleen cells were isolated and human engraftment detected by FACS with CD34 and CD10 antibodies. The left plot shows the isotype control sample and the right one the CD34 and CD10 antibodies stained sample were more than 98% of human CD10 positive cells (Q2 + Q4) were detectable. hCD34 = detection of human CD34 antigen in the FITC channel of the FACS, hCD10 = detection of human CD10 antigen in the PE channel of the FACS.

From three mice with human engraftment cells were used for a retransplantation experiment (Table 9). Frozen BM of one mouse transplanted with hyperdiploid sample #7145 and one with TEL/AML1 sample #140 was used and retransplanted into two and one mice respectively. From the mice #2, transplanted with TEL/AML1 ALL sample #131, and the highest human engraftment of >98%, fresh BM and spleen were retransplanted into two and three mice respectively. The three mice transplanted with the hyperdiploid ALL samples #7145 and the TEL/AML1 ALL sample #140 showed no human engraftment when they were examined 13-19 weeks later. From the five mice retransplanted with TEL/AML1 ALL sample #131, four had a human engraftment ranging between 32-93% (Table 9 and Figure 28) and one mouse died of unknown reasons.

ALL #	ALL Subtype	Mouse #	Time post transpl.	% human cells
131	TEL-AML1	1	100 days	22% CD34 in BM / 93% CD45 in spleen
		2	118 days	32% CD45 in spleen
		4	126 days	64% CD45 in spleen
		5	132 days	97% CD19 in spleen

Table 9: 1st retransplantation of human ALL samples into NOD/*scid* mice (experiment #1). ALL samples with successful human engraftment in NOD/*scid* mice after 1st retransplantation of human ALL samples are shown with with ALL # (3.4.4), the specific ALL subtype, the # of the transplanted mice, the time after transplantation when the mice were analysed and the percentage of human engraftment in different organs detected by the described specific human CD antibodies.

From human cells in the spleen of one of the mice, retransplanted with TEL/AML1 ALL sample #131, two subpopulations with either CD34$^-$CD19$^+$ or CD34$^+$CD19$^+$ expression of CD antigens were sorted and analysed for gene expression (Figure 31).
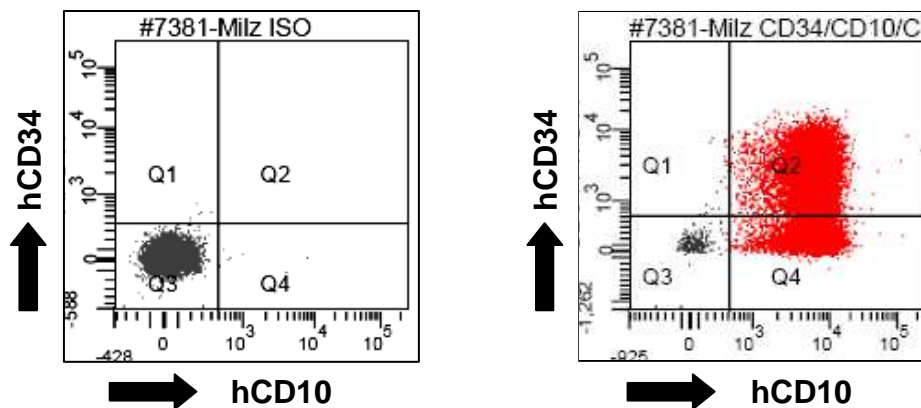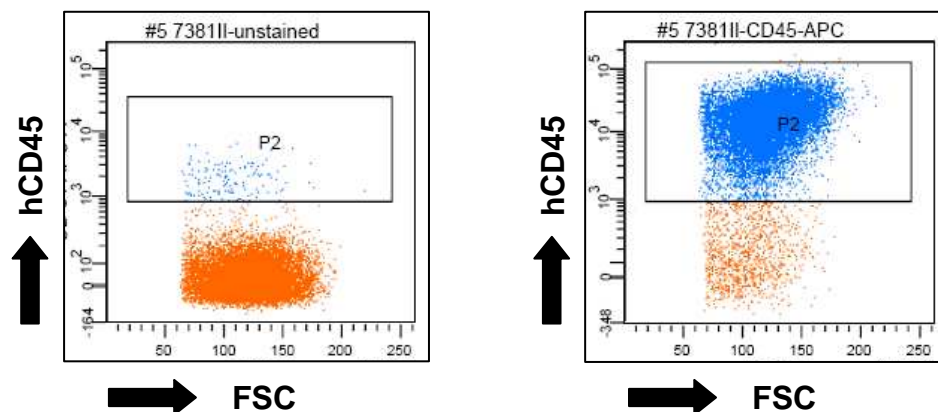

Figure 28: Engraftment of ALL sample #131 after 1st retransplantation into NOD/*scid* mice #1. Spleen cells were isolated and human engraftment detected by FACS with CD45 antibody. The left plot shows the unstained control sample and the right one the CD45 antibody stained sample were more than 93% of human cells (P2) were detectable. hCD45 = detection of human CD45 antigen in the APC channel of the FACS, FSC = forward scatter of the FACS.

The engrafted human cells from the spleen of one of the mice retransplanted with TEL/AML1 sample #131 were retransplanted a second time (Table 10). Four different mice were transplanted with $2x10^6$ fresh spleen cells each. Between 6-12 weeks later the mice were analysed and all mice showed a human engraftment ranging between 0.7% and 91% (Table 10 and Figure 31).

ALL #	ALL Subtype	Mouse #	Time post transpl.	% human cells
131	TEL-AML1	1	43 days	3.1% CD45 in BM
		2	43 days	0.7% CD45 in BM
		3	74 days	29% CD45 in blood / 70% CD45 in BM / 82% CD10 in spleen
		4	78 days	91% CD19 in spleen

Table 10: 2nd retransplantation of human ALL samples into NOD/*scid* mice (experiment #1). ALL samples with successful human engraftment in NOD/*scid* mice after 2nd retransplantation of human ALL samples are shown with ALL # (3.4.4), the specific ALL subtype, the # of the transplanted mice, the time after transplantation when the mice were analysed and the percentage of human engraftment in different organs detected by the described specific human CD antibodies.

From the spleen of mice #4, showing a human engraftment of more than 91% detected by CD19 expression, subpopulations were sorted (Figure 29 and Figure 30). Two populations with CD34⁻CD10⁺CD19⁺ or CD34⁺CD10⁺CD19⁺ antigen expression were gained and subsequently analysed for specific gene expression (Figure 31).

Figure 29: Engraftment and sorting of ALL sample #131 after 2nd retransplantation into NOD/*scid* mice #4 (control). Spleen cells were isolated and human cells detected and sorted by FACS with CD34, CD19 and CD10 antibodies. The plot shows the unstained control sample stained with CD34 and CD19 antibodies. hCD34 = detection of human CD34 antigen in the FITC channel of the FACS, hCD19 = detection of human CD19 antigen in the APC channel of the FACS.
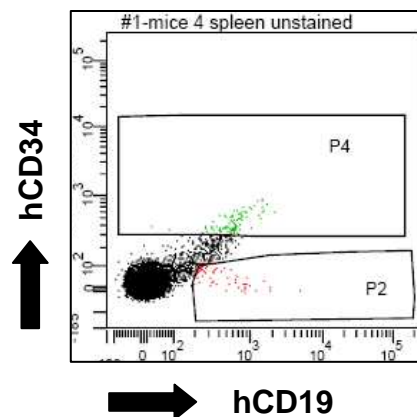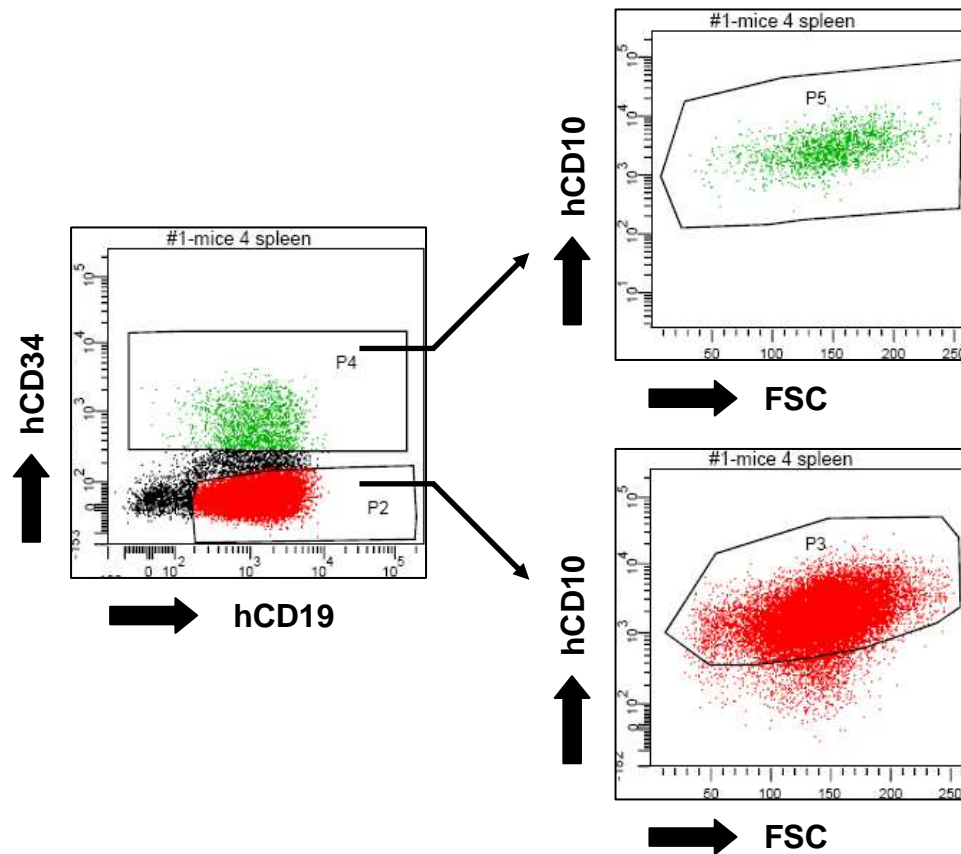
Figure 30: Engraftment and sorting of ALL sample #131 after 2nd retransplantation into NOD/*scid* mice #4. Spleen cells were isolated and human cells detected and sorted by FACS with CD34, CD19 and CD10 antibodies. The left plot shows the sample stained with CD34 and CD19 antibodies were more than 91% of the cells were of human origin (P2 = CD34⁻CD19⁺, P4 = CD34⁺CD19⁺). Shown are the sorting gates of the CD34⁺CD19⁺CD10⁺ subpopulation (right upper plot) sorted via gate P4 and P5 and of the CD34⁻CD19⁺CD10⁺ subpopulation (right lower plot) sorted via gate P2 and P3. hCD34 = detection of human CD34 antigen in the FITC channel of the FACS, hCD19 = detection of human CD19 antigen in the APC channel of the FACS, hCD10 = detection of human CD10 antigen in the PE channel of the FACS, FSC = forward scatter of the FACS.

In a subsequent second experiment (# 2) ALL samples from eight different patients, four with TEL/AML1 rearrangement or hyperdiploid karyotype respectively, were used and transplanted into one mouse per patient. A mouse transplanted with TEL/AML1 sample #43 and a human engraftment of >94% in the spleen (detected by CD10) was used for sorting. The sorted CD34⁻CD10⁺CD19⁺ subpopulation was used to analyse the OAZ expression level (Figure 31). The CD34⁺CD10⁺CD19⁺ subpopulation seen in the other engrafted ALL samples was absent. From another mouse transplanted with TEL/AML1 sample #192 and a human engraftment of 65% in the spleen (detected by CD19) unsorted cells were used to analyse the gene expression level (Figure 31).

4.6.1 OAZ Expression *in-vivo*

The transplantation of frozen ALL cells into NOD/*scid* mice led to an engraftment of initially transplanted human cells in 9 of 28 mice (32%), not depending on the initial viability and subtype of the thawed ALL cells. Serial retransplantation of isolated cells was successful twice for TEL/AML1 sample #131 with an engraftment of human cells in almost all mice transplanted. The engrafted human cells were isolated from BM or spleen and sorted into subpopulations if possible. These engrafted ALL samples were subsequently analysed for the expression of OAZ (Figure 31), EBF1 and BMP2 (data not shown).
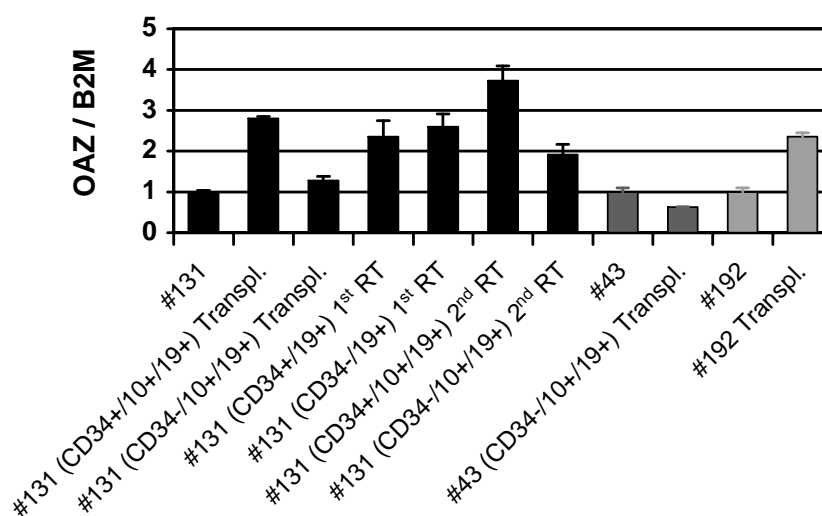

Figure 31: Quantification of OAZ expression by real time PCR of engrafted ALL samples. OAZ expression levels quantitated by real time PCR in ALL patient samples transplanted into NOD/*scid* mice. Cells were isolated from mice BM or spleen and sorted into subpopulations if possible. Bars show mean (± sd) OAZ expression relative to B2M (normalised to 1 for each of the original samples) for the ALL sample #131, the $CD34^+CD10^+CD19^+$ and $CD34^-CD10^+CD19^+$ subpopulations from the initially transplantation, the $CD34^+CD19^+$ and $CD34^-CD19^+$ subpopulations from the 1st retransplantation, the $CD34^+CD10^+CD19^+$ and $CD34^-CD10^+CD19^+$ subpopulations of the 2nd retransplantation, the ALL sample #43, the $CD34^-CD10^+CD19^+$ subpopulation from the initially transplantation, the ALL sample #192 and the unsorted population from the initially transplantation. Transpl. = transplantation, 1st RT = 1st retransplantation and 2nd RT = 2nd retransplantation.

The transplanted and engrafted cells of ALL sample #131 showed an OAZ expression in the same log range as the original measured patient sample. The OAZ expression was slightly increased in the $CD34^-CD10^+CD19^+$ subpopulation from the initial transplantation and was almost 4-fold higher in the $CD34^+CD10^+CD19^+$ subpopulation from the 2nd retransplantation. The differences detected could not be stated as significant. The OAZ expression in the transplanted ALL sample #43 was slightly decreased and in the transplanted ALL sample #192 more than 2-fold increased. The expression of EBF1 and BMP2 was also measured in the engrafted samples and the values were in the same log range as the initial transplanted ALL sample (data not shown). In conclusion, the phenotype of the transplanted ALL cells

remained relatively constant *in-vivo* and showed a constantly detectable but not significantly varying gene expression of the analysed genes OAZ, BMP2 and EBF1. Obviously, the initially measured expression values were not experimental artifacts due to the freezing and thawing of ALL patient samples or other handling procedures.

4.7 Disturbance of B-cell differentiation in HSCs

The aberrant upregulation of OAZ in TEL/AML1 rearranged ALL detected by real time PCR (3.3.2) and its interaction with the crucial B-cell development factor EBF1 were shown in an *in-vitro* system by Co-IP after transfection (3.13.6). A TEL/AML1 rearrangement in HSCs or B-lymphoid progenitors is considered the initial event in leukaemia development. An accumulation of additional mutations including an upregulation of OAZ might be sufficient to cause a full leukaemia phenotype through induction of the characteristic maturation arrest[1]. The aim of this work was to study potential mechanisms of the maturation arrest in B-lymphopoiesis focusing on the interplay between OAZ and EBF1. A γ-retroviral expression system was used (Figure 32) to modulate the expression of candidate genes[144].
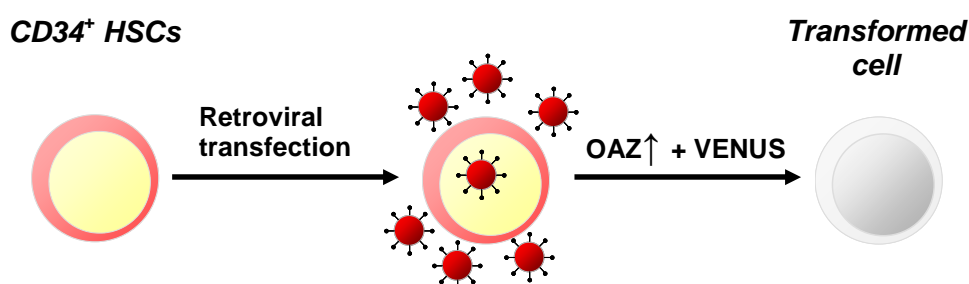
Figure 32: Schematic representation of retroviral infection of CD34^{+} HSCs leading to an expression of OAZ and the reporter protein VENUS. HSCs = hematopoietic stem cells, OAZ↑ + VENUS = OAZ and VENUS expression in the infected cells.

For this purpose, the CDS of OAZ was subcloned into the retroviral vector R1331-pRMys-iV (Figure 33). The vector harbours an expression cassette for the yellow fluorescent protein Venus as a reporter downstream of an internal ribosomal entry site (IRES) (Figure 34). Phoenix-gp cells were co-transfected (3.12.10) with the OAZ expression construct R1331-FlagHsOAZ(wt) or the empty control vector R1331-pRMys-iV in combination with suitable packaging plasmids encoding retroviral proteins with the help of the cacium-phoshate method.
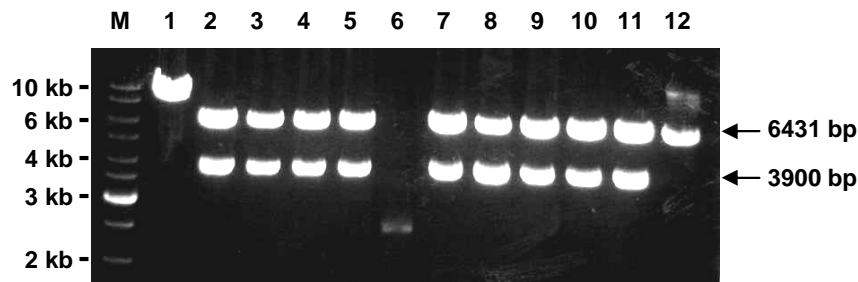
Figure 33: Subcloning of hOAZ into R1331-pRMys-iV vector. *EcoRI* digest of 12 clones of subcloned hOAZ CDS ligated in R1331-pRMys-iV vector separated on a 1 % TAE-Agarose gel. Size of hOAZ CDS insert is 3900 bp and of R1331-pRMys-iV backbone 6431 bp. M (GeneRuler DNA Ladder Mix size marker), 1-12 (number of different plasmid clones).
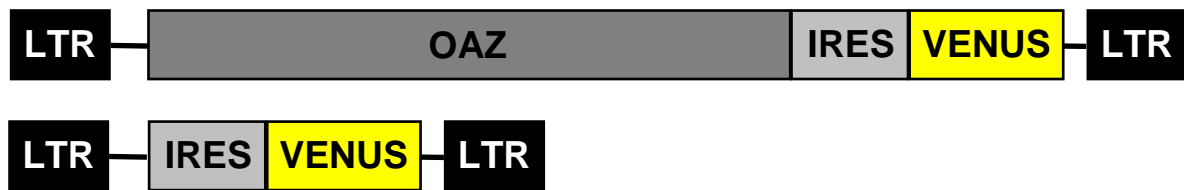
Figure 34: Retroviral OAZ expression constructs R1331-FlagHsOAZ(wt) (top) and R1331-pRMys-iV (bottom). LTR = long terminal repeat, IRES = internal ribosomal entry site

Retroviral supernatants were harvested and suitable titres ≥1x10^6 (3.12.11) were used for the infection of CD34$^+$ cells (HSC fraction) isolated from umbilical cord blood by immunomagnetic CD34$^+$ selection (3.12.8) of mononuclear cells (3.12.7) (Figure 35). The titres for the R1331-pRMys-IV control vector were always significantly higher in comparison to the R1331-FlagHsOAZ(wt) vector. Retroviral infection of CD34$^+$ cells (3.12.13) led to a genomic integration of the retroviral vector and a subsequent expression of OAZ and the VENUS reporter protein (Figure 36)[144]. The provirus was passed down to the next generation, through the stable integration into the genome of the target cell, when infected cells propagated. OAZ expressing cells could be detected by flow cytometric methods via the co-expression of the yellow fluorochrome VENUS in the infected cells.

Figure 35: FACS analysis of cord blood after CD34$^+$ selection. Number of human CD34 expressing cells after immunomagnetic CD34$^+$ selection. Shown is an unstained (left) and CD34 antibody stained (right) sample. hCD34 = detection of human CD34 antigen in the PE channel of the FACS.

The infection efficiencies of CD34$^+$ cells infected with the OAZ-virus ranged between 1.3%-35.3% (mean 12.7%±14.6%) and from 6.1%-63.6% (mean 28.8%±27.6%) for the control-virus. VENUS expressing cells were sorted (3.12.6) to a purity of greater than 95% (Figure 36).

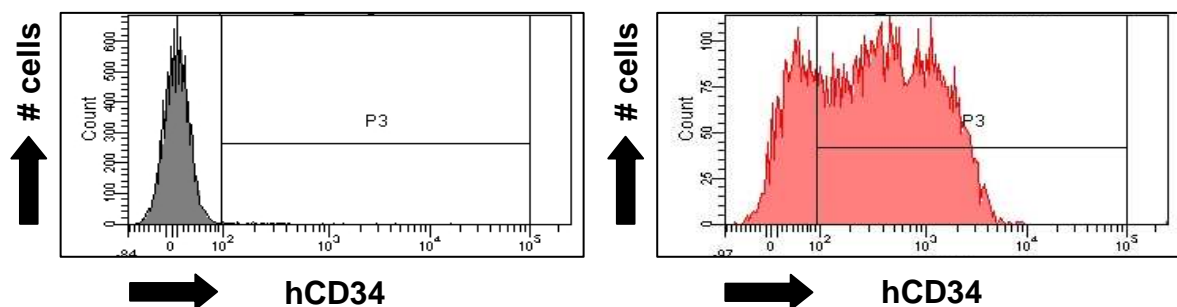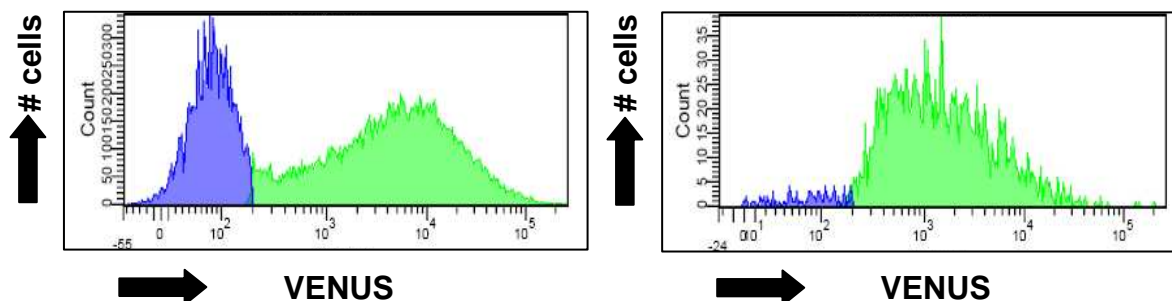**Figure 36: FACS analysis of retroviral infected CD34$^+$ cells**. Number of VENUS expressing cells after infection with R1331-pRMys-iV, before (left) and after sorting (right). Expression of VENUS is shown in green and negative not infected cells are shown in blue.

Infected cells of high purity were used for further *in-vitro* culture under B-cell differentiation conditions (3.12.14). Between 5x10^3-2x10^4 CD34$^+$ cells (per well of a 24-well plate) were resuspended in B-cell differentiation medium and were cultured for 5-15 days to proliferate and differentiate to the B-cell lineage. This was supported by a telomerase-immortalised human BM stromal cell line (hTERT-BMSC)[137] and a suitable combination of the human cytokines SCF, FLT3-L and IL-7 (Figure 37)[152,153,154].
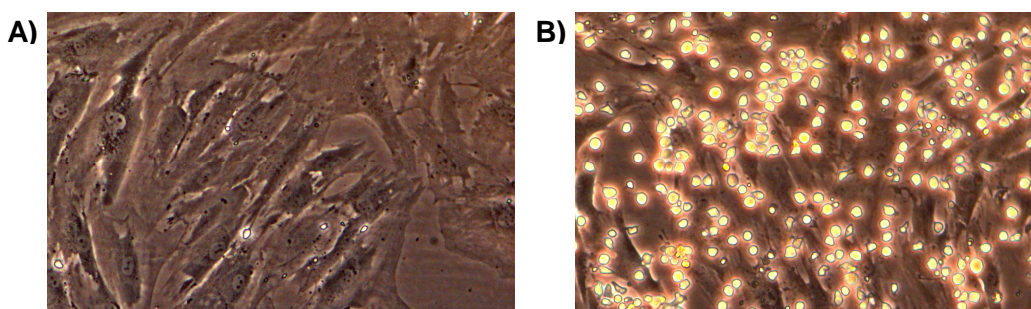
Figure 37: Dense stromal layer of hTERT-BMSC (A) and CD34$^+$ cells seeded on top of hTERT-BMSC (B). Phase contrast microscopy images; 400x magnification.

The presence of mesenchymal cells facilitates the growth and differentiation of primitive haematopoietic cells *In-vitro* and the maintenance of leukaemic cells[163,164]. At defined time points after cell expansion (cell population doubling within 3-4 days) they were detached from the stromal layer preventing contamination with hTERT-BMSC. Isolated cells were analysed by FACS which showed that on average 94% (± 1.7%) of the cells expressed VENUS i.e. the initially sorted cell population was maintained and expanded without loss of retroviral expression.

4.7.1 Detection of OAZ expression in infected cells

OAZ expression was quantitated for all samples showing only basal or absent levels in control-virus infected cells (Figure 38). By contrast, OAZ expression in with OAZ-retrovirus infected cells was 5-500-fold (mean 8.3-fold±6.2) higher except for one sample (Figure 38). The retrovirally-driven OAZ expression increased during the culture period and reached levels comparable to the analysed ALL samples.
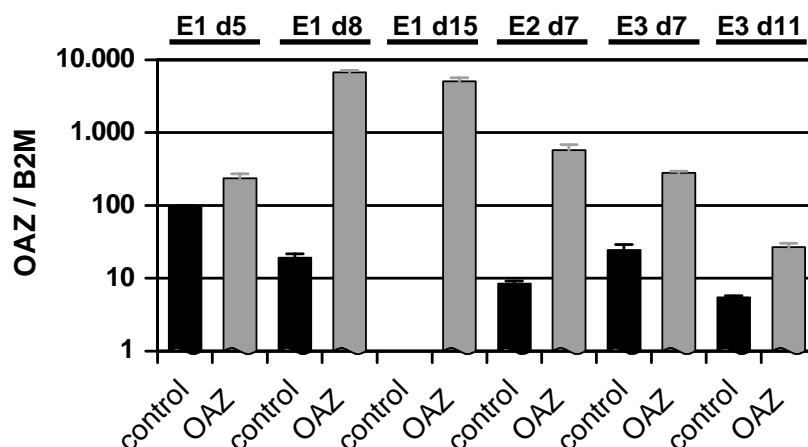
Figure 38: Quantification of OAZ expression by real time PCR of retroviral infected and subsequently cultured CD34+ cells. OAZ expression levels quantitated by real time PCR in CD34+ cells infected with OAZ or control retrovirus, sorted for VENUS expression and cultured for 5-15 days on a dense layer of hTERT-BMSC in B-cell differentiation medium. Bars show OAZ expression relative to B2M. E1, E2 and E3 = experiment 1, 2 and 3; d = day.

Harvested cells were also used for the isolation of protein (3.13.1) showing a constitutively and strong expression of OAZ during the observed *in-vitro* culture period (Figure 39).
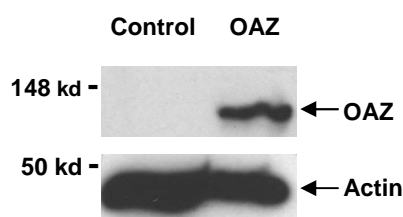
Figure 39: Detection of OAZ in whole protein lysate of retroviral infected and subsequently cultured CD34+ cells. 8% SDS-PAGE gel; PVDF membrane; detection of OAZ (top) by Santa Cruz anti-hOAZ antibody (1:1000) and detection of Actin (bottom), which served as loading control, by Sigma Aldrich anti-hActin antibody (1:3000).

4.7.2 Expression of B-cell specific surface markers

Retrovirally infected cells were analysed via FACS (3.12.5) towards the expression of B-cell specific CD antigens. Depending on the period of time, B-cell progenitors and later on immature B-cells were expected to arise from the initially seeded CD34+ cells during culture. The absolute number or relative amount of these B-cell subgroups should significantly differ

between cells infected with OAZ- or control-virus because of OAZ's interaction with EBF1. According to the classification of human B-cells and progenitors[59], antibodies against human CD34, CD10 and CD19 were used to characterise the cultured cells. CD34^{+} is expressed on HSCs[37,38], myeloid, T-lymphoid and B-lymphoid progenitors up to the Pro-B cell stage, whereas CD10 is an early B-lymphoid marker and CD19 a marker characteristic for committed B-cells expressed on cells from the Pro-B stage to mature B-cells (1.2). Due to the relatively low number of cells available after *in-vitro* culture only samples from one independent experiment could be comprehensively analysed for the expression of the described surface CD antigens. The cells from experiment #1 were analysed after 5, 8 and 15 days of culture. OAZ expression in infected cells led to a significant reduction of the antigens CD34 and CD19. After 5 days of culture 27.1% of the control cells expressed CD34 which was expressed on only 2.8% of OAZ-virus infected cells. 13.1% of the control cells expressed the B-cell marker CD19 contrary to 1.8% in the OAZ-virus cells (Figure 40).
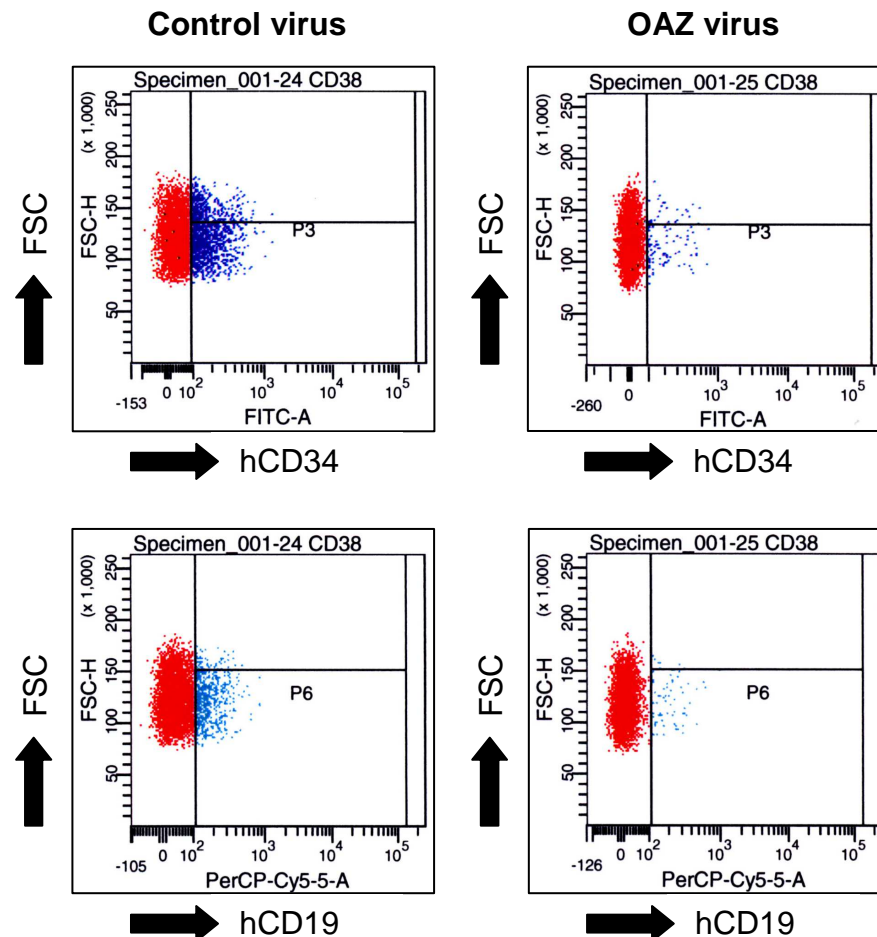
Figure 40: FACS analysis of retroviral infected CD34^{+} cells cultured for 5 days on stromal cells. Cultured cells retroviral infected with control (left plots) or OAZ virus were detached from the stromal layer and haematopoietic and B-cell development was detected by CD34 (upper plots) and CD19 (lower plots) antibodies. Reduction of CD34 and CD19 expression was detectable in cells infected with OAZ virus meaning a repression of B-cell development. hCD34 = detection of human CD34 antigen in the FITC channel of the FACS, hCD19 = detection of human CD19 in the PerCP-Cy5.5 channel of the FACS and FSC = forward scatter of the FACS.

The detection of CD10 gave no consistent results, but it is likely that the cells which expressed CD19 co-expressed CD10 as well (1.2). After 8 days of culture 16.9% of the control cells expressed CD34 which was almost 10-fold more than for the OAZ-virus infected cells were only 1.7% of the cells expressed CD34. 7.6% of the control cells and 1.4% of the OAZ-virus infected cells expressed CD19. The cells isolated after 15 days showed no evaluable results in the FACS analysis. The analysis of the two samples from day 5 and 8 showed additionally that the expression of CD19 decreased during this period of time suggesting that the culture conditions used were not fully sufficient to support the generation and expansion of B-cells with high efficiency and stringency. But nevertheless, it can be concluded that the expression of OAZ in HSCs led to a repression of the ability of haematopoietic cells to differentiate to the B-cell lineage, probably by interfering with EBF1.

4.7.3 Repression of EBF1 target genes

Cultured cells infected with OAZ-virus showed a significant reduction of the present populations expressing CD34 and CD19 under conditions that should support normal B-cell growth. This negative effect on the generation of B-cells is most likely mediated by a binding of OAZ to EBF1, a crucial factor in the regulation of B-cell development, leading to its sequestration (4.5). Therefore EBF1 expression was quantitated to analyse if there was any correlation between OAZ expression and the expression of EBF1 in the infected cells (Figure 41). Like in the ALL samples analysed before (4.4.2) no obvious correlation was detectable.
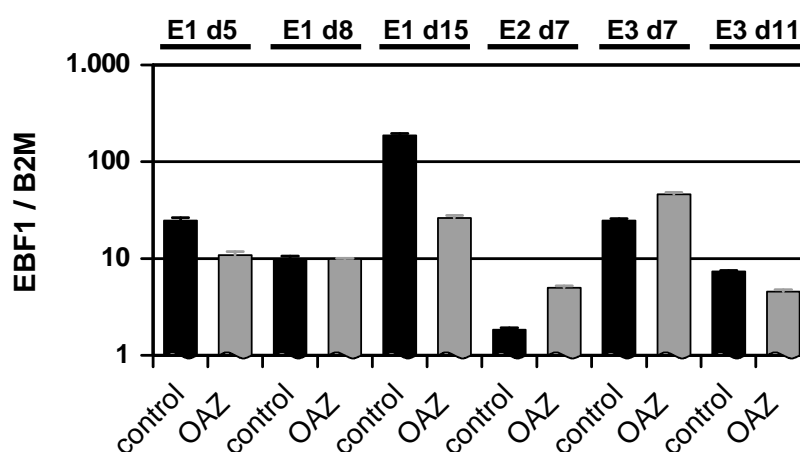
Figure 41: Quantification of EBF1 expression by real time PCR of retroviral infected and subsequently cultured CD34^{+} cells. EBF1 expression levels quantitated by real time PCR in CD34^{+} cells infected with OAZ or control retrovirus, sorted for VENUS expression and cultured for 5-15 days on a dense layer of hTERT-BMSC in B-cell differentiation medium. Bars show EBF1 expression relative to B2M. E1, E2 and E3 = experiment 1, 2 and 3; d=day.

Preliminary gene expression analysis of transcriptional regulators of B-lymphopoiesis (1.2) was performed via semi-quantitative RT-PCR (data not shown). PU.1 a regulator of myeloid and lymphoid development and E2A encoding the essential B-lymphoid regulators E12 and

E47 were easily detectable but with no obvious differences between control- and OAZ-virus infected cells. PAX5 acting downstream of EBF1 in the regulation of B-cell development had only basal expression levels in the analysed cells. RAG1 and IL-7R expression was not detectable and the expression of the terminal deoxynucleotidyl transferase (TdT) transcript did not show a differential pattern in the analysed cells. By contrast, the expression of the known direct EBF1 target genes CD79a (Igα), CD79b (Igβ), IGLL1 (λ5) and VpreB, necessary for the proper formation of the pre-B-cell receptor (pre-BCR), were apparently reduced in the cells infected with the OAZ-virus. The pre-BCR mediates the proliferation and expansion of B-cell progenitors and is essential for the generation of B-cells in general. Downregulation or block of pre-BCR expression has serious effects on normal B-cell development characteristic for an EBF1 knock-out. Real time PCR was used to analyse the downregulation of the EBF1 target genes more precisely and to quantitate the expression levels. Differences in EBF1 expression obviously directly correlate with the expression of direct EBF1 target genes making it necessary to normalise the EBF1 levels of the samples. This made it possible to quantitate the molecular effects of OAZ expression on the regulation of EBF1 and EBF1 target genes.

For CD79a and CD79b comparable samples from three independent experiments (E1 d5, E2 d7 and E3 d7), cultured *in-vitro* for 5-7 days post infection, were analysed (Figure 42). The expression of CD79a was significantly (p<0.02) reduced with an average of more than 63% in the cells infected with OAZ-virus, whereas the strength of CD79a repression varied between 45% and more than 80%.

Figure 42: Quantification of CD79a and CD79b expression by real time PCR of retroviral infected and subsequently cultured CD34$^+$ cells. CD79a and CD79b expression levels quantitated by real time PCR in CD34$^+$ cells infected with OAZ or control retrovirus, sorted for VENUS expression and cultured on a dense layer of hTERT-BMSC in B-cell differentiation medium. Bars show mean ± sd of the samples E1 d5, E2 d7 and E3 d7. Bars show CD79a and CD79b expression relative to EBF1 normalized to 1 for cells infected with control virus. E1, E2 and E3 = experiment 1, 2 and 3; d = day and $2^{-\Delta\Delta CP}$ = the real time PCR data is reported as a difference between ΔCP of Control and OAZ virus infected cells, where ΔCP is defined as the difference between the crossing point (CP) of the target gene and the EBF1 gene. Asterisks, analysis of means with Student's t-test; *, p<0.02; **, p<0.01.

The effect of OAZ expression on the EBF1-mediated expression of CD79b was even more pronounced. CD79b expression was highly significant (p<0.01) reduced with an average of more than 73% with a variation between 68% and more than 80% in the different cells infected with the OAZ-virus.

For IGLL1 and VpreB comparable samples from two independent experiments (E2 d7 and E3 d7), cultured *in-vitro* for one week after infection, were analysed (Figure 43). The expression of IGLL1 was highly significant (p<0.01) reduced in the OAZ-virus infected cells with an average of more than 81% and very low variation. The strongest effect of OAZ-virus infection on EBF1 target gene expression was observed for VpreB. The OAZ-virus infected cells showed in average a reduction of more than 87% in the expression level.
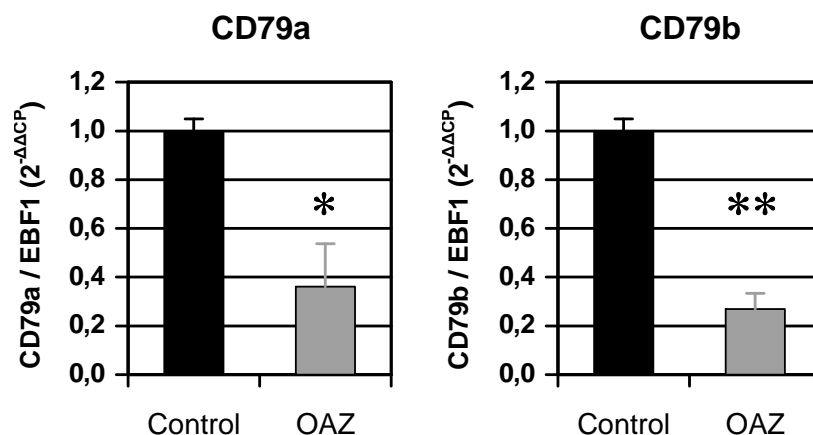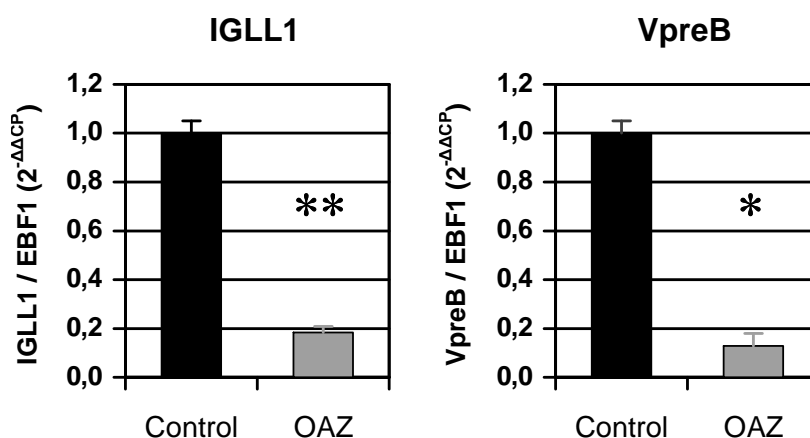

Figure 43: Quantification of IGLL1 and VpreB expression by Real Time PCR of retroviral infected and subsequently cultured CD34$^+$ cells. GLL1 and VpreB expression levels quantitated by real time PCR in CD34$^+$ cells infected with OAZ or control retrovirus, sorted for VENUS expression and cultured on a dense layer of hTERT-BMSC in B-cell differentiation medium. Bars show mean ± sd of the samples E2 d7 and E3 d7. Bars show IGLL1 and VpreB expression relative to EBF1 normalised to 1 for cells infected with control virus. E1, E2 and E3 = experiment 1, 2 and 3; d = day and $2^{-\Delta\Delta CP}$ = the real time PCR data is reported as a difference between ΔCP of Control and OAZ virus infected cells, where ΔCP is defined as the difference between the crossing point (CP) of the target gene and the EBF1 gene. Asterisks, analysis of means with Student's t-test: ∗, p<0.02; ∗∗, p<0.01.

In summary, enforced OAZ expression in human CD34$^+$ cells by retroviral infection was sufficient to downregulate the expression of four direct EBF1 target genes. Possibly by forming a protein-protein complex which leads to sequestration of EBF1 as shown before (4.5).

5 Discussion

Based on previous genome-wide transcriptome analyses the present study focused on the supposable aberrant activation of the BMP2-dependent pathway and its direct target protein OAZ. An activation of BMP2 signalling likely is a specific aberration in ALL that drives and maintains the leukaemic state of the cells. It was discovered that BMP2 and OAZ showed a strong expression in TEL/AML1 rearranged ALL contrary to haematopoietic control cells. Because OAZ is normally not expressed in B-cells, this implies a possible role of OAZ in leukaemic transformation due to its known role in negatively regulating EBF1 and the EBF1-mediated activation of target genes. Aberrant expression of OAZ in company with first hit events like the TEL/AML1 rearrangement could contribute to the characteristic maturation block and the initiation or propagation of leukaemia.

It was shown that OAZ and EBF1 interact on the protein level leading to EBF1 sequestration. This recapitulates recent knowledge. OAZ expression also remained constant and significantly high in ALL cells transplanted into NOD/*scid*. Furthermore we were able to show for the first time that expression of OAZ in haematopoietic progenitor cells in an *in-vitro* culture system was able to block B-cell differentiation. OAZ significantly blocked the activation of the crucial EBF1 target genes CD79a, CD79b, IGLL1 and VpreB which are necessary for proper pre-B-cell receptor (pre-BCR) formation and B-cell development. Additional *In-vitro* and *in-vivo* studies in the near future could modulate the expression of OAZ on the background of the TEL/AML1 rearrangement in haematopoietic cells defining its potential role in leukaemic transformation. This hopefully will lead to new promising and innovative treatment strategies targeting its noxious effects on B-cell differentiation

5.1 BMP2-signalling in ALL

During this work it was shown that the cytokine BMP2 was highly expressed in the TEL/AML1 ALL cell line REH consistent with other studies[161]. The Smad proteins which transducer the BMP- signal from the cell surface to the nucleus[99,105,107], were also significantly expressed. This suggests BMP2 signalling activity in these ALL cell lines. In contrast to that, BMP2 expression in other ALL cell lines was substantially lower. In normal haematopoietic stem cells Smad signalling is involved in self-renewal[114,119]; an abnormal upregulation of Smad signaling could therefore alter this crucial regulative program. Direct mutations in Smad genes are usually rare in leukaemia, but disruption or alterations have been linked to leukaemic transformation[114,119]. In analogy to the cell line analyses, a large cohort of ALL patient samples underwent a gene expression analysis of the BMP2 pathway.

The expression of BMP2 was significantly higher in TEL/AML1 rearranged ALL and hyperdiploid ALL patient samples in comparision to the haematopoietic control cells validating the initial transcriptom profiling data and the cell line analysis.

A strong Smad1 expression was observed in the TEL/AML1 ALL subgroup along with a homogenous expression of Smad4 and Smad5 in all ALL subgroups. Smad molecules are necessary for BMP and TGF-β signalling in general[99,104,105] congruent with the expression of Smads in all cell lines and the ALL patient samples. Other Smads than Smad1/5 can be activated by different TGF-β family ligands than BMP2, leading to the activation of divergent regulative programs. High Smad1 expression could therefore be specific for TEL/AML1 rearranged ALL, which would correlate with the upregulation of BMP2, the cytokine whose receptor binding leads to Smad1 phosphorylation[105].

The question was if and how an active BMP2 signalling pathway could contribute to leukaemia or if this was just an epiphenomenon of leukaemia development itself. One characteristic of leukaemic cells is that they can indefinitely self-renew and expand like HSCs[3] due to direct interactions with the nourishing bone marrow environment[165]. BMP2 signalling in bone marrow[161] is possibly necessary for the regulation of normal HSC and B-cell progenitor establishment and differentiation. BMP2 expression is able to block the proliferation of HSCs preserving their undifferentiated phenotype and repopulation capacity[122]. Aberrant upregulation of this complex signalling network in leukaemia could help to overcome the dependence of direct cell-cell contact and adherence with the bone marrow stroma, which facilitates normal HSC and B-cell progenitor growth and differentiation and supports ALL cells *in-vitro*[163,164], and could deregulate the proliferation and differentiation capacity of transformed cells.

5.2 OAZ upregulation in pre-B ALL

OAZ is a regulator of signal transduction playing multifunctional regulative roles by mutually exclusive use of different zinc-fingers in the context of BMP-signalling[110] and EBF1 interaction[128,131] and maybe in general. OAZ is not expressed in normal haematopoietic cells[133], thus an upregulation of OAZ in ALL could be of great relevance. The analysis of material from ALL cell lines and patients exhibited a remarkebly high expression in the TEL/AML1 rearranged samples. This correlates with a gene expression profiling study of paediatric B-ALL cases showing a more than 2-fold higher OAZ expression in TEL/AML1 rearranged cases in comparison to other subgroups[166]. The differences to the normal cells were striking and the expression was up to 173-fold higher. In addition the analysis of the cell line REH showed a strong expression of OAZ on protein level. This is important because

mRNA levels are relevant indicators for gene expression, but do not reflect the real functional situation in the analysed cells, which is mainly regulated by the translated proteins.

OAZ was initially detected in several different tissues of the rat by RT-PCR only[128]. Other groups were able to detect OAZ mRNA levels in human tissues by northern blot analysis or RT-PCR. They found only low levels in haematopoietic tissues[132] or no expression in sorted B-cells at all[133]. It is remarkable that up to date nobody was able to detect OAZ on protein level in primary cells. This could partially explain our own experimental challenges to detect OAZ with conventional techniques, immunoprecipitation or FACS in leukaemic patient samples. Alternatively, it could be that the absolute OAZ protein levels in the analysed leukaemic cell lysates were below the detection limits of the used techniques although OAZ was transcriptionally upregulated.

Nevertheless, the upregulation of OAZ on the mRNA level could have a significant impact on the translation of the OAZ protein with potentially severe functional consequences in the transforming process of lymphoblasts. Abnormal high protein levels of OAZ in leukaemic cells could be suitable for a simultaneous regulation of BMP2-signalling and EBF1-mediated B-cell differentiation even though only one binding partner can bind to OAZ at the same time. Redundant expression of OAZ in ALL might be sufficient to bind all present EBF1 molecules and anyhow leave enough free OAZ molecules left for interacting in BMP2-signalling.

5.3 OAZ's possible role in BMP signalling

The cell type specific zinc-finger protein OAZ is not expressed during lymphopoiesis[133], supporting the assumption that its abnormal expression in HSCs or B-cell progenitors leads to a deregulation of the cellular homeostasis. OAZ is highly pathway specific by cooperating with BMP-activated Smad1 but not with Smad2 which is activated by TGF-β. The only known mammalian target gene of OAZ so far is Smad6, a specific inhibitor of BMP-mediated signalling[111]. Upon BMP4 stimulation OAZ can form a complex with Smad1/4 leading to an activation of the Smad6 gene[167]. Smad6 expression leads to a competition with Smad1, and possibly Smad5/8, for binding to Smad4 and a reduction of BMP4-mediated signalling. In this context OAZ acts within an inhibitory auto-feedback loop of Smad signaling.

BMP2 and BMP4 are highly homologous[102], binding the same receptors and R-Smads and acting cooperatively in essential developmental processes. Both are implicated in many regulative processes[126,168]. Despite their high degree of homology BMP2 and BMP4 are not exchangeable and redundant in their biological function in the regulation of human haematopoiesis contrary to the observed situation in other species[169,170]. Striking differences

were found when examining their role in early erythropoiesis[171,172]. BMP2 can affect the induction of early erythroid cells in company with the TGF-β family ligand activin A, contrary to BMP4[172], which is however able to induce CD34$^+$ progenitor cells to differentiate to megakaryoctyes, an effect which was not observed for BMP2[171]. Both cytokines possibly differentially cooperate or compete with other ligands, like activin A, in binding to the BMP receptors. Thus it is very likely that BMP2 and BMP4 signalling is also contingent upon cell type specific downstream factors besides OAZ, leading to an exclusive transmission of BMP2 or BMP4 signals only. It could also be that BMP2- or BMP4-binding to the BMP receptor complex is specifically detected leading to differential regulation of target genes. So far it is not known if BMP2 can also activate the Smad6 gene in company with OAZ, which is reasonably due to its high homology with BMP4[102].

For TEL/AML1 rearranged ALL this is an open question that could be of main relevance. BMP4 expression was not detectable in the TEL/AML1 cell line REH contrary to all other ALL cell lines tested, which invariably showed significant BMP4 mRNA levels. If and how BMP4 and Smad6 are expressed in ALL patients samples is unknown and could be of primary interest in the understanding of the role of BMP-signalling in leukaemia. The used ALL patient samples therefore ought to be further analysed for BMP4 and Smad6 expression in the near future (work in progress). In cells in which BMP4 is not expressed, BMP2 signalling might lead to different regulatory processes. An activated complex of Smad1/4 and OAZ in leukaemic cells might not be able to bind to the Smad6 gene if activated by BMP2. Another possibility is that in leukaemic cells Smad1/4/OAZ can bind to Smad6, which in turn does not lead to activation, but deactivation of the gene, due to so far unknown additional co-factors, an interaction with TGF-β signalling or a "cross-talk" with other non-Smad signalling pathways like Notch, p38 mitogen-activated protein kinase and Toll[112,113].

5.4 OAZ: A regulator of EBF1

The other known role of OAZ is its regulation of the early B-cell factor (EBF1). OAZ can form a complex with EBF1, preventing the formation of functional EBF1 homodimers necessary for recognition and binding of DNA sequences with specific EBF1 binding-sites[128,131]. Expression of EBF1 is indispensable for the development and differentiation of B-cells by directing haematopoietic progenitors to the B-lymphoid lineage[71] and by activating transcription of B-cell specific genes[79,85,86,87,173]. B-cell differentiation in EBF$^{-/-}$ mice is blocked between the early-B and pro-B cell stage leading to a complete absence of functional Ig expressing mature B-cells[67]. Although OAZ is usually not expressed in haematopoietic cells it can inhibit the activation of the B-cell specific target genes CD79b and IGLL1 in an artificial luciferase-reporter based system in HEK-293 cells[132]. Upregulation of OAZ in HSCs or B-cell

progenitors could therefore block the EBF1-mediated differentiation, supporting leukaemia development by leading to the characteristic B-cell maturation arrest observed in B-ALL[1].

To analyse a possible connection between OAZ upregulation and EBF1-mediated B-cell development, EBF1 expression was measured in ALL samples and normal HSC and B-cell progenitor subsets. As expected, EBF1 was expressed during all stages of B-cell development with a profile that was concordant with the known expression profile of EBF1 during normal B-lymphopoiesis with expression peaks in pro- and pre-B cells[72,91]. The expression of EBF1 in the ALL samples included in this study was usually higher than in the normal control cells. This correlates with recent findings from larger ALL series, which showed that only ~3% of the cases had a mono- or bi-allelic deletion of EBF1 leading to its downregulation[32]. Another study analysed 33 cases with paediatric B-ALL; they found submicroscopic lesions in the EBF1 gene in only 6% of the cases, with possible functional impact[34]. The expression level of EBF1 in BM stromal cells was similar to that of Pro-B cells. A fact that was quite astonishing, but could possibly be explained by recent results showing a potential dual role of EBF1 in regulation of B-lymphopoiesis on the one hand and regulation of genes in bone marrow stromal cells on the other hand[174].

5.5 A model of leukaemia development

Based on the described possible functional impact of activated BMP2 signalling and an upregulation of the zinc-finger protein OAZ during leukaemia initiation and propagation, which could at least have pathogenic impact on TEL/AML1 rearranged ALL, a hypothetical model for the development of ALL was proposed: This model led to an experimental setup for the testing of this hypothesis (Figure 44).
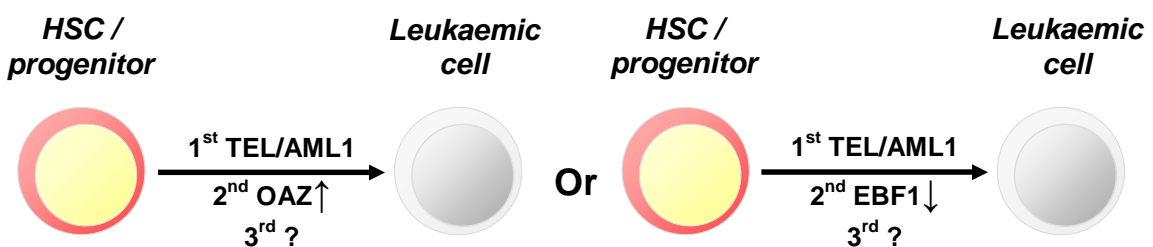
Figure 44: Hypothetical model for the development of acute lymphoblastic leukaemia. HSCs or hematopoietic B-cell progenitors are the suspected origin of the initial TEL-AML1 rearrangement. Additional critical secondary and tertiary events such as the aberrant upregulation of the zinc-finger protein OAZ on the one hand or vice versa the knock-down or deletion of EBF1 on the other hand could be able to induce a B-cell maturation arrest in the TEL-AML1 transformed cells. This in consequence could lead to an initiation and progression of a leukaemic clone and the development of gross leukaemia at the end. Shown are two experimental systems with HSCs/progenitors as targeted cells in which by artificial expression of the TEL/AML1 fusion gene (1st TEL/AML1) in company with the overexpression of OAZ (2nd OAZ↑) or the knock-down of EBF1 (2nd EBF1↓) and unknown other events (3rd ?) the transformation into a leukemic cell should be induced.

A first hit event such as the TEL/AML1 rearrangement in HSCs or B-cell progenitors (CD34^{+} cells) followed by a second critical hit at the B-cell differentiation pathway for instance by functional loss of EBF1[32] either by secondary mutation or indirectly by OAZ overexpression might prepare the ground for leukaemic transformation. Though OAZ can inactivate the factor EBF1, essential for the development of functional B-lymphocytes, an aberrantly increased OAZ level or vice versa a knock-down or deletion of EBF1 should have serious consequences for the differentiation of B-cells. The result could be a maturation arrest, one of the significant characteristics of leukaemia[1]. In company with other malignant events like the reactivation of stem cell programs as the BMP2 signalling pathway and/or mutations in critical cell cycle regulators (e.g. CDKN2A) these orchestrated events could finally overrun normal cellular control mechanisms and lead to the development of leukaemia.

The validation of the hypothetical model for the development of leukaemia could permit a new promising approach for the treatment of the disease which could be tested in an experimental model (Figure 45). Blasts from paediatric ALL patients, possessing a high expression level of OAZ, could be induced to differentiate to functional B-cells. If OAZ is responsible for the previously described B-cell maturation arrest this would sequentially lead to a cure of leukaemia.
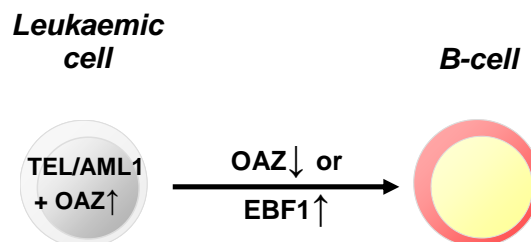
Figure 45: Experimental model for the treatment of acute lymphoblastic leukaemia. Leukaemic cells of precursor B-ALL generally having a growth advantage by possessing stem cell characteristics like the indefinite ability of self renewal and are blocked on an inoperable stage characteristic for progenitor B-cells. Patients with TEL-AML1 rearranged ALL and strong upregulation of OAZ (TEL/AML1 + OAZ↑) are a possible target of therapy by either effective downregulation of OAZ (OAZ↓) or a sufficient overexpression of EBF1 (EBF1↑) in the leukaemic cells leading to a breakup of the leukaemia intrinsic maturation arrest and a recovery of the normal hematopoiesis and a cure of leukaemia at last.

In a realistic therapeutic strategy in humans it nevertheless will be difficult to directly knock-down the transcription factor OAZ or to effectively upregulate EBF1 necessary to compete with the deleterious OAZ/EBF1 protein complex. For the development of a promising therapeutic approach it therefore is important to further focus on the exposure of the so far totally unknown reasons for the OAZ upregulation in leukaemic cells. The deciphering of these processes and upstream mechanisms in the regulation of OAZ are a basic prerequisite which could lead to new strategies for the treatment of ALL in the future.

5.6 OAZ has relevance for leukaemia *in-vivo*

To analyse if the high OAZ expression in ALL cells had any relevance for the *in-vivo* situation the NOD/*scid* mice was used as a model for human leukaemia development[135,136,175].

A cohort of 28 ALL patient samples was transplanted leading to an engraftment in 9 of the mice. The low engraftment rate stood in contrast to usually much higher engraftment rates obtained in other studies[136,175]. In one study analysing engraftment of ALL in NOD/*scid* mice all samples showed engraftment, differences were only observed depending on the initially transplanted cell numbers which were always higher 2.5×10^6 per mouse[175]. In another experimental setup between $2-50 \times 10^6$ human CD34$^+$ cells were transplanted and an engraftment was detectable for up to 6.5 months afterwards. Engraftment reached levels as high as 96% in the bone marrow, but was clearly dependent on the initially used number of cells[136]. The reasons that in our study up to six months after transplantation only 32% of the mice showed human engraftment at all were most likely due to the sometimes very low cell recoveries and vitalities. For some mice less than 1×10^5 vital cells were transplanted. Freshly isolated ALL cells should therefore preferentially be used for further transplantation experiments if possible, because freeze thaw cycles decrease the viability of the cells.

Expanded leukaemic cells were sorted to test if the initially observed OAZ expression in the transplanted samples was an image of the bulk population or a compound of divergent expression levels in subfractions of the blasts. The expression values of OAZ and BMP2 were usually equal or higher than in the original patient samples and showed no significant subfraction-specific differences. This makes it likely that their expression has relevance for the engraftment and proliferation of leukaemic cells *in-vivo* and the sustainment of the B-cell maturation arrest because engraftment of leukaemic cells in NOD/*scid* mice reflects the original disease in the human[175,176]. Phenotypic and genotypic characteristics of the cells are retained over many serial retransplantation steps.

5.7 OAZ disturbs the B-cell differentiation

As a first functional experimental setup the impacts of OAZ expression on HSCs or B-cell progenitors were analysed. If OAZ is able to block EBF1-mediated activation of crucial programs necessary for B-cell development, it would give a direct link to the maturation arrest observed in leukaemia[1]. For the first time it was shown that OAZ expression in haematopoietic progenitors was able to reduce the expression of CD34 and the B-cell marker CD19 meaning that OAZ inhibited the differentiation of the cells to the B-cell lineage.

Albeit the conditions used were obviously not optimal for B-cell development because only up to 13.1% of the control cells expressed CD19 after 5-15 days of culture. Most of the cells possibly differentiated to the myeloid lineage, supported by recent findings in our group showing an increase in the expression of the myeloid marker CD33 during culture of cells with the used stromal cells and medium. Additionally usually different hardly comparable combinations of cytokines and other mouse or stroma cell lines were used in other studies.

The fact that the cells did not efficiently differentiate to the B-cell lineage is possibly related to the infection procedure used, that was optimised for the CD34^{+} cells, which contained the cytokines FLT3-L, SCF, TPO and IL-6[177]. FLT3-L and SCF - despite their well established crucial role in B-cell development - and TPO can lead to proliferation of CFU-Blast cells[178]. TPO is also known for its essential role in the development and differentiation of megakaryocytes necessary for platelet building[179]. Treatment of CD34^{+} cells with IL-6 results in an increase of the number of the myeloid colony-forming unit-macrophage (CFU-M) and can support the differentiation of monocytes[180].

Another reason for low B-cell recoveries could be the relatively low period of time the cell had for differentiation. In other studies CD19 expression of HSCs cultured on stromal layers started after 1 week but cells usually needed 2-6 weeks for efficient B-cell differentiation[151,153]. Nevertheless significant differences between cells infected with OAZ and control-virus were detectable, supporting the assumption that OAZ expression in haematopoietic cells has severe consequences on B-cell differentiation.

Detection of significant OAZ expression in the infected cells showed a reduction of B-cell specific surface markers. This alteration is likely related to the shown and described sequestration of EBF1 by OAZ[128,131,132]. There was no correlation between EBF1 and OAZ expression in the infected cells comparable to the situation in the analysed ALL patients. To analyse the effects of OAZ expression on the expression of EBF1 target genes, semi-quantitative RT-PCR was performed. The essential B-cell commitment factor PAX5[68,69] was only barely detectable, consistent with the incomplete differentiation of the cells to the B-cell lineage. PAX5 acts downstream of EBF1, in its absence, B-cell development is arrested between pro- and pre-B cell stage[69,90]. RAG1 and IL7R expression were not detectable at all. The majority of the cells were likely not restricted to the lymphoid lineage, which is accompanied by RAG1 expression[181]. The EBF1 expression possibly was also not sufficient for effectively activating RAG1[67] that is participating with RAG2 in V(D)J recombination of Ig genes during B-cell differentiation[182]. It is believed that B-cell differentiation begins in CLPs with the expression of low levels of EBF1 in response to PU-1 and IL-7 signalling[44,64]. This

supports the presumption that the analysed cells were not already restricted to the B-cell lineage and would explain the undetectable IL7R expression. Additionally it is controversial which role IL7R signalling plays in humans during B-cell development, contrary to its undisputable critical role in mice[183].

A striking difference in gene expression was detectable for the known direct EBF1 target genes CD79a (Igα), CD79b (Igβ), IGLL1 (λ5) and VpreB[79,85,173]. These proteins are necessary for the proper formation of the pre-BCR, which is expressed in pre-B cells and an important checkpoint in B-cell development and proliferation[58,56,57]. The pre-BCR mediates the expansion of B-cell progenitors and the generation of B-cells in general. Real time PCR analysis of the pre-BCR components showed a significant reduction of CD79a and CD79b in OAZ-virus infected cells. Both genes are transcribed from different chromosomes making synergistic effects unlikely. The expression of IGLL1 and VpreB in OAZ-virus infected cells were also significantly reduced. In summary it was observed for the first time that OAZ expression in haematopoietic progenitors was able to efficiently and significantly reduce the expression of four direct EBF1 target genes under the control of native promoters. The functional impacts for the upregulation of OAZ observed in ALL patient samples are apparent.

The critical role for aberrant OAZ expression during haematopoiesis is supported by several studies using the AKXD mice model. The AKXD mice are susceptible for leukaemia and lymphomas as a result of viral integration[184]. Mouse Evi3 is highly homologous to OAZ and both are frequent targets of retroviral integrations in AKXD B-cell lymphomas[133,185,186]. Lymphomas with OAZ or Evi integrations are supposed to be blocked at an early stage of B-cell development supported by specific expression of B-cell markers and Ig heavy chain rearrangement[185,186]. OAZ, which is normally not expressed in B-cells, and Evi3 are highly expressed following viral integration[133,185]. It was assumed that Evi3 and EHZF, its human homologue, and not OAZ are the essential players of the zinc-finger protein family implicated in regulation of EBF1 during B-cell development[132,185,187]. Both are like OAZ multifunctional in their role in enhancing BMP- and inhibiting EBF1-mediated transcriptional activity of target genes[132,186]. There were controversial results after analysis of several tumours with viral Evi3 integration[186] leading to the hypothesis that Evi3 expression results in a downregulation of EBF target genes, while in leukaemogenic cells Evi3 expression leads to an upregulation of EBF target genes[186].

This conclusion is contrary to our results. Evi3 is expressed in murine B-cells[133] and EHZF is abundant in human CD34[+132] and CD133[+188] progenitors and decreases during

differentiation. The assumptions of the normal roles of Evi3, EHZF and OAZ in normal haematopoiesis are supported by the results gained during this work showing almost no expression of OAZ in normal haematopoietic subsets and its aberrant expression in pre-B ALL. EHZF expression was found in most AML cases but was almost absent in B-ALL[132,166]. It is likely that Evi3 and EHZF are the regulators of EBF1 during normal B-cell development and the haematopoietic counterparts of OAZ, which regulates olfactory and neuronal development by interaction with EBF1. Why only exceedingly low numbers of B-ALL cases showed upregulation of EHZF is unknown[166], but this could be related to the processes responsible for the upregulation of OAZ in ALL. Molecular alterations in leukaemic transformation like the TEL/AML1 rearrangement might initiate further processes that involve the deregulation of upstream effectors of OAZ that lead to its subsequent activation.

Reasons why OAZ is upregulated in ALL remain elusive down to the present day. Analyses of the OAZ promoter region might be helpful because one could assume that the transcription of OAZ is downregulated in haematopoietic cells via methylation[189], a process that might be reverted during leukaemia development. Other possibilities are retroviral integrations into the OAZ promoter, which can lead to a strong increase in OAZ expression as it was shown in the AKXD mice model[133,185] or a genomic gain at the OAZ gene locus on chromosome 16q due to amplification. Preliminary analysis of ALL cell lines, especially of the TEL/AML1 rearranged ALL cell line REH, nevertheless showed no indication for an altered OAZ promoter region. Further analysis of ALL patient samples and ALL cell lines need therefore to be performed to get a deeper insight into the molecular mechanisms leading to abnormal OAZ expression in ALL.

6 Summary

A specific form of childhood leukaemia is the precursor B-lineage acute lymphoblastic leukaemia (pre-B ALL), in which progenitors of the B-lymphocytes go awry. Previous transcriptome-wide analyses on ALL patient samples showed an aberrant activation of the BMP2-dependent pathway in the leukaemic cells. The goal of the present study was to assess the biological relevance of BMP2 signalling and its potential transcriptional targets in ALL of childhood. We hypothesised that an activated BMP2-pathway either reflects a state of differentiation of leukaemic cells or rather a specific aberration of ALL which drives and maintains the malignant phenotype. During this work it was discovered that BMP2 and its signalling target OAZ were highly expressed in TEL/AML1 rearranged ALL patient samples in comparison to normal haematopoietic stem cell and B-cell progenitor control samples. OAZ is normally not expressed in haematopoietic cells implying a potential role of OAZ in the pathogenesis of ALL. Aberrant activity of OAZ might block the EBF1-mediated transcriptional activation of target genes, which are essential for normal B-cell differentiation and development. The net effect could be a maturation arrest, one of the characteristic features of leukaemia. A first hit-event like the TEL/AML1 rearrangement in HSCs or B-cell progenitors, followed by an aberrant expression of OAZ through still undefined mechanisms, might be sufficient or at least contribute to the initiation or propagation of leukaemia. The first step in the functional analysis of OAZ expression recapitulated recent knowledge and showed the specific interaction of OAZ and EBF1 on the protein level, disrupting EBF1 function by sequestration. Further significant OAZ expression was detectable in engrafted ALL cells that were serially transplanted into NOD/*scid* mice. For the first time it was possible to show that OAZ expression in haematopoietic progenitors in an *in-vitro* culture based system was able to inhibit B-cell differentiation and to significantly downregulate the gene expression of the direct EBF1 target genes CD79a, CD79b, IGLL1 and VpreB necessary for proper B-cell development. Further *in-vitro* and *in-vivo* studies which allow for modulation of OAZ activity on the background of the TEL/AML1 rearrangement in haematopoietic cells might be able to define the role of OAZ as a bona fide target in leukaemia development and may lead to alternative, innovative treatment strategies directed towards its deleterious effects on B-cell differentiation.

7 List of abbreviations

µ	micro
A	adenosine or deoxyadenosine
Ac	acetate
AC3	type III adenylyl cyclase
add	addition
ALL	acute lymphoblastic leukaemia
amp	ampicillin
APC	allophycocyanin
APC-H7	allophycocyanin-H7
APS	ammonium persulfate
ATCC	American Type Culture Collection
B-cell	bursal or bone marrow derived cell
BCR	B-cell receptor
BMP	bone morphogenetic protein
BMPR	bone morphogenetic protein receptor
BMSC	bone marrow stromal cells
bp	base pairs
BRE	BMP responsive element
C	cytosine
CAPS	N-cyclohexyl-3-aminopropanesulfonic acid
CD	cluster of differentiation
cDNA	complementary DNA
CDS	coding sequence
CFU-m	colony-forming unit-macrophage
Cl	cloride
CLP	common lymphoid progenitor
CMP	common myeloid progenitor
CMV	cytomegalovirus
CP	crossing point
ddH$_2$O	double distilled water
del	deletion
DEPC	diethylpyrocarbonat
DMEM	Dulbecco's modified Eagle's medium
DMSO	dimethyl sulfoxide
DNA	deoxyribonucleic acid
DSMZ	Deutsche Sammlung von Mikroorganismen und Zellkulturen GmbH
DTT	dithiothreitol
E-B-cell	early-B-cell
EBF	early B-cell factor
EBFAZ	early B-cell factor associated zinc finger protein
ECL	electrochemiluminescence
EDTA	ethylenediaminetetraacetic
eGFP	enhanced green fluorescent protein
ErP	erythrocyte precursor
EtOH	ethanol
F	fluorine

FACS	fluorescence-activated cell sorting
FBS	fetal bovine serum
FITC	fluorescein isothiocyanate
FLT3-L	FLT3 Ligand
fw	forward
g	gram
G	guanosine
GDF	growth and differentiation factor
GMP	granulocyte macrophage precursor
h	human
H	heavy
H	hydrogene
HA	hemagglutinin
HBSS	Hank's buffered salt solution
HC	heavy chain
HEPES	(4-(2-hydroxyethyl)-1-piperazineethanesulfonic acid)
HRP	horseradish peroxidase
HSC	haematopoietic stem cell
IFN	interferone
Ig	immunoglobulin
IL-	interleucine
IM-B-cell	immature B-cell
inv	inversion
IP	Immunoprecipitation
IRES	internal ribosomal entry site
I-Smad	Inhibitory Smad
IU	infectous units
K	potassium
kan	kanamycin
l	litre
L	light
LB	Luria-Bertani
LC	light chain
Lin	lineage-specific markers
LOH	loss of heterozygosity
LSC	leukaemic stem cell
LT	long-term
LTR	long terminal repeat
m	mouse
m	milli
M	mol(ar)
MAPK	Mitogen-activated protein kinase
MCS	multiple cloning site
MEM	modified Eagle's medium
MEP	megakaryocyte erythrocyte precursor
Mg	magnesium
MIS	Müllerian inhibiting substance
MkP	megakaryocyte precursor
ml	milli
MOPS	3-(N-morpholino)propanesulfonic acid

MPP	multipotent progenitor cell
mRNA	messenger RNA
n	nano
Na	sodium
NCBI	National Center for Biotechnology Information
neo	neocin
NK	natural killer
nt	nucleotides
NTP	nucleoside triphosphate
O	oxygen
OAZ	Olf/EBF1-associated zinc finger protein
OMP	olfactory marker protein
p	petit
p	poly
p	pico
p	phospho
P	phosphate
PAGE	polyacrylamide gel electrophoresis
PC5	R-phycoerythrin-Cy5.1
PCR	polymerase chain reaction
PE	R-phycoerythrin
PE-Cy7	R-phycoerythrin-Cy7
PerCP-Cy5.5	peridinin chlorophyll protein-Cy5.5
PMSF	phenylmethylsulfonylfluorid
PP	pyrophosphate
pre-B-cell	precursor B-cell
pro-B-cell	progenitor B-cell
puro	puromycin
PVDF	polyvinylidene fluoride
q	queue
RAG	recombination activating gene
rev	reverse
RNA	ribonucleic acid
rpm	rounds per minute
RPMI	Roswell Park Memorial Institute medium
R-Smad	receptor activated Smad
RT	room temperature
RT	real-time
SBE	Smad binding element
SCF	stem cell factor
SDS	sodium dodecyl sulfate
Ser	serine
SFEM	serum free expansion media
shRNA	short hairpin RNA
ST	short-term
t	translocation
T	deoxythymidine
T	thymidine
TAE	Tris-acetate-EDTA
TBS	Tris-buffered saline

TBST	Tris-buffered saline Tween
TdT	terminal deoxynucleotidyl transferase
TE	Tris-EDTA
TEMED	tetramethylethylenediamine
TGF-β	transforming growth factor beta
TPO	thrombopoietin
Tris	tris(hydroxymethyl)aminomethane
v	volume
v	version
V	vanadium
V(D)J	variable(diversity)joining genes
w	weight
wt	wild type
YFP	yellow fluorescent protein
zeo	zeocin

8 Literature

1   C. H. Pui and S. Jeha, *Nature reviews* **6** (2), 149 (2007).

2   L. I. Zon, *Nature* **453** (7193), 306 (2008).

3   E. Passegue, C. H. Jamieson, L. E. Ailles et al., *Proceedings of the National Academy of Sciences of the United States of America* **100 Suppl 1**, 11842 (2003).

4   C. H. Pui, M. V. Relling, and J. R. Downing, *The New England journal of medicine* **350** (15), 1535 (2004).

5   S. A. Armstrong and A. T. Look, *J Clin Oncol* **23** (26), 6306 (2005).

6   A. G. Knudson, *Seminars in cancer biology* **3** (3), 99 (1992).

7   B. Vogelstein and K. W. Kinzler, *Trends Genet* **9** (4), 138 (1993).

8   D. Hanahan and R. A. Weinberg, *Cell* **100** (1), 57 (2000).

9   C. H. Pui and W. E. Evans, *The New England journal of medicine* **339** (9), 605 (1998).

10 J. H. Kersey, *Blood* **90** (11), 4243 (1997).

11 C. H. Pui and W. E. Evans, *The New England journal of medicine* **354** (2), 166 (2006).

12 M. Schrappe, B. Camitta, C. H. Pui et al., *Leukemia* **14** (12), 2193 (2000).

13 T. R. Golub, G. F. Barker, S. K. Bohlander et al., *Proceedings of the National Academy of Sciences of the United States of America* **92** (11), 4917 (1995).

14 A. Zelent, M. Greaves, and T. Enver, *Oncogene* **23** (24), 4275 (2004).

15 H. Mori, S. M. Colman, Z. Xiao et al., *Proceedings of the National Academy of Sciences of the United States of America* **99** (12), 8242 (2002).

16 M. Hotfilder, S. Rottgers, A. Rosemann et al., *Blood* **100** (2), 640 (2002).

17 A. Castor, L. Nilsson, I. Astrand-Grundstrom et al., *Nature medicine* **11** (6), 630 (2005).

18 C. A. Quijano, D. Moore, 2nd, D. Arthur et al., *Leukemia* **11** (9), 1508 (1997).

19 C. Cobaleda, N. Gutierrez-Cianca, J. Perez-Losada et al., *Blood* **95** (3), 1007 (2000).

20 A. A. George, J. Franklin, K. Kerkof et al., *Blood* **97** (12), 3925 (2001).

21 M. Fischer, M. Schwieger, S. Horn et al., *Oncogene* **24** (51), 7579 (2005).

22 M. Morrow, S. Horton, D. Kioussis et al., *Blood* **103** (10), 3890 (2004).

23 P. Andreasson, J. Schwaller, E. Anastasiadou et al., *Cancer genetics and cytogenetics* **130** (2), 93 (2001).

24 D. F. Tough and J. Sprent, *Immunologic research* **14** (1), 1 (1995).

25 H. Okada, T. Watanabe, M. Niki et al., *Oncogene* **17** (18), 2287 (1998).

26 M. Morrow, A. Samanta, D. Kioussis et al., *Oncogene* **26** (30), 4404 (2007).

27 T. Enver, S. Tsuzuki, J. Brown et al., *Annals of the New York Academy of Sciences* **1044**, 16 (2005).

28 S. Tsuzuki, M. Seto, M. Greaves et al., *Proceedings of the National Academy of Sciences of the United States of America* **101** (22), 8443 (2004).

29 D. Hong, R. Gupta, P. Ancliff et al., *Science (New York, N.Y* **319** (5861), 336 (2008).

30 S. P. Romana, M. Le Coniat, H. Poirel et al., *Leukemia* **10** (1), 167 (1996).

31 A. T. Maia, A. M. Ford, G. R. Jalali et al., *Blood* **98** (2), 478 (2001).

32	C. G. Mullighan, S. Goorha, I. Radtke et al., *Nature* **446** (7137), 758 (2007).
33	C. Cobaleda, A. Schebesta, A. Delogu et al., *Nature immunology* **8** (5), 463 (2007).
34	R. P. Kuiper, E. F. Schoenmakers, S. V. van Reijmersdal et al., *Leukemia* **21** (6), 1258 (2007).
35	T. Reya, S. J. Morrison, M. F. Clarke et al., *Nature* **414** (6859), 105 (2001).
36	D. S. Krause, M. J. Fackler, C. I. Civin et al., *Blood* **87** (1), 1 (1996).
37	K. J. Payne and G. M. Crooks, *Immunological reviews* **187**, 48 (2002).
38	D. DiGiusto, S. Chen, J. Combs et al., *Blood* **84** (2), 421 (1994).
39	A. Galy, M. Travis, D. Cen et al., *Immunity* **3** (4), 459 (1995).
40	J. Cheng, S. Baumhueter, G. Cacalano et al., *Blood* **87** (2), 479 (1996).
41	L. Healy, G. May, K. Gale et al., *Proceedings of the National Academy of Sciences of the United States of America* **92** (26), 12240 (1995).
42	T. W. LeBien and T. F. Tedder, *Blood* **112** (5), 1570 (2008).
43	C. Nunez, N. Nishimoto, G. L. Gartland et al., *J Immunol* **156** (2), 866 (1996).
44	M. Kondo, I. L. Weissman, and K. Akashi, *Cell* **91** (5), 661 (1997).
45	L. L. Rumfelt, Y. Zhou, B. M. Rowley et al., *The Journal of experimental medicine* **203** (3), 675 (2006).
46	T. Ishii, M. Nishihara, F. Ma et al., *J Immunol* **163** (7), 3612 (1999).
47	J. Hagman and K. Lukin, *Current opinion in immunology* **18** (2), 127 (2006).
48	S. Roessler and R. Grosschedl, *Seminars in immunology* **18** (1), 12 (2006).
49	F. Gounari, I. Aifantis, C. Martin et al., *Nature immunology* **3** (5), 489 (2002).
50	Y. S. Li, R. Wasserman, K. Hayakawa et al., *Immunity* **5** (6), 527 (1996).
51	D. Reynaud, N. Lefort, E. Manie et al., *Blood* **101** (11), 4313 (2003).
52	T. W. LeBien, B. Wormann, J. G. Villablanca et al., *Leukemia* **4** (5), 354 (1990).
53	K. Lassoued, C. A. Nunez, L. Billips et al., *Cell* **73** (1), 73 (1993).
54	F. Melchers, H. Karasuyama, D. Haasner et al., *Immunology today* **14** (2), 60 (1993).
55	S. A. Omori and R. Wall, *Proceedings of the National Academy of Sciences of the United States of America* **90** (24), 11723 (1993).
56	R. J. Benschop and J. C. Cambier, *Current opinion in immunology* **11** (2), 143 (1999).
57	F. Melchers, *Nat Rev Immunol* **5** (7), 578 (2005).
58	T. W. LeBien, *Blood* **96** (1), 9 (2000).
59	B. Blom and H. Spits, *Annual review of immunology* **24**, 287 (2006).
60	J. Hagman and K. Lukin, *Trends in immunology* **26** (9), 455 (2005).
61	S. L. Nutt and B. L. Kee, *Immunity* **26** (6), 715 (2007).
62	D. Reynaud, I. A. Demarco, K. L. Reddy et al., *Nature immunology* **9** (8), 927 (2008).
63	J. H. Wang, A. Nichogiannopoulou, L. Wu et al., *Immunity* **5** (6), 537 (1996).
64	R. P. DeKoter and H. Singh, *Science (New York, N.Y* **288** (5470), 1439 (2000).
65	G. Bain, E. C. Maandag, D. J. Izon et al., *Cell* **79** (5), 885 (1994).
66	Y. Zhuang, P. Soriano, and H. Weintraub, *Cell* **79** (5), 875 (1994).
67	H. Lin and R. Grosschedl, *Nature* **376** (6537), 263 (1995).
68	I. Mikkola, B. Heavey, M. Horcher et al., *Science (New York, N.Y* **297** (5578), 110 (2002).
69	S. L. Nutt, B. Heavey, A. G. Rolink et al., *Nature* **401** (6753), 556 (1999).

70	D. Liberg, M. Sigvardsson, and P. Akerblad, *Molecular and cellular biology* **22** (24), 8389 (2002).
71	K. Lukin, S. Fields, J. Hartley et al., *Seminars in immunology* **20** (4), 221 (2008).
72	R. Gisler, S. E. Jacobsen, and M. Sigvardsson, *Blood* **96** (4), 1457 (2000).
73	J. Hagman, C. Belanger, A. Travis et al., *Genes & development* **7** (5), 760 (1993).
74	M. M. Wang and R. R. Reed, *Nature* **364** (6433), 121 (1993).
75	L. A. Cirillo and K. S. Zaret, *Molecular cell* **4** (6), 961 (1999).
76	J. Xu, S. D. Pope, A. R. Jazirehi et al., *Proceedings of the National Academy of Sciences of the United States of America* **104** (30), 12377 (2007).
77	S. Mella, C. Soula, D. Morello et al., *Gene Expr Patterns* **4** (5), 537 (2004).
78	S. Garel, F. Marin, R. Grosschedl et al., *Development (Cambridge, England)* **126** (23), 5285 (1999).
79	J. Hagman, A. Travis, and R. Grosschedl, *The EMBO journal* **10** (11), 3409 (1991).
80	L. Borghesi, J. Aites, S. Nelson et al., *The Journal of experimental medicine* **202** (12), 1669 (2005).
81	E. M. Smith, R. Gisler, and M. Sigvardsson, *J Immunol* **169** (1), 261 (2002).
82	B. L. Kee and C. Murre, *The Journal of experimental medicine* **188** (4), 699 (1998).
83	A. C. Berardi, E. Meffre, F. Pflumio et al., *Blood* **89** (10), 3554 (1997).
84	J. M. Pongubala, D. L. Northrup, D. W. Lancki et al., *Nature immunology* **9** (2), 203 (2008).
85	P. Akerblad, M. Rosberg, T. Leanderson et al., *Molecular and cellular biology* **19** (1), 392 (1999).
86	P. Akerblad and M. Sigvardsson, *J Immunol* **163** (10), 5453 (1999).
87	R. Gisler, P. Akerblad, and M. Sigvardsson, *Molecular immunology* **36** (15-16), 1067 (1999).
88	C. S. Seet, R. L. Brumbaugh, and B. L. Kee, *The Journal of experimental medicine* **199** (12), 1689 (2004).
89	S. Roessler, I. Gyory, S. Imhof et al., *Molecular and cellular biology* **27** (2), 579 (2007).
90	P. Urbanek, Z. Q. Wang, I. Fetka et al., *Cell* **79** (5), 901 (1994).
91	M. E. Hystad, J. H. Myklebust, T. H. Bo et al., *J Immunol* **179** (6), 3662 (2007).
92	M. Sigvardsson, D. R. Clark, D. Fitzsimmons et al., *Molecular and cellular biology* **22** (24), 8539 (2002).
93	S. Hirokawa, H. Sato, I. Kato et al., *European journal of immunology* **33** (7), 1824 (2003).
94	H. Maier and J. Hagman, *Seminars in immunology* **14** (6), 415 (2002).
95	C. C. Goodnow, *Proceedings of the National Academy of Sciences of the United States of America* **93** (6), 2264 (1996)
96	K. Kudrycki, C. Stein-Izsak, C. Behn et al., *Molecular and cellular biology* **13** (5), 3002 (1993).
97	J. Massague, *Nat Rev Mol Cell Biol* **1** (3), 169 (2000).
98	G. I. Patterson and R. W. Padgett, *Trends Genet* **16** (1), 27 (2000).
99	J. Massague and D. Wotton, *The EMBO journal* **19** (8), 1745 (2000).
100	E. S. Lander, L. M. Linton, B. Birren et al., *Nature* **409** (6822), 860 (2001).
101	G. Manning, D. B. Whyte, R. Martinez et al., *Science (New York, N.Y* **298** (5600), 1912 (2002).

102   J. Massague, *Annual review of biochemistry* **67**, 753 (1998).

103   J. Massague and Y. G. Chen, *Genes & development* **14** (6), 627 (2000).

104   Y. Shi and J. Massague, *Cell* **113** (6), 685 (2003).

105   J. Massague, J. Seoane, and D. Wotton, *Genes & development* **19** (23), 2783 (2005).

106   M. Kretzschmar, F. Liu, A. Hata et al., *Genes & development* **11** (8), 984 (1997).

107   M. Kawabata, T. Imamura, and K. Miyazono, *Cytokine & growth factor reviews* **9** (1), 49 (1998).

108   L. J. Jonk, S. Itoh, C. H. Heldin et al., *The Journal of biological chemistry* **273** (33), 21145 (1998).

109   O. Korchynskyi and P. ten Dijke, *The Journal of biological chemistry* **277** (7), 4883 (2002).

110   A. Hata, J. Seoane, G. Lagna et al., *Cell* **100** (2), 229 (2000).

111   M. Ku, S. Howard, W. Ni et al., *The Journal of biological chemistry* **281** (8), 5277 (2006).

112   A. Herpin and C. Cunningham, *The FEBS journal* **274** (12), 2977 (2007).

113   M. Raida, J. H. Clement, R. D. Leek et al., *Journal of cancer research and clinical oncology* **131** (11), 741 (2005).

114   F. W. Ruscetti, S. Akel, and S. H. Bartelmez, *Oncogene* **24** (37), 5751 (2005).

115   N. O. Fortunel, A. Hatzfeld, and J. A. Hatzfeld, *Blood* **96** (6), 2022 (2000).

116   K. Park, S. J. Kim, Y. J. Bang et al., *Proceedings of the National Academy of Sciences of the United States of America* **91** (19), 8772 (1994).

117   L. Garrigue-Antar, T. Munoz-Antonia, S. J. Antonia et al., *Cancer research* **55** (18), 3982 (1995).

118   S. Markowitz, J. Wang, L. Myeroff et al., *Science (New York, N.Y* **268** (5215), 1336 (1995).

119   H. K. Lin, S. Bergmann, and P. P. Pandolfi, *Oncogene* **24** (37), 5693 (2005).

120   I. Rios, R. Alvarez-Rodriguez, E. Marti et al., *Development (Cambridge, England)* **131** (13), 3159 (2004).

121   G. Bhardwaj, B. Murdoch, D. Wu et al., *Nature immunology* **2** (2), 172 (2001).

122   M. Bhatia, D. Bonnet, D. Wu et al., *The Journal of experimental medicine* **189** (7), 1139 (1999).

123   J. An, V. Rosen, K. Cox et al., *Experimental hematology* **24** (7), 768 (1996).

124   C. Kersten, E. A. Sivertsen, M. E. Hystad et al., *BMC immunology* **6** (1), 9 (2005).

125   J. M. Wozney, V. Rosen, A. J. Celeste et al., *Science (New York, N.Y* **242** (4885), 1528 (1988).

126   B. L. Hogan, *Current opinion in genetics & development* **6** (4), 432 (1996).

127   M. F. Mehler, P. C. Mabie, D. Zhang et al., *Trends in neurosciences* **20** (7), 309 (1997).

128   R. Y. Tsai and R. R. Reed, *J Neurosci* **17** (11), 4159 (1997).

129   W. A. Alcaraz, D. A. Gold, E. Raponi et al., *Proceedings of the National Academy of Sciences of the United States of America* **103** (51), 19424 (2006).

130   J. Turner and M. Crossley, *Trends in biochemical sciences* **24** (6), 236 (1999).

131   R. Y. Tsai and R. R. Reed, *Molecular and cellular biology* **18** (11), 6447 (1998).

132   H. M. Bond, M. Mesuraca, E. Carbone et al., *Blood* **103** (6), 2062 (2004).

133   S. Warming, P. Liu, T. Suzuki et al., *Blood* **101** (5), 1934 (2003).

134   R. Feinbaum, *Current protocols in molecular biology / edited by Frederick M. Ausubel ... [et al* **Chapter 1**, Unit1 5 (2001).

135   M. Prochazka, H. R. Gaskins, L. D. Shultz et al., *Proceedings of the National Academy of Sciences of the United States of America* **89** (8), 3290 (1992).

136   J. C. van der Loo, H. Hanenberg, R. J. Cooper et al., *Blood* **92** (7), 2556 (1998).

137   K. Mihara, C. Imai, E. Coustan-Smith et al., *British journal of haematology* **120** (5), 846 (2003).

138   T. Dull, R. Zufferey, M. Kelly et al., *Journal of virology* **72** (11), 8463 (1998).

139   V. Sandrin, B. Boson, P. Salmon et al., *Blood* **100** (3), 823 (2002).

140   F. Di Nunzio, B. Piovani, F. L. Cosset et al., *Human gene therapy* **18** (9), 811 (2007).

141   P. D. Zamore, T. Tuschl, P. A. Sharp et al., *Cell* **101** (1), 25 (2000).

142   R. Zufferey, D. Nagy, R. J. Mandel et al., *Nature biotechnology* **15** (9), 871 (1997).

143   T. Nagai, K. Ibata, E. S. Park et al., *Nature biotechnology* **20** (1), 87 (2002).

144   T. Kitamura, Y. Koshino, F. Shibata et al., *Experimental hematology* **31** (11), 1007 (2003).

145   M. F. Kramer and D. M. Coen, *Current protocols in molecular biology / edited by Frederick M. Ausubel ... [et al* **Chapter 15**, Unit 15 1 (2001).

146   F. Sanger, S. Nicklen, and A. R. Coulson, *Proceedings of the National Academy of Sciences of the United States of America* **74** (12), 5463 (1977).

147   C. A. Heid, J. Stevens, K. J. Livak et al., *Genome research* **6** (10), 986 (1996).

148   J. Vandesompele, K. De Preter, F. Pattyn et al., *Genome biology* **3** (7), RESEARCH0034 (2002).

149   M. Goldstein and S. Watkins, *Current protocols in molecular biology / edited by Frederick M. Ausubel ... [et al* **Chapter 14**, Unit 14 6 (2008).

150   T. M. Dexter and E. Spooncer, *Annual review of cell biology* **3**, 423 (1987).

151   M. Nishihara, Y. Wada, K. Ogami et al., *European journal of immunology* **28** (3), 855 (1998).

152   S. Saeland, V. Duvert, D. Pandrau et al., *Blood* **78** (9), 2229 (1991).

153   J. I. Ohkawara, K. Ikebuchi, M. Fujihara et al., *Leukemia* **12** (5), 764 (1998).

154   A. J. Shah, E. M. Smogorzewska, C. Hannum et al., *Blood* **87** (9), 3563 (1996).

155   M. M. Bradford, *Analytical biochemistry* **72**, 248 (1976).

156   J. D. Dignam, R. M. Lebovitz, and R. G. Roeder, *Nucleic acids research* **11** (5), 1475 (1983).

157   N. C. Andrews and D. V. Faller, *Nucleic acids research* **19** (9), 2499 (1991).

158   S. R. Gallagher, *Current protocols in molecular biology / edited by Frederick M. Ausubel ... [et al* **Chapter 10**, Unit 10 2A (2006).

159   S. Gallagher, S. E. Winston, S. A. Fuller et al., *Current protocols in molecular biology / edited by Frederick M. Ausubel ... [et al* **Chapter 10**, Unit 10 8 (2008).

160   R. M. Harland, *Proceedings of the National Academy of Sciences of the United States of America* **91** (22), 10243 (1994).

161   K. Detmer, T. A. Steele, M. A. Shoop et al., *Blood cells, molecules & diseases* **25** (5-6), 310 (1999).

162   C. Li, K. Ando, Y. Kametani et al., *Experimental hematology* **30** (9), 1036 (2002).

163   A. Manabe, K. G. Murti, E. Coustan-Smith et al., *Blood* **83** (3), 758 (1994).

164   K. G. Murti, P. S. Brown, M. Kumagai et al., *Experimental cell research* **226** (1), 47 (1996).

165 J. C. Wang and J. E. Dick, *Trends in cell biology* **15** (9), 494 (2005).

166 M. E. Ross, X. Zhou, G. Song et al., *Blood* **102** (8), 2951 (2003).

167 W. Ishida, T. Hamamoto, K. Kusanagi et al., *The Journal of biological chemistry* **275** (9), 6075 (2000).

168 S. Davis, S. Miura, C. Hill et al., *Developmental biology* **270** (1), 47 (2004).

169 M. Maeno, P. E. Mead, C. Kelley et al., *Blood* **88** (6), 1965 (1996).

170 F. Li, S. Lu, L. Vida et al., *Blood* **98** (2), 335 (2001).

171 S. Jeanpierre, F. E. Nicolini, B. Kaniewski et al., *Blood* **112** (8), 3154 (2008).

172 V. Maguer-Satta, L. Bartholin, S. Jeanpierre et al., *Experimental cell research* **282** (2), 110 (2003).

173 M. Sigvardsson, M. O'Riordan, and R. Grosschedl, *Immunity* **7** (1), 25 (1997).

174 A. Lagergren, R. Mansson, J. Zetterblad et al., *The Journal of biological chemistry* **282** (19), 14454 (2007).

175 R. B. Lock, N. Liem, M. L. Farnsworth et al., *Blood* **99** (11), 4100 (2002).

176 A. Borgmann, C. Baldy, A. von Stackelberg et al., *Pediatric hematology and oncology* **17** (8), 635 (2000).

177 J. Cammenga, B. Niebuhr, S. Horn et al., *Cancer research* **67** (2), 537 (2007).

178 C. De Bruyn, A. Delforge, D. Bron et al., *Journal of hematotherapy* **6** (2), 93 (1997).

179 K. Kaushansky, *Annals of the New York Academy of Sciences* **1044**, 139 (2005).

180 A. W. Kamps, D. Hendriks, J. W. Smit et al., *Medical oncology (Northwood, London, England)* **16** (1), 46 (1999).

181 H. Igarashi, S. C. Gregory, T. Yokota et al., *Immunity* **17** (2), 117 (2002).

182 S. D. Fugmann, A. I. Lee, P. E. Shockett et al., *Annual review of immunology* **18**, 495 (2000).

183 J. A. Prieyl and T. W. LeBien, *Proceedings of the National Academy of Sciences of the United States of America* **93** (19), 10348 (1996).

184 M. L. Mucenski, B. A. Taylor, N. A. Jenkins et al., *Molecular and cellular biology* **6** (12), 4236 (1986).

185 S. Warming, T. Suzuki, T. P. Yamaguchi et al., *Oncogene* **23** (15), 2727 (2004).

186 K. E. Hentges, K. C. Weiser, T. Schountz et al., *Oncogene* **24** (7), 1220 (2005).

187 H. M. Bond, M. Mesuraca, N. Amodio et al., *The international journal of biochemistry & cell biology* **40** (5), 848 (2008).

188 H. Hemmoranta, S. Hautaniemi, J. Niemi et al., *Stem cells and development* **15** (6), 839 (2006).

189 E. Prokhortchouk and P. A. Defossez, *Biochimica et biophysica acta* **1783** (11), 2167 (2008).

9 Danksagung